To the Graduate Council:

I am submitting herewith a thesis written by Naomi Parker entitled "Ross Sea Polynya Phytoplankton bloom dynamics : Ultraviolet-B Effects". I have examined the final copy of this thesis for form and content and recommend that it be accepted in partial fulfullment of the requirements for the degree of Master of Science, with a major in Ecology.

Walker O. Smith, Major Professor

We have read this thesis
and recommend its acceptance :

Accepted for the Council:

Associate Vice Chancellor and
Dean of the Graduate School

ROSS SEA POLYNYA

PHYTOPLANKTON BLOOM DYNAMICS :

ULTRAVIOLET-B EFFECTS

A Thesis

Presented for the

Master of Science

Degree

The University of Tennessee, Knoxville

Naomi Parker

May 1997

ACKNOWLEDGEMENTS

• I would like to firstly thank my major professor, Dr. Walker Smith for giving me the opportunity to work on this project and for his support, advice and review of the manuscript.

• I also extend thanks to my other comittee members, Dr. Dewey Bunting for help with statistical analyses and Dr. Jackie Grebmeier for reviewing the manuscript.

• Much thanks must also go to Ann-Maree White, Scott Polk, Sylvie Mathot, Shuhua Hu, Kendra Daly and Lee-Ann Monty who helped me in so many ways with advice, encouragement and just generally putting up with me and keeping me sane.

• Thanks to my family for their support and for keeping in touch in spite of the cost of phone calls and for being there for me.

• Thanks also to my friends for their friendship and encouragement and for helping make Knoxville home for a while. In particular Lach, for all those emails and Corey for listening and talking at the appropriate time.

• Thanks to the Captain and crew of the Nathaniel B. Palmer for their help and patience and to all the scientific team involved in the Ross Sea Polynya Project for an interesting, stimulating and enjoyable time at sea.

• This work was supported by NSF grant OPP-9317587 to Walker Smith.

• Finally, thanks to my heavenly Father for loving and sustaining me in all things.

ABSTRACT

Stratospheric ozone depletion in the austral spring results in increased fluxes of Ultraviolet - B (UV-B) radiation (280 - 320 nanometers) to the earth's surface which is biologically harmful to phytoplankton. The potential effects of ultraviolet-B radiation on the Ross Sea polynya spring phytoplankton blooms were investigated through measurements of UV-B penetration (along with other wavelengths) into the water column and through field experiments on phytoplankton responses to variations in UV-B levels. This work was carried out during two research cruises, the first from November 10 to December 8, 1994 under significantly ozone depleted conditions, and the second from December 16 to January 14, 1995/96 when 'normal' ozone levels were present. UV-B was found to penetrate to biologically significant depths, extending through almost the entire mixed layer at the longer wavelengths. The vertical attenuation coefficients (K) for all wavelengths measured varied greatly throughout the polynya and were positively correlated with integrated chlorophyll concentrations, reflecting the importance of phytoplankton as attenuators of light. The dominant alga of the early spring in the polynya is *Phaeocystis* sp., while later in the season diatoms, particularly *Nitzschia subcurvata,* become numerically dominant. Primary production in surface waters increased under UV-B exclusion during both cruises, suggesting the possibility that current measurements of productivity for the area using UV-opaque incubation vessels may be overestimated. Experiments in which UV-B exposure of phytoplankton was varied indicated that in the Ross Sea *Phaeocystis* is better able to tolerate enhanced UV-B conditions. To my knowledge this has not been observed previously, since in other environments diatoms have been found to be more tolerant to increased UV-B fluxes. It is suggested that the cellular geometry of the dominant Ross Sea polynya diatom (*Nitzschia subcurvata*) which is small and solitary, may be one reason for this discrepancy, as all diatoms studied for their UV-B tolerance have been either larger or occurred in chains. The higher UV-B tolerance of *Phaeocystis* may increase its competitiveness over diatoms in the early spring, although lack of pre-ozone data make it impossible to quantify the effect. The poorer nutritional value of *Phaeocystis* compared to diatoms implies that any benefit of ozone depletion for *Phaeocystis* may have a negative impact on the ecosystem as a whole by decreasing the amount of energy transferred to higher trophic levels, both pelagic and benthic. More work needs to be done to determine the impact of this effect and the implications for the area of continued ozone depletion.

TABLE OF CONTENTS

Chapter			Page
1.	Introduction		1
	1.1	The Ross Ice Shelf Polynya	2
	1.2	Controls on Phytoplankton Blooms	7
		1.2.1 Light	8
		1.2.2 Macronutrients	10
		1.2.6 Micronutrients	11
		1.2.4 Grazing	12
		1.2.3 Vertical Flux of Particles	13
		1.2.5 Bacterial Activity	14
		1.2.6 Physical Factors	15
	1.3	UV Radiation and the Ozone Hole	16
		1.3.1 DNA Damage	18
		1.3.2 Primary Productivity	19
		1.3.3 Defense Mechanisms	20
		1.3.4 Pigments	20
		1.3.5 Variable Effects	21
2.	Materials and Methods		23
	2.1	Sample Sites	23
	2.2	Light Measurements	24
	2.3	UV-B Incubations	31
	2.4	Water Collection	32
	2.5	Chlorophyll *a*	34
	2.6	HPLC Pigments	35
	2.7	Primary Productivity	37
	2.8	Photosynthetic Parameters	38
	2.9	Microscopic Analysis	40
	2.10	Particulate Carbon and Nitrogen	41

3. Results 43
3.1 Daily Irradiances 43
3.2 Ozone Concentrations 44
3.3 Profiling Ultraviolet Radiometer Profiles 51
3.4 UV Experiments 67
3.4.1 Chlorophyll 72
3.4.2 Phytoplankton Assemblages 73
3.4.3 Pigment Concentrations 89
3.4.4 Primary Production 95
3.4.5 Photosynthetic Parameters (1995 only) ... 95

4. Discussion and Conclusions 106
4.1 Discussion 106
4.2 Conclusions 117

References Cited 119

Appendices 134
Appendix A NASA Press Release 135
Appendix B Instrument / Model comparison ... 137
Appendix C 1994 Microscopy Data 139
Appendix D 1995 Microscopy Data 140

Vita 150

LIST OF TABLES

		Page
2.1	Summary of parameters measured at each station for RSP^{2}94	27
2.2	Summary of parameters measured at each station for RSP^{2}95	29
3.1	Average and integrated irradiances for RSP^{2}94 determined by the model of Legendre et al. (1993) from mid-day irradiances.	45
3.2	Average and integrated irradiances for RSP^{2}95 determined by the model of Legendre et al. (1993) from mid-day irradiances.	46
3.3	Comparison of two PAR sensors and the Legendre et al. (1993) model approximation of integrated daily irradiance for RSP^{2}95.	47
3.4	Vertical attenuation coefficients from PUV profiles - RSP^{2}94.	63
3.5	Vertical attenuation coefficients from PUV profiles - RSP^{2}95.	64
3.6	Vertical attenuation coefficient simple correlation matrix for RSP^{2}94.	65
3.7	Vertical attenuation coefficient simple correlation matrix for RSP^{2}95.	66
3.8	Vertical attenuation coefficient simple correlation matrix for RSP^{2}94 (*Phaeocystis*-dominated stations only).	68
3.9	Vertical attenuation coefficient simple correlation matrix for RSP^{2}95 (diatom-dominated stations only).	69
3.10	Chlorophyll *a* measurements from 1994 UV experiments.	72
3.11	Chlorophyll equivalent measurements from 1995/96 UV experiments.	74
3.12	Summary of changes in cell numbers for RSP^{2}94 UV experiments.	79
3.13	Summary of changes in cell numbers for RSP^{2}95 UV experiments.	85
3.14	Concentrations of pigments from UV experiments as determined by HPLC for RSP^{2}94.	90
3.15	Concentrations of pigments from UV experiments as determined by HPLC for RSP^{2}95.	91
3.16	Productivity measurements from UV experiments for RSP^{2}94.	96
3.17	Productivity measurements from UV experiments for RSP^{2}95.	97
3.18	Summary of changes in P/I parameters over time for RSP^{2}95 UV 5-day experiments.	99

LIST OF FIGURES

		Page
1.1	Location of the study area.	3
1.2	Seasonal progression of ice/polynya formation.	4
1.3	Interannual variability in Antarctic sea ice (images from Gloersen et al., 1992).	5
2.1	Location of sampling stations for RSP^{2}94.	25
2.2	Location of sampling stations for RSP^{2}95.	26
2.3	Absorption and transmission spectra for mylar screens used in UV-B incubations.	33
2.4	Idealised curve of specific photosynthetic rate (P) as a function of irradiance (I) illustrating the photosynthetic parameters.	39
3.1	PAR as measured by two radiometers and approximated from midday irradiances by the Legendre et al. (1993) model.	48
3.2	Ozone concentrations over the Antarctic continent on the 10th of November 1994 (in dobson units).	49
3.3	Ozone concentrations over the Antarctic continent on the 8th of December 1994 in dobson units).	50
3.4	Ozone concentrations over the Antarctic continent on the 10th of November 1995 (in dobson units).	52
3.5	Ozone concentrations over the Antarctic continent on the 8th of December 1995 (in dobson units).	53
3.6	Ozone concentrations over the Antarctic continent on the 16th of December 1995 (in dobson units).	54
3.7	Ozone concentrations over the Antarctic continent on the 14th of January 1996 (in dobson units).	55
3.8	Variation in stratospheric ozone concentrations over the Ross Sea polynya during RSP^{2}95.	56
3.9	Locations of PUV 500 profile stations for RSP^{2}94.	57
3.10	Locations of PUV 500 profile stations for RSP^{2}95.	58
3.11	Depth penetration of 1% of surface UV-B into the water column.	59

3.12	Water column light profiles as measured by the PUV 500 ultraviolet radiometer - Station 24, 1995.	60
3.13	Water column light profiles as measured by the PUV 500 ultraviolet radiometer - Station 27, 1995.	61
3.14	Locations of stations where UV experiments were initiated for $RSP^2$94.	70
3.15	Locations of stations where UV experiments were initiated for $RSP^2$95.	71
3.16	Change in chlorophyll a over time in experiments A (top), and B (bottom).	75
3.17	Change in chlorophyll a over time in experiments C (top), and D (bottom).	76
3.18	Change in chlorophyll a over time in experiments E (top), and F (bottom).	77
3.19	Change in chlorophyll a over time in experiments G (top), and H (bottom).	78
3.20	Changes in cell concentration over time for experiments 1 and 3.	80
3.21	Changes in cell concentration over time for experiments 4 and 5.	81
3.22	Change in cell numbers over time in experiment 2 for *Phaeocystis* (top), and diatoms (bottom).	83
3.23	Change in cell numbers over time in experiment 6 for *Phaeocystis* (top), and diatoms (bottom).	84
3.24	Change in cell numbers over time in experiment D for *Phaeocystis* (top) and diatoms (bottom).	87
3.25	Change in cell numbers over time in experiment G for *Phaeocystis* (top) and diatoms (bottom).	88
3.26	Changes in concentrations of fucoxanthin (top), and hex-fucoxanthin (bottom) for experiment B.	92
3.27	Changes in concentrations of fucoxanthin (top), and hex-fucoxanthin (bottom) for experiment D.	93
3.28	Changes in concentrations of fucoxanthin (top), and hex-fucoxanthin (bottom) for experiment G.	94
3.29	Change in production rates over time for UV experiments D (top) and G (bottom).	98

3.30 Photosynthesis as a function of irradiance for experiment D after 3 days under the three different UV regimes. 100

3.31 Photosynthesis as a function of irradiance for experiment D after 5 days under the three different UV regimes. 101

3.32 Change in photosynthetic parameters over time for Experiment D. 103

3.33 Photosynthesis as a function of irradiance for experiment D after 3 (top) and 5 (bottom) days under total light conditions. 104

3.34 Photosynthesis as a function of irradiance for experiment D after 3 (top) and 5 (bottom) days under total UV-B exclusion. 105

4.1 Micrographs of *Phaeocystis* (small round cells) and *Nitzschia subcurvata* (long thin cells). 114

1. INTRODUCTION

The Ross Sea polynya is the site of an extensive phytoplankton bloom in the austral spring, with high chlorophyll concentrations and primary production rates. The role of the region in global and Southern Ocean carbon budgets has been a subject of much recent interest, and the investigation of controls on the initiation and development of these blooms is also under question. Several large field programs have been initiated in the region to study the system, including the Ross Sea Polynya Project, U. S. JGOFS (Joint Global Ocean Flux Study) and ROAVERRS (Research on Ocean Atmosphere Variability and Ecosystem Response in the Ross Sea).

In this thesis, the role of ultraviolet-b (UV-B) radiation in this system will be discussed based on data collected in the spring of 1994 and the spring/summer of 1995/96. Ozone depletion occurs over the Antarctic continent in the austral spring resulting in higher levels of UV-B reaching the earth's surface at a time of bloom initiation and development. The purpose of this project was to determine in what way ozone depletion in the area of the Ross Sea might effect bloom dynamics and productivity. The dominant phytoplankton species in the Ross Sea in the early spring is *Phaeocystis* sp., while the assemblage is dominated by diatoms, in particular *Nitzschia subcurvata*[1], later in the year. A second aim of the work was to determine what differential impact UV-B effects have on these assemblages. In the remainder of this chapter, the dynamics of the polynya and its blooms are discussed along with a summary of factors which may play a role in bloom regulation. Finally, the possible effects and implications of ultraviolet radiation on this system are addressed.

---

1 The species referred to throughout the thesis as *Nitzschia subcurvata* is identified as *Pseudo-Nitzschia subcurvata* by the conventions of Tomas (1996).

1.1 THE ROSS ICE SHELF POLYNYA

The Ross Sea polynya is located in the south central sector of the Ross Sea (Figure 1.1). A polynya is an oceanic region surrounded by dense ice cover which remains either partially or totally ice free at times and under climatological conditions where we would expect the waters to be ice covered. Polynyas are generally classified as one of two types (Smith et al., 1990). One type is a latent heat polynya, which is maintained by winds or currents in combination with a physical feature such as a coastline or channel constriction. In this case the winds or currents remove the ice as it is formed, while the physical feature prevents existing ice from entering the region. The second form is a sensible heat polynya, in which sufficient oceanic heat enters the surface waters to prevent ice from forming. This upward heat transfer can occur through vertical mixing of heat from deeper water or through upward advection of heat by such mechanisms as upwelling (Muench, 1990). The Ross Sea polynya is generally thought to be a latent heat polynya, with katabatic winds that blow off the Ross Ice Shelf removing ice as it forms. There is, however, a suggestion that sensible heat processes are also operative, although there is at this time little evidence to support this mechanism (Gloersen et al., 1992). While reduced in ice cover compared to the surrounding region throughout the year, the polynya is essentially ice free for several months in the austral summer and becomes contiguous with the Southern Ocean in late January (see Figure 1.2 for the seasonal progression of ice extent). There is considerable interannual variability within the polynya in both size and position of the open water (Figure 1.3). Satellite images of the polynya from 1978 to 1993 have shown the polynya 'opening' (defined as less than 50 % ice cover) as early as October 13 (1980) and as late as November 22 (1981) (Arrigo et al., submitted).

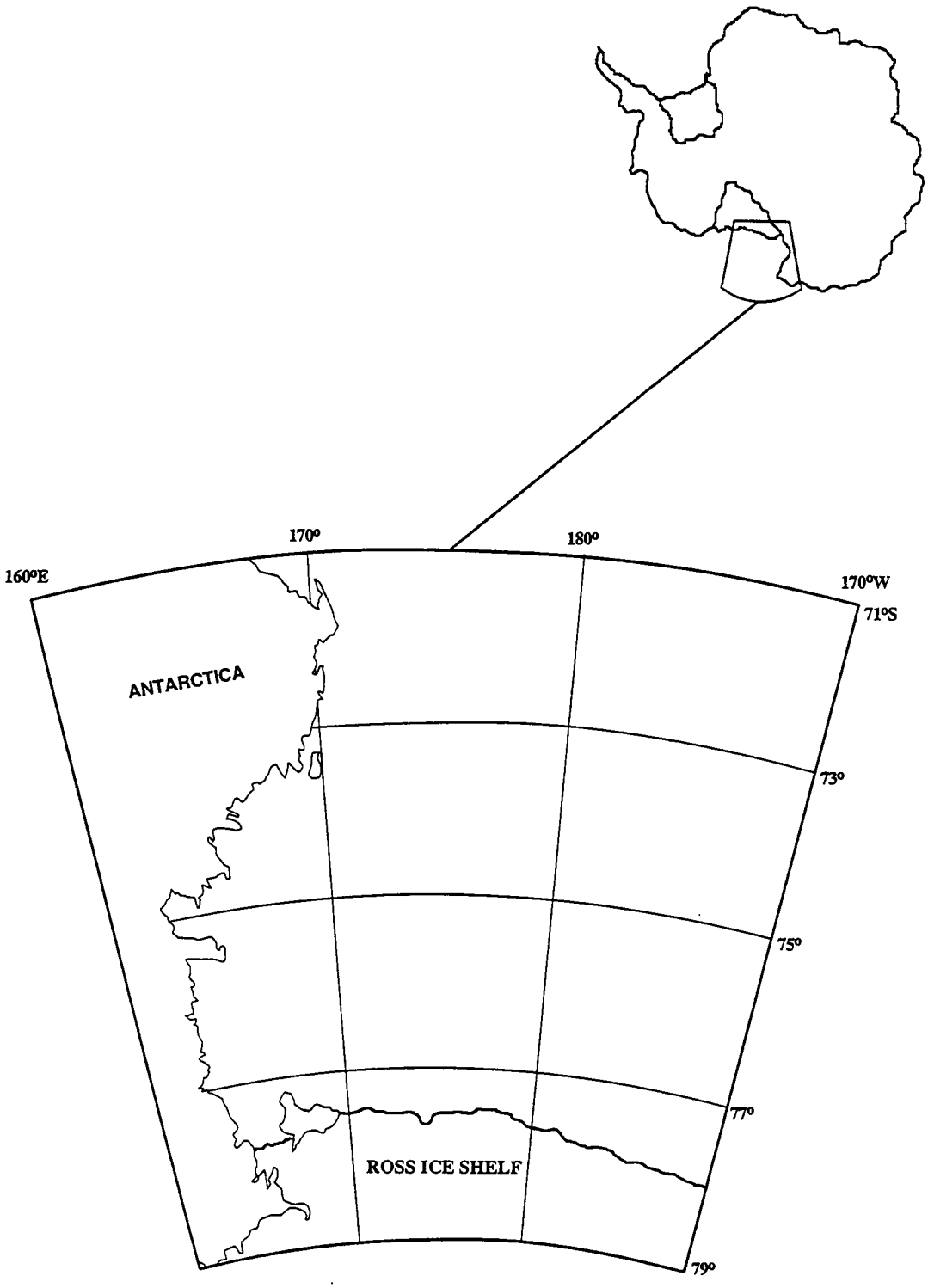

Figure 1.1 Location of the study area

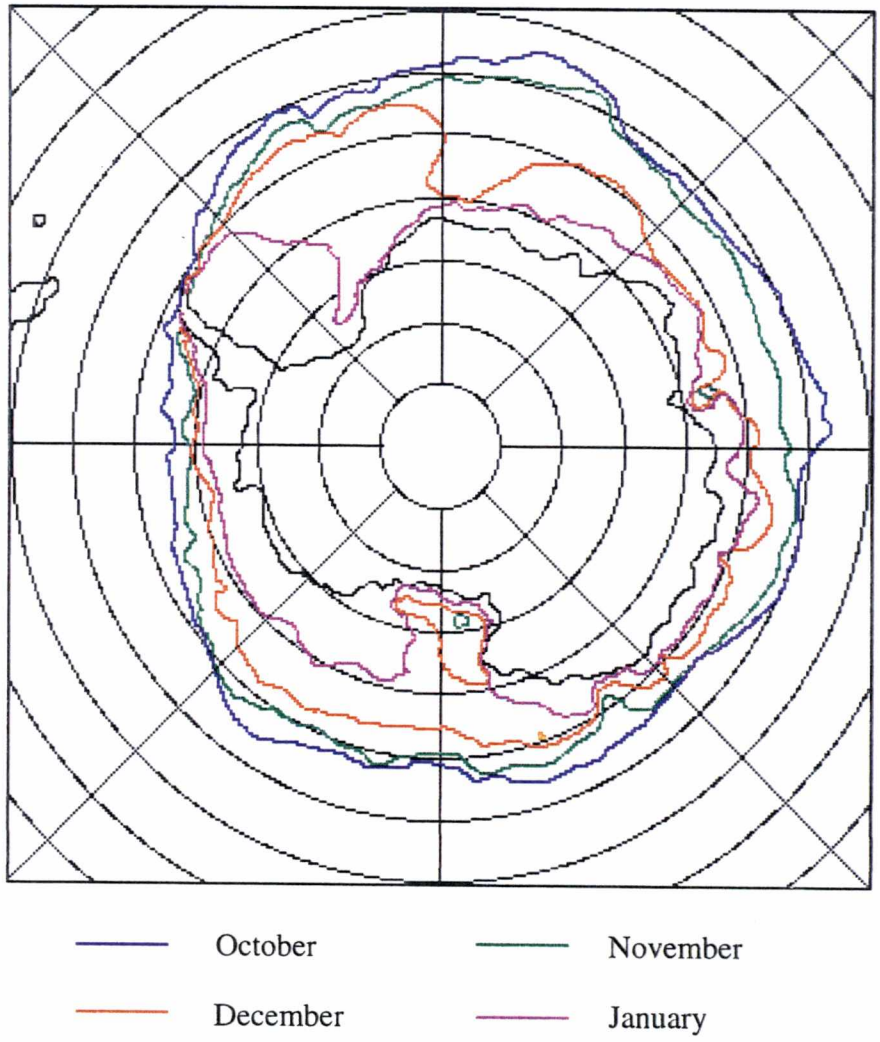

Figure 1.2 Seasonal progression of ice/polynya formation. Lines indicate approximately 30% ice cover (outermost line is October and innermost is January; adapted from Gloersen et al., 1992).

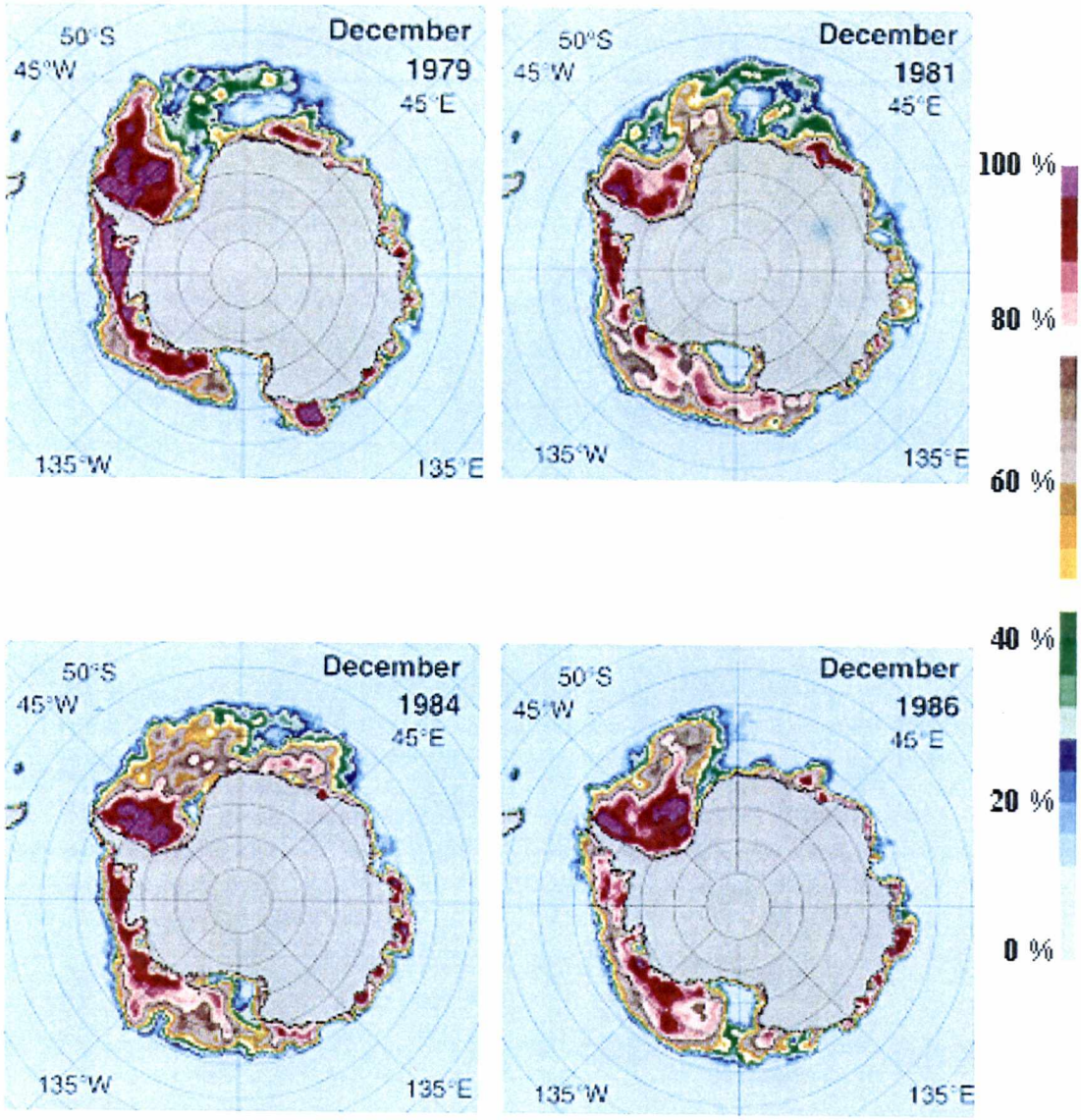

Figure 1.3 Interannual variability in Antarctic sea ice (images from Gloersen et al., 1992).

The Ross Sea polynya during the austral spring is ecologically dynamic. It is the site of Antarctica's most predictable and spatially extensive phytoplankton bloom (Comiso et al., 1993). The breakup of the ice in the early spring coincides with the seasonal increase in irradiance and the development of phytoplankton blooms. These blooms are comprised predominantly of *Phaeocystis antarctica* early in the season in the central polynya area while later in the season several diatoms dominate the phytoplankton assemblage, with *Nitzschia subcurvata* being the most abundant of these. The bloom dynamics of the Ross Sea have been described as a succession of *Phaeocystis* to diatoms during the growing period (Lancelot et al., 1997). The actual situation, however, is far more complex, with most species being present at all times in varying abundances and with a great deal of spatial heterogeneity. Leventer and Dunbar (1996) describe two regions within the polynya from sediment trap samples at Ross Sea sites in January 1990 - February 1992. In the southwestern Ross Sea near the coast (76°30'S, 167°30'E), an assemblage of large diatoms was observed including *Flagilariopsis curta* (maximum of 92%). At a more easterly site (76°30'S, 175°W), a diverse assemblage with a greater contribution of non-diatom species was seen. At this second site *Phaeocystis* was found along with dinoflagellates, *Flagilariopsis cylindrus, F. kerguelensis* and *Thalassiosira gracilis*. DiTullio and Smith (1996) found (in the late austral summer of 1992) greater concentrations of fucoxanthin, a pigment indicative of diatoms, near the coast of Victoria Land and in the northern part of the Ross Sea, while 19'-hexanoyloxyfucoxanthin (a *Phaeocystis* marker) was more prevalent in the south central region. In the spring and summer of 1994 and 1995, respectively, large diatoms were found to be dominant in the southwestern part of the polynya and in the far east. The central portion of the polynya was *Phaeocystis* dominated, with diatoms always present and becoming more numerically important later in the season, particularly the small pennate diatom *Nitzschia subcurvata* (Garrison and Gowing, unpublished data). Chlorophyll concentrations in

these Ross Sea Polynya blooms have previously been estimated through satellite ocean color imagery to reach 40 $\mu g\ L^{-1}$, with production rates of 3.9 g C $m^{-2}\,day^{-1}$ (Arrigo and McClain, 1994), although discrete measurements of chlorophyll from the region have never exceeded 16 $\mu g\ L^{-1}$.

The Ross Sea Polynya Project (RSP^2) was initiated to investigate this productive system. The first cruise to the region was conducted from November 10 - December 8, 1994, and a second cruise took place from December 16, 1995 - January 14, 1996. The primary aim of the Ross Sea Polynya Project was to determine the causes of the phytoplankton blooms, their early bloom dynamics and their impact on the microbial and zooplankton-based food webs.

1.2 CONTROLS ON PHYTOPLANKTON BLOOMS

Phytoplankton blooms occur in oceanic, coastal and freshwater regions. They are among the most dramatic of ecological events, literally turning the waters where they occur soupy green. Phytoplankton blooms are characterized by high cell numbers (> 10^6 cells ml^{-1}) and high chlorophyll concentrations (> 1.0 $\mu g\ L^{-1}$). In many cases they can be caused by anthropogenic influences, such as eutrophication caused by run-off from farmland and the altering of waterways for human use disrupting physical conditions. Phytoplankton blooms attributable to natural causes are also common, and those which occur in the Ross Sea are examples of these. Phytoplankton blooms can occur in frontal zones (e.g. Yoder et al., 1994), marginal ice edge zones (Smith and Sakshaug, 1990), and in areas of upwelling (Barber and Smith, 1981). Blooms result when the average photosynthetic rate in the mixed column is larger than the average loss rate (Sakshaug et

al., 1991). This condition is a result of the interplay of various biological, chemical and physical factors. In the Ross Sea, dominance of *Phaeocystis* in spring and early summer followed by higher abundances of diatoms is a result of the interaction of these various factors. Those factors which are potentially important in the Ross Sea system are as follows :

1) Light,
2) Macronutrients,
3) Micronutrients,
4) Grazing,
5) Vertical flux of particles,
6) Bacterial activity,
7) Physical factors, such as temperature, stratification and winds.

1.2.1 LIGHT

Light is an important controlling mechanism in phytoplankton assemblages at all latitudes and drives many of the seasonal cycles seen in these populations. Light in the Antarctic undergoes great fluctuations throughout the year. For areas below the Antarctic circle, 24-hour photoperiods occur for periods of the summer, while in the winter 24-hour darkness occurs (Smith and Sakshaug, 1990). Phytoplankton require light for growth, and use it to convert carbon dioxide to biomass through photosynthesis; consequently, variations in light have a significant impact on phytoplankton communities. In the Antarctic the light regime is made more complex by the presence of sea ice. Light intensity varies with the thickness of the ice and also varies with snow cover, as even a light covering of snow can reduce light transmission significantly (Maykut and Grenfell, 1973; Karentz, 1991). The angle of the sun, sky conditions (clouds, haze, etc.), and sea

state also effect how deeply light penetrates into the water column (Jerlov, 1976; Kirk, 1994; Mobley, 1994).

The amount of light that is available to phytoplankton is strongly influenced by the physical movement of the water. Water in the ocean is in a constant state of flux, with vertical mixing occurring in the surface layer due to wind stress. The depth of this surface mixed layer, which is marked by an abrupt change in density, determines how long a given phytoplankter is resident in the euphotic zone where light is adequate for photosynthesis (down to approximately 0.1% of surface irradiance). If the mixed layer is deeper than the critical depth (the depth at which integrated water column production is equal to integrated water column respiration), then positive growth and accumulation of biomass cannot occur. Alternatively, if the mixed layer depth is less than the critical depth, positive growth and accumulation of biomass results (Sverdrup, 1953; Nelson and Smith, 1991). It has been suggested by many authors that the main limiting factor for phytoplankton growth in Antarctic waters is light (e.g., Smith and Sakshaug, 1990). In the Ross Sea it is likely that phytoplankton are light limited at the beginning of the spring, when deep mixed layers prevent bloom development (Smith, unpublished data). In the spring and summer shallow mixed layers develop as a result of melt water input and surface warming, ensuring that light is not limiting to phytoplankton.

The previous discussion has been limited to photosynthetically active radiation or visible light (PAR = 400 - 700 nm). Ultraviolet radiation levels, especially UV-B wavelengths of 280 - 320 nm, can also play an important role in bloom dynamics. Under natural conditions UV-B reduces productivity and is damaging to phytoplankton cells. Under ozone depletion with enhanced UV-B in the austral spring, these shorter wavelengths may play an even greater role. UV-B damages DNA, decreases primary production and

pigment content, and also shows a great deal of variation in its effects on different phytoplankton species. These effects are further discussed in section 1.3.

1.2.2 MACRONUTRIENTS

Macronutrients (nitrate, phosphate and silicate) can be very important in the control and development of phytoplankton blooms. A bloom cannot be initiated without sufficient nutrients to enable rapid growth rates and sustenance of the bloom. The ratios of one nutrient to another can also be important. For example, siliceous organisms such as diatoms and silicoflagellates require higher levels of silicon (Jacques, 1989), whereas other phytoplankton groups, (e.g., prymnesiophytes, cryptomonads, cyanobacteria or dinoflagellates) do not have a high requirement for this nutrient. If ambient silicate levels are low, non-siliceous species would likely have a competitive advantage (Sommer, 1994).

In many systems, changes in nutrient levels through terriginous inputs or upwelling events can initiate bloom formation, while the exhaustion of these nutrients results in their decline. The Southern Ocean is a special case in that macronutrient levels are always high (Mitchell and Holm-Hansen, 1991) and drawdown of these nutrients is rare, although nitrate depletion has been observed at the ice edge (Nelson and Smith, 1986) and in coastal regions (Holm-Hansen et al., 1989b). Thus, although high nutrient levels are always required for bloom formation, this condition is continually met in Antarctic systems and more specifically in the Ross Sea. In the Ross Sea other factors appear to be more important to bloom dynamics than macronutrient concentrations.

1.2.3 MICRO-NUTRIENTS

It has been suggested that micronutrients, such as iron, vitamin B12, copper, molybdenum and manganese can play a large role in the regulation of phytoplankton growth dynamics (Duce, 1986; Martin et al., 1991; Coale et al., 1996). These trace constituents are involved in all metabolic processes of phytoplankton, including photosynthesis, respiration and nutrient assimilation (Morel et al., 1991a). Micronutrient deficiency is considered to be particularly important in areas where even though macronutrients are high, chlorophyll levels are generally low (high nutrient, low chlorophyll, or HNLC areas). One example of an HNLC system is the equatorial Pacific. In this area macronutrients are upwelled to the surface, and although biomass and net production rates are considerable, they are not as high as they could be if all of the nutrients available were utilized. Both grazing (discussed in section 1.2.4) and iron limitation have been suggested as limiting the biomass of these regions (Cullen, 1991; Coale et al., 1996).

The main source of iron to the surface of the ocean is through eolian dust from terrestrial sources, which contributes approximately three times more than other sources such as riverine input and runoff (Duce, 1986; Morel et al., 1991b; Duce and Tindale, 1991). As a result, bodies of water that are far removed from land and atmospheric fallout often have lower iron concentrations. This trace metal deficiency hypothesis was first put forward for Antarctic waters by Hart (1934) and was revived with the development of clean techniques for trace metal studies (e.g., Martin and Fitzwater, 1988). Martin et al. (1994) carried out an experiment where they seeded a 64 km^2 area of the equatorial Pacific with iron. This iron addition resulted in a doubling of plant biomass, a three-fold increase in chlorophyll and a four-fold increase in plant production. Similar increases were found in a chlorophyll-rich plume downstream of the Galapagos Islands, which

was presumably naturally enriched in iron by resuspension from sediments. These findings indicated that iron limitation can control rates of phytoplankton productivity and biomass in the ocean (Martin et al., 1994). Martin et al. (1990a) also carried out experiments on the effect of iron addition on phytoplankton growth in the Ross Sea (although these were bottle experiments rather than seeding of the actual water column) and found that phytoplankton growth at three stations in the Ross Sea region were limited by iron availability; a fourth station, nearest to the coast had higher ambient iron concentrations and was not iron limited. DiTullio and Sedwick (1996) found that iron concentrations were quite low in the Ross Sea polynya in the late spring of 1995 (0.2 nM) and suggested that these low concentrations of iron may regulate the *Phaeocystis* blooms in the seasonal ice zone. Martin et al. (1990b) originally suggested that iron input from retreating ice may help to trigger phytoplankton growth, and therefore increased distance from the receding ice edge would result in a gradual reduction in iron concentrations and in production. The influence of iron and other micronutrient concentrations on Ross Sea bloom dynamics at this time is equivocal, but potentially could play an important role.

1.2.4 GRAZING

Grazing can play an important role in the development and control of phytoplankton blooms. There are many different sizes of grazers, ranging from nanoflagellate heterotrophs (2 - 20 μm; e.g. choanoflagellates) to the microheterotrophic dinoflagellates and cilliates (20 - 200 μm) to the mesozooplankton such as krill (Euphausiids), copepods and amphipods (0.2 - 20 mm). These various grazers can all have significant impacts on bloom dynamics through grazing the various size classes of prey. There is considerable evidence that naturally occurring concentrations of krill are capable of virtually 'clearing'

an area of phytoplankton, and also of altering the species distribution of the assemblage by selectively grazing the larger components of the phytoplankton (Price et al., 1988; Graneli et al. 1993). Large krill swarms have been observed in the Ross Sea through acoustic observations (Azzali and Kalinowski, 1996) but are limited to the north, suggesting that krill swarms are not a large factor in the dynamics of the ice shelf polynya bloom. Microzooplankton have been found to play an important role in the control of production in Antarctic waters (Buma et al. 1991; Lancelot et al., 1993; Burkill et al., 1995) and in some cases potential grazing rates can exceed rates of primary production (Mathot et al., 1992). Many authors have suggested that microzooplankton, because of their size and metabolic rates, are readily able to keep up with the growth rates of phytoplankton and control their growth (Cushing, 1959; Frost, 1991; Becquevort et al., 1992; Lancelot et al., 1993). In the summer of 1995/96, large numbers of heterotrophic dinoflagellates (as well as fecal pellets of these organisms) were observed in the polynya bloom (Lessard and Gowing, unpublished data), which suggests that grazing may contribute significantly to the regulation and decline of the Ross Sea blooms.

1.2.5 VERTICAL FLUX OF PARTICLES

The vertical flux of particles through the water column and from the euphotic zone can play an important role in bloom dynamics by controlling loss rates. Sinking particles also remove nutrients and biomass from the bloom waters. The flux of particles is dependent on factors such as their specific gravity and their incorporation into fecal pellets or aggregates (marine snow), as well as the physical conditions of the water column (Honjo, 1990). Jaeger et al. (1996) found that fecal pellets and aggregates made up >70% of the particle flux by mass at two stations within the Ross Sea study area. In floating sediment trap samples from December/January of 1995/96, many mini-pellets,

probably released by heterotrophic dinoflagellates, were observed along with particle aggregates of *Phaeocystis* and diatoms (Gowing, unpublished data). Asper et al. (1996b) reported relatively low flux rates of 0 - 250 mg C m^{-2} d^{-1} for November 1994 in the Ross Sea polynya at a time when there was high and increasing primary productivity (up to 6 g C m^{-2} d^{-1}; Smith and Gordon, 1997). In the later stages of the bloom in December/January 1995/96 Asper et al. (1996a) reported sinking speeds of between 4 and 200 m d^{-1} and flux rates of 100 - 800 mg C m^{-2} d^{-1} (Asper, personal communication) when primary production averaged 1 g C m^{-2} d^{-1} (Smith, unpublished data). These high flux rates later in the season suggest that increased aggregation and flux of particles from the water column may play an important role in the control of the standing stocks of the Ross Sea blooms.

1.2.6 BACTERIAL ACTIVITY

In the last two decades the importance and abundance of marine bacteria has been recognized (Ducklow and Carlson, 1992). It is widely accepted that approximately 50% of the primary production in temperate and tropical marine and fresh water systems is processed by bacteria each day (Ducklow and Carlson, 1992 and references therein). Bacteria can influence phytoplankton indirectly by their impact on macronutrient dynamics. Bacteria are an important part of the microbial loop which cycles nutrients; they use dissolved organic matter released from phytoplankton as a substrate for growth and produce ammonium, which is preferred over nitrate as a nitrogen source for phytoplankton growth (Ducklow and Carlson, 1992). In this way bacteria remineralize nutrients in the euphotic zone so that the nutrients can be re-used by phytoplankton, and potentially extend the bloom period (Putt et al., 1994). Bacterial production rates increased dramatically during the course of the 1994 and 1995 Ross Sea blooms (Carlson

et al., 1997) and therefore may be important in bloom dynamics, although the high ambient concentrations of macronutrients mean that the process of remineralization may be less crucial in this system.

Another process by which bacteria may influence phytoplankton dynamics in a more direct way is through the chelation of metals. Bacteria produce iron chelating ligands (siderophores) which they excrete in order to complex and ultimately assimilate dissolved iron; this, along with their high surface-to-volume ratios, enables them to successfully compete with phytoplankton for iron (Kirchman, 1996; Pakulski et al., 1996). Bacteria have been found to contain more iron than phytoplankton (Tortell et al., 1996) and thus, if iron is indeed limiting to phytoplankton in the Ross Sea as discussed above (section 1.2.3), bacteria may be reducing the available iron even further.

1.2.7 PHYSICAL FACTORS

Many physical factors are important in bloom dynamics. Mixed layer depths have been mentioned previously in the discussion of light in section 1.2.1. The effect of winds on mixing rates and depths is also important as greater wind speeds, and longer duration winds often result in deeper mixed depths. Decreases in salinity due to meltwater input, along with increases of temperature in the spring and summer, help to produce a stratified water column that is absent in winter when mixed layers extend throughout the water column (Smith, unpublished data). Reduced wind speeds and ice cover also set up suitable conditions for phytoplankton growth. The timing of stratification and breaking up of ice in the polynya varies from year to year, and as a result the timing of the onset of blooms also varies. Arrigo et al. (1997) present data which suggest that the timing of polynya opening is dependent on winter temperatures that determine ice thicknesses in the

Ross Sea rather than wind stress. They also suggest that, contrary to what would be expected, earlier opening of the polynya results in a later start to the bloom as a result of stronger winds earlier in the year maintaining deep mixed layers. The various mechanisms which bring about the stratification of the water column are essential to phytoplankton growth, and as such physical processes are of primary importance in bloom formation.

1.3 UV RADIATION AND THE OZONE HOLE

Ultraviolet B radiation consists of the wavelengths between 280 and 320 nanometers. It is the most biologically harmful component of sunlight which reaches the earth's surface (the shorter wavelength UV-C is potentially more harmful but is completely absorbed by the atmosphere; Calkins and Thordardottir, 1980; Karentz, 1991). However, the ozone layer in the stratosphere blocks most of the harmful UV-B radiation. In 1985 researchers from the UK's Halley station on the Antarctic peninsula first reported that an observed thinning of the ozone layer over the Antarctic region during the austral spring was probably a result of the anthropogenic input of compounds such as chlorofluorocarbons into the earth's atmosphere (Farman et al., 1985). These compounds are very stable and have long residence times in the atmosphere, and due to atmospheric circulation can ultimately be transported to the stratosphere where the chlorine molecules break ozone (O_3) bonds. The destruction of the ozone then results in a thinning of the ozone layer (Frederick and Lubin, 1994).

The production of the ozone hole has been a predictable event each austral spring for the last decade and a half, although it varies somewhat in size and in location. In 1987 an

international agreement to reduce and ultimately halt the emissions of ozone destroying substances was implemented. This agreement, called the Montreal Protocol, has more than 150 countries as signatories. These countries account for approximately 92% of the estimated global consumption of ozone destroying substances. The measures outlined in the Montreal Protocol have now been put into effect by many of the signatory countries. However, due to the long life of the compounds in question, full recovery of the atmospheric system would occur only after a century or more following complete termination of the emissions of these gases into the atmosphere (Kurylo, 1990), and this is not scheduled until early in the 21st century. Encouragingly, there has been an observed decrease in the atmospheric concentration of one of the ozone depleting substances, methyl chloroform (NASA press release July 20, 1995 - Appendix A). It has also been stated that the peak in the buildup of chlorofluorocarbons has been reached as a result of Montreal protocol directives barring future non-compliance with the protocol (Hofmann, 1996; Normile, 1996).

The scientific community has been endeavoring to determine the implications of ozone depletion for various ecosystems since its discovery. One area of concentrated effort has been on the marine ecosystem of the Southern Ocean. UV radiation is able to penetrate to depths of 50 m, and in highly stratified waters with shallow mixed layers, such as those that occur in marginal ice edge zones, this can result in phytoplankton being exposed to high UV levels for long periods of time. It is important to determine how phytoplankton may be affected by the increases in UV radiation, as they form the base of the food web, and as such any impact of ozone depletion may be felt throughout the rest of the ecosystem (El-Sayed et al., 1990).

The levels of UV-B reaching the ocean surface in spring under ozone depletion are comparable to, or greater than those experienced in mid-summer. This results in a greatly extended period where organisms are exposed to high UV-B radiation levels (Frederick and Snell, 1988). The concern for Antarctic ecosystems is based on the assumption that the organisms in these regions evolved under lower UV-B levels and consequently do not have defenses adequate to cope with the elevated UV-B. Much of the research on the consequences of ozone depletion in Antarctica has focused on trying to determine what kinds of protection these organisms have.

1.3.1 DNA DAMAGE

UV-B radiation has been found to have deleterious effects on phytoplankton in several ways. The direct biological effects of UV-B result from the absorption of specific wavelengths by biomolecules and the resultant dissipation of that energy by photochemical reactions (Vincent and Roy, 1993). This can result in DNA and RNA damage through the formation of base lesions. If these changes in molecular structure are not repaired, they can interfere with DNA synthesis and RNA transcription, essentially disrupting the translation of the genetic code. This DNA damage is potentially debilitating, mutational, or lethal (Karentz, 1994). At least three major cellular mechanisms interact with UV-damaged DNA to restore the original genetic code: photoreactivation, excision repair, and recombinational repair (Cleaver and Kraemar, 1989 as cited by Karentz and Lutze, 1990). Photoreactivation is a single enzyme system activated by visible light that corrects one class of pyrimidine dimer in DNA. Excision repair is a system that corrects a range of DNA damage by removal and replacement. Recombinational repair is a complex process in which damaged DNA is reconstructed through DNA replication and strand exchange. These repair mechanisms work best at

low levels of damage (Karentz and Lutze, 1990).

1.3.2 PRIMARY PRODUCTIVITY

The effect of elevated UV-B on primary production and photosynthesis has received much attention over the last two decades. Increased UV-B levels have been found to cause photoinhibition of photosynthesis (Lorenzen, 1979; Smith and Baker, 1979; Smith and Baker, 1980; El-Sayed, 1990, Prezelin et al., 1994). UV radiation has, however, only recently (since the late 1970s) been considered to be a significant factor in biological oceanographic studies, and it has been suggested that the standard technique of measuring productivity by ^{14}C-uptake in polycarbonate (or other UV opaque) bottles may overestimate primary production by as much as 1.5 times on a sunny day (Lorenzen, 1979). Estimates of the effect on annual primary productivity caused by elevated UV-B levels vary. Smith et al. (1992) estimate a 2% to 4% decrease in the annual productivity and a 6 - 12 % decrease over a 6 week period in spring in the marginal ice edge zone. Holm-Hansen et al. (1989a) estimated decreases in annual productivity at $< 0.15\%$ and decreases in daily production in the spring on the order of 3-15%, and Arrigo (1994) estimated less than 1% reduction in gross primary productivity. All of these estimates are far less than natural interannual variability, which is approximately +/- 25 % (Smith, et al., 1988). However, these estimates are clearly measurable on a daily or weekly scale, and the ecological impact of these reductions in springtime productivity is yet to be determined (Smith et al., 1992).

1.3.3 DEFENSE MECHANISMS

Much research has been focused on the determination of the kinds of defenses Antarctic organisms have to elevated springtime UV-B levels. Some have physical barriers such as shells, feathers, and fur which exclude UV. Vertical migration has also been observed in many organisms, so that they are in lower light levels when UV levels are at their highest. This behavior has been observed in dinoflagellates, pennate diatoms in estuarine sediments and *Oscillatoria* (cyanobacteria trichomes) in microbial mats (Vincent and Roy, 1993). The primary reason for this behavior is probably not UV avoidance, but this is a secondary benefit of the behavior. For those species without such defenses, other means of protection have been found. Many Antarctic marine organisms have been found to contain mycosporine-like amino acids (MAAs) which absorb strongly in the UV-B portion of the spectrum (Karentz et al., 1991b; Vincent and Roy, 1993; Karentz, 1994). MAAs have been reported in corals (Dunlap et al., 1986), seastars (Nakamura et al., 1981), ascidians (Kobayashi et al., 1981), zoanthids (Ito and Hirata, 1977), fish (Dunlap et al., 1989), dinoflagellates (Carreto et al., 1990), red algae (Sivalingham et al., 1974a,b), and diatoms (Karentz, 1994). Compounds which absorb strongly between 250 and 370 nm have also been found in colonial *Phaeocystis* sp., although the actual compounds have not been identified (Marchant et al., 1991; Davidson and Marchant, 1994). It is generally accepted that the photosynthetic organisms synthesize the MAAs which are subsequently assimilated by animals through ingestion or through translocation from symbionts (Karentz, 1991; Shick et al., 1992; Karentz, 1994).

1.3.4 PIGMENTS

UV-B radiation has been found to destroy chlorophyll and accessory pigments in both micro- and macroalgae (Dohler, 1984 ; Wood, 1987 ; Bidigare, 1989 ; El-Sayed et al.,

1990). Chlorophyll *a* has been observed to be selectively reduced in long-term (24-48 hours) exposures to UV-B while other pigments remained unchanged (Bidigare, 1989; El-Sayed et al., 1990). In other experiments reductions in all pigments have been observed under higher UV-B irradiances (El-Sayed et al., 1990). Shorter experiments (4 hours) have shown no appreciable loss of photosynthetic pigmentation (El-Sayed et al., 1990). The mixed layer depth, mixing rates and depth of UV light penetration into waters which experience increased exposures of UV-B will determine the significance of the impact on pigmentation since they determine the length of exposure. It has been suggested that the destruction of these photosynthetic pigments by UV-B radiation may be a major factor in the reduction of productivity (El-Sayed et al., 1990).

1.3.5 VARIABLE EFFECTS

The impact of UV-B on phytoplankton has been found to show a considerable amount of variation from one species to another (Karentz et al., 1991a; Davidson and Marchant, 1994; Karentz, 1994) and it has been suggested that this may result in a species shift within assemblages (Worrest et al., 1978; Karentz, 1991; Davidson and Marchant, 1994). It is difficult to determine how this will effect communities on a whole. An alteration of the community composition could significantly impact successional patterns and primary producer-consumer trophodynamics (Worrest et al., 1981). However, due to the short life cycle of phytoplankton, such changes would be expected to occur relatively quickly, and pre-ozone hole data are scarce. Inter- and intra-annual variability in species composition is also very high, so that even if pre-ozone hole data were available, comparisons would be difficult (Karentz, 1994). A significant finding for the Ross Sea is that *Phaeocystis* has been found to have a lower tolerance to increases in UV-B than diatoms in other Antarctic regions (Karentz and Spero, 1995) and in culture

experiments (Davidson and Marchant, 1994; Karentz, 1994) This could result in a shift away from *Phaeocystis* dominance toward diatom dominance with increased UV-B levels and the concomitant alteration of the extant food web.

2. MATERIALS AND METHODS

The determination of the potential impact of UV-B on Ross Sea phytoplankton was addressed in three ways. Firstly, surface measurements of photosynthetically active radiation (PAR) and four UV-B wavelengths were recorded throughout the two cruises. Secondly, on most days a profiling radiometer was deployed at approximately local noon to measure the underwater light field, again in the PAR and four UV-B wavelength regions. Thirdly, a series of experiments were carried out in which natural phytoplankton assemblages were exposed to varying levels of UV-B radiation for 24 hours or several days (up to 7 days). During these experiments chlorophyll, pigments, primary productivity, cell abundances, and in 1995/96, photosynthetic parameters, were measured at various time intervals to determine whether there was any differential response in these parameters to the different light regimes. In addition to the aforementioned data, some data from the wider group was incorporated into the analyses; integrated chlorophyll, particulate carbon, particulate nitrogen and productivity measurements were obtained from Walker Smith for comparison with light profiles. The methods for the various measurements are outlined below.

2.1 SAMPLE SITES

The first cruise of the Ross Sea Polynya Project (RSP^{2}94) took place in austral spring/summer of 1994 between November 10 and December 8. The second cruise (RSP^{2}95) was carried out in the austral summer of 1995/96 between December 16, 1995

and January 14, 1996. The sites occupied during the two cruises are shown in figures 2.1 and 2.2. The transect along 76° 30' S was occupied twice in the first cruise and three times during the second. These transects provided data on the temporal variations of the phytoplankton standing stocks. The northward transects yielded spatial information on the variations in phytoplankton biomass and assemblages within the polynya in relation to physical factors. Chlorophyll measurements were taken at all stations, and all other parameters (primary productivity, particulate carbon and nitrogen, light profiles, initiation of UV experiments) were determined at a subset of these stations. These measurements are summarized in tables 2.1 and 2.2.

2.2 LIGHT MEASUREMENTS

During both field seasons a Biospherical Instruments PUV (Profiling Ultraviolet Radiometer) 511 continuously recorded light levels from the ship's mast during each cruise, although instrument problems on the 1994 cruise resulted in some data gaps. The PUV 511 has 5 optical channels, four in the UV portion of the spectrum (308, 320, 340, and 380 nm) and one broad band PAR (Photosynthetically Active Radiation; 400-700 nm) channel. On the 1994 cruise these data were collected at 1 second intervals, and in 1995/96 at 10 second intervals. The PUV 500 is the underwater profiling component of the PUV package and has the same optical channels as the surface radiometer. The PUV 500 was deployed once per day at approximately local noon to a maximum depth of 80 m; care was taken to avoid the ship's shadow. The wire angle was also monitored carefully throughout the cast in an attempt to keep the instrument upright. Data files from

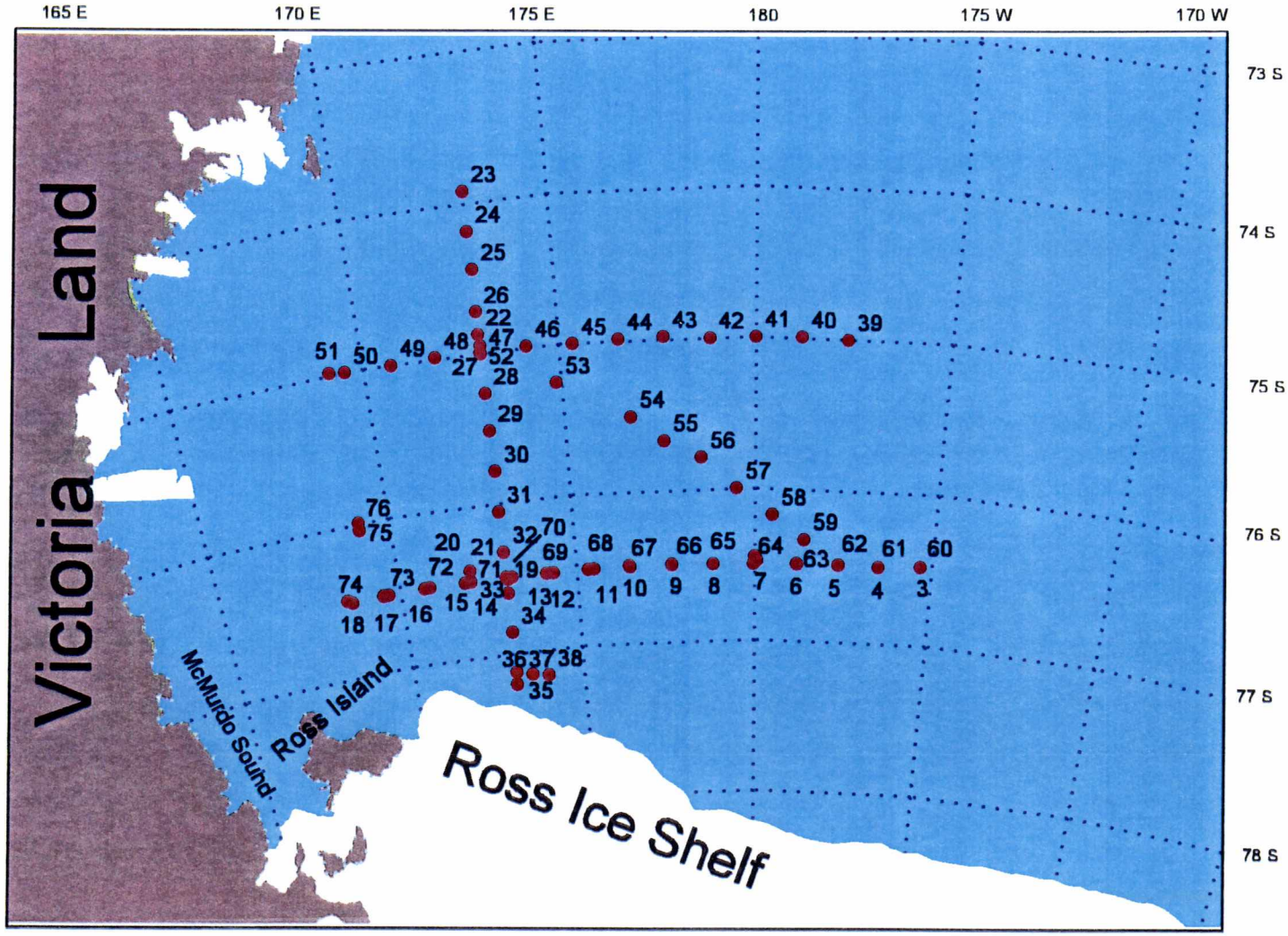

Figure 2.1 : Location of sampling stations for RSP^{2}94.

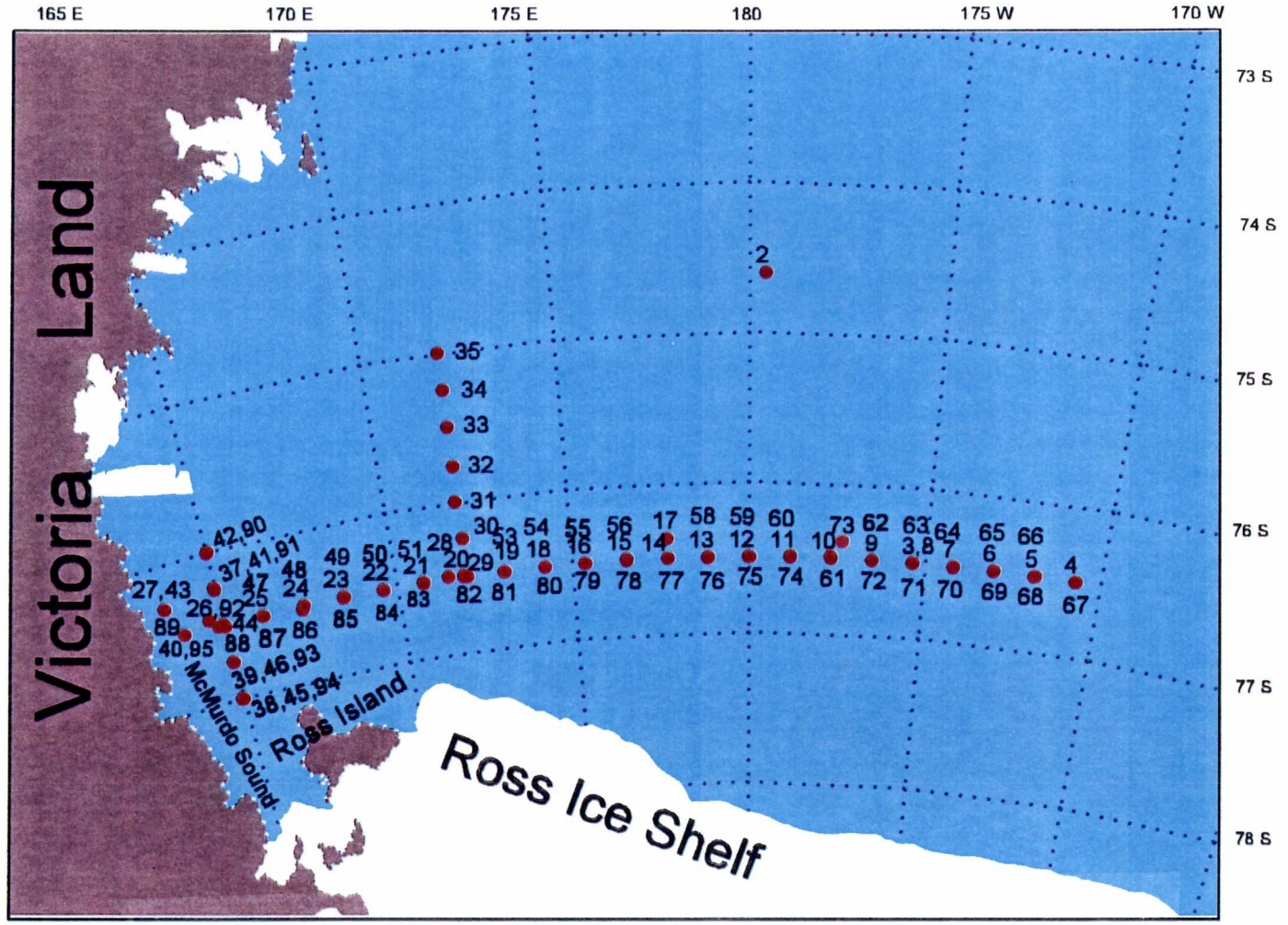

Figure 2.2 : Location of sampling stations for RSP^{2}95.

Table 2.1 : Summary of parameters measured at each station for RSP²94.

Station No.	Chl	Prod.	Exp.	PUV	C, N	Station No.	Chl	Prod.	Exp.	PUV	C, N
1	✓	✓				21	✓	✓			✓
2	✓				✓	22	✓				✓
3	✓				✓	23	✓	✓			✓
4	✓	✓			✓	24	✓				✓
5	✓	✓			✓	25	✓	✓			✓
6	✓				✓	26	✓		✓	✓	
7	✓	✓		✓	✓	27	✓	✓			✓
8	✓				✓	28	✓				
9	✓	✓		✓	✓	29	✓	✓			✓
10	✓				✓	30	✓	✓			✓
11	✓	✓			✓	31	✓	✓		✓	✓
12	✓				✓	32	✓				✓
13	✓	✓	✓	✓	✓	33	✓	✓			✓
14	✓				✓	34	✓				✓
15	✓	✓			✓	35	✓	✓			✓
16	✓	✓				36	✓	✓	✓	✓	✓
17	✓	✓			✓	37	✓	✓			✓
18	✓	✓		✓	✓	38	✓	✓	✓	✓	✓
19	✓	✓	✓	✓	✓	39	✓	✓		✓	✓
20	✓	✓			✓	40	✓				

Note : Checks indicate where a particular parameter was measured. Chl= Fluorometric chlorophyll, Prod= ^{14}C Primary productivity, Exp.= Experimental incubations, PUV=PUV500 Profiler deployed, C,N= Particulate carbon and nitrogen.

Table 2.1 : Continued.

Station No.	Chl	Prod.	Exp.	PUV	C, N
41	✓	✓			✓
42	✓				
43	✓	✓			✓
44	✓			✓	✓
45	✓	✓			✓
46	✓				
47	✓	✓		✓	✓
48	✓				
49	✓	✓			
50	✓				
51	✓	✓			
52	✓	✓			
53	✓	✓		✓	✓
54	✓	✓			✓
55	✓				
56	✓	✓			✓
57	✓			✓	
58	✓	✓			
59	✓				
60	✓	✓		✓	✓

Station No.	Chl	Prod.	Exp.	PUV	C, N
61	✓				✓
62	✓	✓			✓
63	✓				✓
64	✓	✓			✓
65	✓			✓	✓
66	✓	✓			✓
67	✓				✓
68	✓	✓			✓
69	✓				✓
70	✓	✓		✓	✓
71	✓				✓
72	✓	✓			✓
73	✓				✓
74	✓	✓			✓
75	✓	✓		✓	✓
76	✓				✓
77	✓	✓			✓

Table 2.2 : Summary of parameters measured at each station for RSP²95 [abbreviations as in Table 2.1].

Station No.	Chl	Prod.	Exp.	PUV	C, N	Station No.	Chl	Prod.	Exp.	PUV	C, N
1	✓	✓			✓	25	✓	✓			✓
2	✓	✓		✓	✓	26	✓	✓	✓		✓
3	✓	✓	✓		✓	27	✓			✓	
4	✓	✓		✓	✓	28	✓	✓			✓
5	✓	✓			✓	29	✓			✓	
6	✓					30	✓				✓
7	✓	✓		✓	✓	31	✓	✓			✓
8	✓					32	✓	✓			
9	✓	✓			✓	33	✓				✓
10	✓	✓			✓	34	✓	✓			
11	✓					35	✓	✓			✓
12	✓	✓		✓	✓	36	✓	✓		✓	✓
13	✓	✓	✓			37	✓				
14	✓	✓			✓	38	✓				
15	✓					39	✓				
16	✓	✓		✓	✓	40	✓	✓			✓
17	✓	✓		✓	✓	41	✓			✓	
18	✓	✓			✓	42	✓	✓			✓
19	✓					43	✓	✓			✓
20	✓	✓			✓	44	✓	✓			✓
21	✓	✓	✓	✓	✓	45	✓				
22	✓	✓			✓	46	✓				
23	✓	✓			✓	47	✓	✓			✓
24	✓			✓		48	✓			✓	✓

Table 2.2 : Continued.

Station No.	Chl	Prod.	Exp.	PUV	C, N
49	✓	✓			✓
50	✓				✓
51	✓				
52	✓				✓
53	✓				
54	✓	✓			✓
55	✓				✓
56	✓	✓	✓	✓	✓
57	✓				✓
58	✓	✓			✓
59	✓				✓
60	✓				
61	✓	✓			✓
62	✓				✓
63	✓			✓	
64	✓				✓
65	✓	✓			✓
66	✓				✓
67	✓				
68	✓	✓			✓
69	✓				
70	✓	✓		✓	✓
71	✓	✓	✓		✓
72	✓	✓			✓
73	✓	✓			✓
74	✓	✓	✓	✓	✓
75	✓	✓			✓
76	✓	✓			✓
77	✓	✓			✓
78	✓	✓		✓	✓
79	✓	✓			✓
80	✓	✓			✓
81	✓	✓			✓
82	✓	✓			
83	✓			✓	✓
84	✓	✓			✓
85	✓	✓			✓
86	✓	✓	✓		✓
87	✓	✓		✓	✓
88	✓	✓			✓
89	✓	✓			✓
90	✓	✓			✓
91	✓	✓		✓	
92	✓	✓			✓
93	✓				
94	✓				
95	✓				

the PUV instruments were later converted to comma separated value files and imported into Microsoft Excel for analysis.

On the 1995/96 cruise a Biospherical Instruments QSR 240 PAR sensor was installed near the incubators to continuously record PAR levels. Recordings were taken at 60 second intervals. The binary data files were imported into Microsoft Excel for analysis and converted to $\mu E\ m^{-2}\ s^{-1}$ and quanta $m^{-2}\ s^{-1}$ using the calibration coefficients provided by Biospherical Instruments.

2.3 UV-B INCUBATIONS

On RSP^{2}94 six UV-B incubations were carried out, and eight were conducted during RSP^{2}95. All UV-B incubations were carried out using Whirlpak polyethylene bags, which are optically clear to UV wavelengths as well as to photosynthetically active radiation (Prezelin et al., 1994). Each bag was rinsed three times in dilute (5%) hydrochloric acid (HCl) and then three times in NANOpure water (>= 18.3 megohm-cm purity with organic filters and final 0.2 µm filter) before use. Water from Niskin bottles was dumped into carboys and the bags were filled from these. Bags were then taped closed to ensure sample integrity.

UV incubations were run for either 24- h or 5 - 8 days under three different light regimes. UV-transparent plexiglas (UVT) was used for 'total light', and two different mylar screens plus UVT were used to give a 'partial UV-B penetration' and 'total exclusion of UV-B' regimes. The transmission and absorption spectra for the two mylar

screens can be seen in figure 2.3. Subsamples from 24-h incubations were taken for fluorometric chlorophyll, HPLC pigments, taxonomic observations and ^{14}C productivity (the latter two taken at the end of the experiment only, while others were measured at 6, 12, 18 and 24 h). For the 5-day incubations chlorophyll was measured each day and pigments, ^{14}C productivity, and species composition measured on days 3 and 5 (photosynthetic parameters were also determined for days 3 and 5 for experiments D and G during RSP^{2}95).

2.4 WATER COLLECTION

Water was collected primarily in Niskin bottles, either 10-l bottles on the CTD (Conductivity, Temperature, Depth) rosette or 30-l bottles which were hung individually on a wire. Some samples were collected using an acid-washed bucket to acquire surface water for characterization of the water column at stations where Profiling Ultraviolet Radiometer (PUV) profiles were conducted but no CTD cast performed. Generally, water for UV experiments was collected using 30-l Niskins and mixed in a 50-l polyethylene carboy before being transferred to bottles or bags. Samples for chemical and biological variables (chlorophyll *a*, particulate organic carbon and nitrogen, nutrients)were collected from the CTD rosette from depths corresponding to 100, 50, 30, 15, 5, 1 and 0.1% of the surface irradiance. Two bottles were closed at each of the seven light depths and the remaining 10 bottles at 5 depths evenly spaced down to 150 meters.

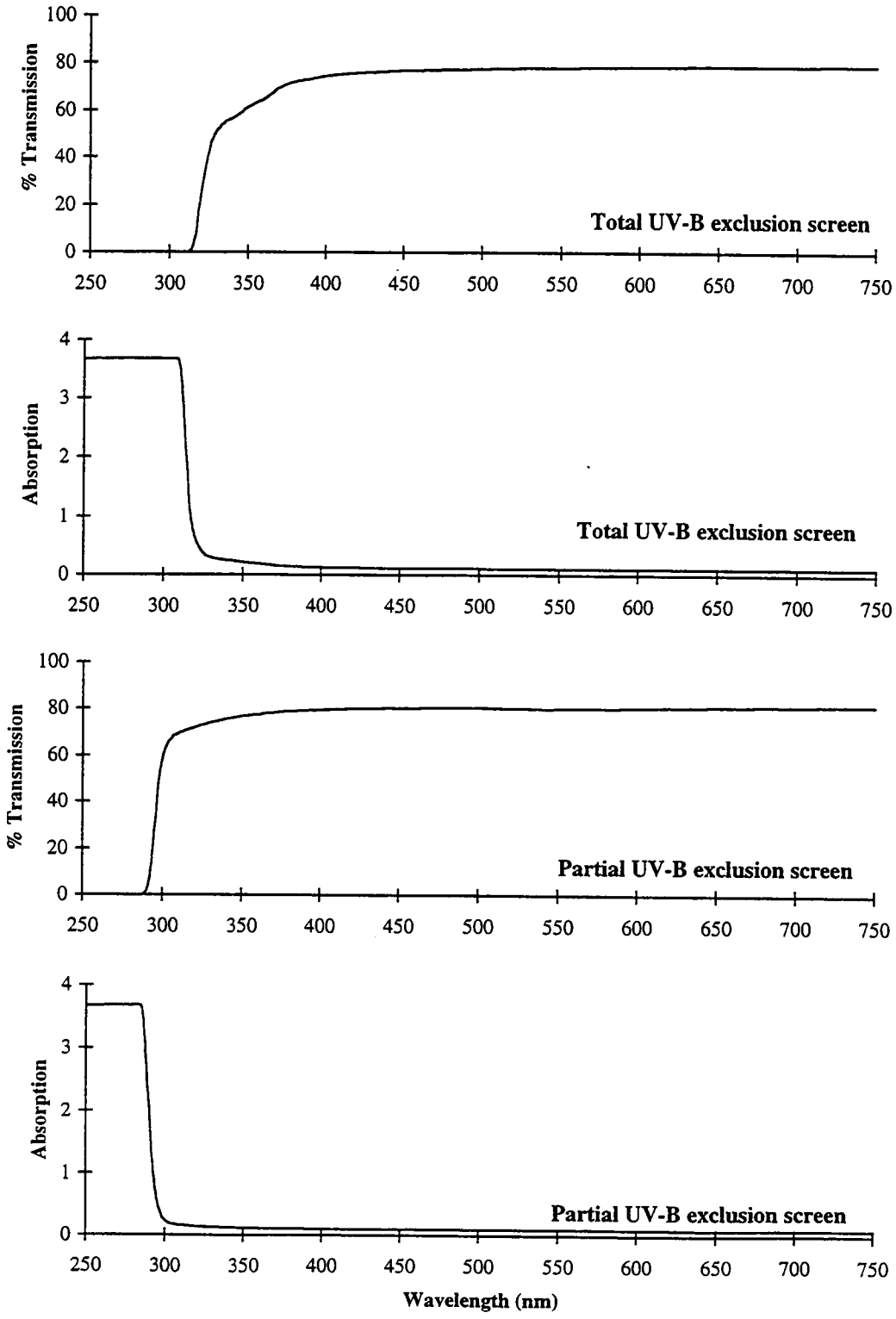

Figure 2.3 : Absorption and transmission spectra for mylar screens used in UV-B incubations.

2.5 CHLOROPHYLL *a*

Chlorophyll *a* concentrations were determined during UV-B experiments as well as for the water column at the stations indicated in Tables 1.1. and 1.2. Chlorophyll *a* was measured fluorometrically using a Turner Designs Fluorometer (Model AU:10). The fluorometer was calibrated at the beginning and end of the two cruises using commercially purified chlorophyll *a* (Sigma Chemicals). Samples of up to 280 ml were filtered onto 25 mm Whatman GF/F glass fiber filters and placed in 15 ml centrifuge tubes with 10 ml of 90% Acetone. The samples were then sonicated in an ice bath (the ice bath prevents heat degradation of the pigments) for 15 minutes followed by an extraction period of at least 10 minutes. On the 1994 cruise both chlorophyll *a* and phaeopigments were determined. Initial fluorescence (F_o) was measured, then 3 drops of 10% hydrochloric acid were added to the sample to convert chlorophyll to phaeopigments. A second fluorescence reading (F_a) was then taken. The concentration of chlorophyll was determined according to Equation 1, and the concentration of phaeopigments according to Equation 2, where K is the calibration factor determined for each fluorometer, V_{ext} is the volume in liters of acetone in which the sample is extracted, and V_{filt} is the volume in liters of water sample filtered. The factor 2.1 represents the theoretical maximum conversion of chlorophyll to phaeopigments.

$$\text{Chlorophyll } (\mu g\ L^{-1}) = \frac{K(F_o - F_a)(V_{ext})}{V_{filt}} \qquad (1)$$

$$\text{Phaeopigments}\left(\mu g\ L^{-1}\right) = \frac{K\left((2.1 \times F_a) - F_o\right)V_{ext}}{V_{filt}} \qquad (2)$$

On the 1995 cruise chlorophyll and phaeopigments were not separated. The extraction procedure was identical, but the acidification step was removed. The concentration of chlorophyll plus phaeopigments was then determined by Equation 3, where F is the fluorescence reading.

$$\text{Chlorophyll} + \text{Phaeopigments}\ (\mu g\ L^{-1}) = F \times \left(\frac{V_{ext}}{V_{filt}}\right) \qquad (3)$$

2.6 HPLC PIGMENTS

Samples for the determination of pigment concentrations by High Performance Liquid Chromatography (HPLC) were taken at various intervals during the UV-B experiments. These samples were filtered onto 25 mm Whatman GF/F filters with an approximate pore size of 0.7 μm. The volume filtered varied between 280 ml and 1000 ml depending on the phytoplankton concentrations (based on the color retained on the filter). The filters were then folded in half, wrapped in aluminium foil, placed in a cryovial, and frozen and stored in liquid nitrogen. Samples were shipped back to the University of Tennessee on dry ice and stored in an ultra-low freezer at -120 °C.

Filters were removed from foil and chopped with a razor blade into 5 to 6 pieces to aid grinding and pigment extraction. The filter pieces were then placed in a 10 ml glass pestle with 1 ml of 90% acetone. The pestle was capped with parafilm to prevent

evaporation, and the sample extracted for approximately half an hour on ice in darkness. The extracted sample was then ground with a hand drill pestle as quickly as possible, and the mortar placed in an ice bath holder to prevent heating while grinding. After grinding the pestle was rinsed with approximately 200 µl of 90% acetone to ensure that all the sample was retained. This was again extracted in the cold and dark for a minimum of 30 minutes.

Following the second extraction the sample was placed in a 1.5 ml gasket-capped cryovial. The cryovial was centrifuged at 14,000 rpm for 3 minutes to remove filter and cell fragments. To make the injection sample, a 2 part sample : 1 part water mixture was made. The total volume of sample (between 200 and 600 µl) varied according to the approximate amount of pigment on the filter. The injection sample was then placed in an 800 µl amber insert for an autosampler vial. Samples were kept cold and dark until ready to be placed in the autosampler for processing.

The HPLC buffer solution (Solvent A) was an 85 : 15, 100 % methanol : 0.5 M Ammonium acetate (aq) mixture. Solvent B was 100% HPLC grade Methanol and Solvent C was 100 % HPLC grade Acetone. Millennium software was used to control a Waters 600 Controller/pump, a Waters 717 Autosampler, a Waters Photodiode Array 996 and a Waters Scanning Fluorescence detector 474. Chromatograms were read at 440 nm and the column was an Alltech adsorbosphere HS C18 5V (150 mm x 4.6 mm).

2.7 PRIMARY PRODUCTIVITY

Rates of primary production were measured in UV experiments under the three different light regimes and also at the stations indicated in Tables 1.1 and 1.2 for the water column. Primary productivity was determined by measuring the uptake of radiolabeled bicarbonate (Smith and Nelson, 1990). For the water column measurements, samples were placed in simulated in situ conditions using neutral density screens to simulate the light depths from which the samples were taken. For the UV experiments, samples were placed under the three different UV-B regimes. Samples of approximately 280 ml (or 500 ml for some UV experiments) were drawn into either bottles or Whirlpak bags, and approximately 20 μCi of $H^{14}CO_3$ (40 μCi for the larger volume) were added. Samples were then placed in on-deck incubators which were kept at in situ temperatures via surface water circulating through the incubators. All incubations were ended after 24 hours (or 3 and 5 days for the long term UV-B experiments) by filtering the entire sample through a Whatman GF/F 25 mm diameter glass fiber filter. Before the final few milliliters of sample were filtered, the filter funnel was rinsed with approximately 5 ml of 0.01 N HCl in seawater to remove inorganic carbonates (Goldman and Dennett, 1985). Each filter was then placed in a scintillation vial and dried at 60°C for at least 24 hours, after which 6 ml of Ecolume (ICN) were added. Three lots of 500 μl were taken from the incubated samples for totals; the sample was put into a scintillation vial along with 6 ml Ecolume. The samples were counted on a Beckman 3600 series scintillation counter and quenching was corrected for using the external standards method. Productivity was then calculated using equations 3 and 4 below.

$$DPM_{ta} = CPM_{tot} \times \left(\frac{2}{E_{tot}} \right) \quad (4)$$

$$\text{Productivity} \left(\text{mg C m}^{-3} \text{ d}^{-1} \right) = \frac{24{,}000 \times 1.05 \times \left[\left(\frac{V_{inc}}{V_f} \right) \times CPM_f \right]}{t \times DPM_{ta} \times E_f} \quad (5)$$

where CPM_{tot} is the average of the three total determinations taken per station, E_{tot} is the average efficiency for those three total determinations, 1.05 is an isotope discrimination factor, 24,000 is the amount of inorganic carbon in seawater (mg m^{-3}), V_f and V_{inc} are the volumes (ml) filtered and incubated, CPM_f is the measured CPMs from the filter at each depth, t the incubation time in h, and E_f the efficiency determined for that filter from the quench curve.

2.8 PHOTOSYNTHETIC PARAMETERS

Productivity (P) vs. irradiance (I) reponses were assessed using a modification of the 'photosynthetron' method of Lewis and Smith (1983). P/I responses were measured for the three UV levels in the long term (5-day) UV experiments on days 3 and 5 on the second cruise only. The photosynthetic parameters, α, β, P_{max}, and I_k (see figure 2.5 for definition of these parameters) were determined through the use of Platt et al.'s (1982) equations 1 and 3 (see Equations 5 and 6 below) using Axum software to fit the data to the model.

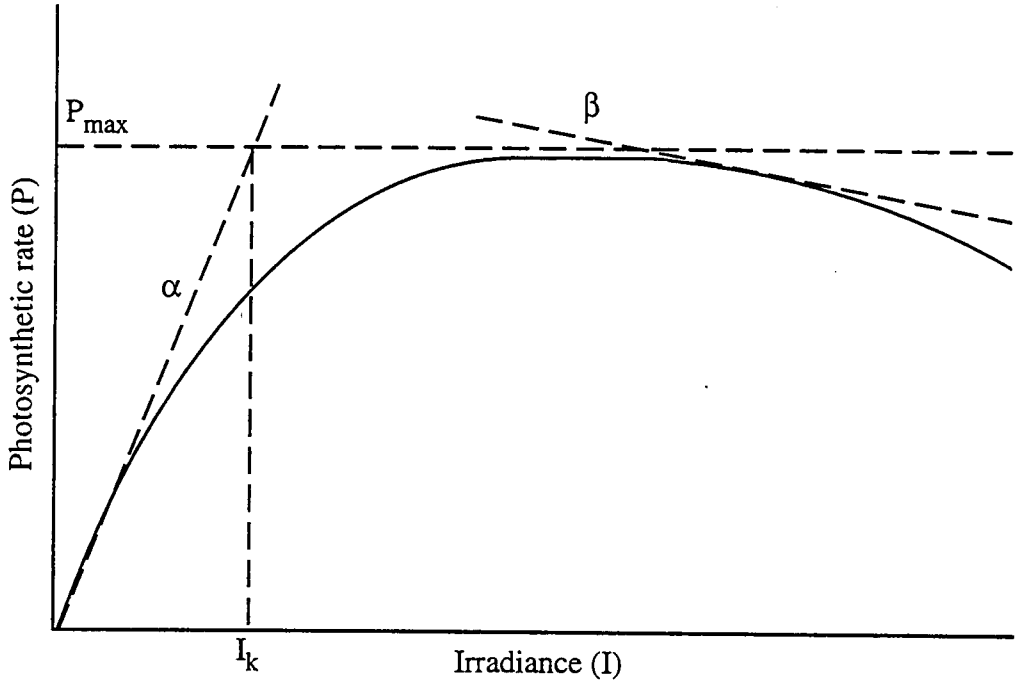

Figure 2.4 Idealised curve of specific photosynthetic rate (P) as a function of irradiance (I), illustrating the photosynthetic parameters. α = the initial slope of the P vs. I curve, P_{max} = the maximum photosynthetic rate, I_k = the saturation onset parameter, and β = the index of photoinhibition.

$$P^B = P_S^B\left[1 - e^{\frac{-\alpha I}{P_S^B}}\right] \times e^{\frac{-\beta I}{P_S^B}} \qquad (5)$$

$$P_m^B = P_S^B\left(\frac{\alpha}{\alpha+\beta}\right)\left(\frac{\beta}{\alpha+\beta}\right)^{\beta/\alpha} \qquad (6)$$

2.9 MICROSCOPIC ANALYSIS

Samples for microscopy were taken during UV-B experiments and also from surface waters at some PUV profile stations to characterize the phytoplankton present. Whole water samples were preserved using one of three fixatives. Some samples were preserved using Lugol's Iodine solution, (approximately 2 ml in 250 ml; Sherr and Sherr, 1993). A modified Lugol's containing 35‰ v/v glutaraldehyde was used for samples containing predominantly *Phaeocystis*, as this has been found to give better preservation of the colonial matrix (Rousseau et al., 1990). These samples were stored in glass bottles and shipped back to the University of Tennessee, Knoxville, for analysis. Other samples were preserved using 50% glutaraldehyde (1 ml per 100 ml seawater). These were then stained with 4',6-diamidino-2-phenylindole (DAPI), which stains DNA such that it fluoresces blue under UV (365 nm) excitation. Samples were then filtered onto 0.8 μm black Poretic filters and placed onto a drop of immersion oil on a microscope slide. Another drop of oil was placed over the filter, which was covered with a glass coverslip. The slides were then frozen. Paraffin wax was used to seal the slide

around the edge of the coverslip to prevent dehydration, and all slides were kept frozen until analysis.

Whole water samples preserved in either Lugol's solution or glutaraldehyde modified Lugol's were settled for a minimum of 6 hours (Utermohl, 1958). The phytoplankton in a minimum of 60 fields of view were counted to give a total of not less than 300 cells. The following equation was then used to determine cell concentration :

$$\text{Abundance (cells L}^{-1}) = \frac{\frac{Cells_{tot}}{FOV_{counted}} \times FOV_{total}}{V_{settled}} \times 1000 \qquad (7)$$

Where $Cells_{tot}$ is the total number of cells counted, $FOV_{counted}$ is the number of fields of view which were enumerated, FOV_{total} is the total number of fields of view in the settling chamber and $V_{settled}$ is the volume of sample settled in liters. Glutaraldehyde fixed samples were observed using a Nikon Labophot-2 Y2F-EFD3 fluorescence microscope with a DAPI filter.

2.10 PARTICULATE CARBON AND NITROGEN

Particulate carbon and nitrogen was measured from Niskin bottles at the stations indicated in Table 1.1 and 1.2 for the water column. These measurements were compared with light PUV radiometer light profiles. Samples for determination of particulate carbon (POC) and nitrogen (PON) concentrations were filtered onto precombusted (450°C for 2 h) 25 mm Whatman GF/F glass fiber filters. Each filter was rinsed with 5-10 ml 0.01 N

HCl in filtered seawater to remove any inorganic carbonates. Filters were then placed in combusted shell vials, covered with combusted foil and dried at 60 °C (Nelson et al., 1989). The vials were then stored in a dessicator prior to shipping. On return to the University of Tennessee the samples were analyzed on a Carlo Erba Instruments CHN EA1108 Elemental Analyzer. Corrections for absorption of dissolved organic carbon and nitrogen by the filter were made by subtracting values from a second filter placed beneath the primary filter and processed identically at the surface and deepest samples for each station. These corrections were typically small, but not negligible. Approximate limits of detection were 0.5 and 0.1 $\mu mol\ l^{-1}$ for carbon and nitrogen, respectively.

3. RESULTS

3.1 DAILY IRRADIANCES

Light concentrations for both RSP[2] cruises varied considerably due to large variations in cloud cover. Problems occurred in the collection of the 1994 PUV 511 light measurements which resulted in many gaps in the data set. As a consequence, daily averages and integrated daily irradiances for both years were determined via the equations of Legendre et al. (1993), which assume constant weather conditions and take into account latitude, solar declination and the fact that at latitudes > 66° 33' S, the sun does not go below the horizon between the 21st of September and the 21st of March. The solar elevation (β) for a given latitude (γ) and solar declination (δ) is a function of the time of the day (t: 0 to 24 h) and was determined using the following relationship:

$$\beta_\tau = \sin^{-1}(c_1 - c_2 \cos\tau) \qquad (8)$$

where $c_1 = \sin\gamma \sin\delta$, $c_2 = \cos\gamma \cos\delta$, and $\tau = 360°$ (t/24 h). Values for δ were obtained from Anon. (1994, 1995 and 1996). The daily irradiance was then calculated from the following equation:

$$Q_s = \left(\frac{86400}{\beta_\tau}\right)\left[\left(1-\frac{2}{\pi}\right)\sin^{-1}(c_1 - c_2) + \left(\frac{2}{\pi}\right)\sin^{-1}(c_1 + c_2)\right]E_t \qquad (9)$$

where Q_s is the daily solar radiation, 86400 is the daylength (s), and E_t is the irradiance measured at any time t during the day. The assumption of constant weather was rarely met in the Ross Sea and resulted in over-estimates on some days and underestimates on others This can be seen in the scatter when the model approximation was compared with the two other sensors for the 1995 data set (Appendix B). Estimated average and integrated daily irradiances for both cruises determined by the Legendre et al. (1993) equations are found in Tables 3.1 and 3.2. The 1995 data collection from the PUV 511 had only two small gaps, and these data are compared to the model approximations and to the PAR data from the QSR 240 in table 3.3 and figure 3.1. The PUV 511 and the QSR 240 were quite consistent, although the QSR 240 consistently measured higher irradiances. Maximum integrated PAR levels in 1995 were higher than those in 1994, although averaged over the cruise total PAR levels were similar, with 1994 having a slightly higher average integrated irradiance. UV levels were similar for the two cruises, although on average were higher in 1995 for all wavelengths except 340 nm.

3.2 OZONE CONCENTRATIONS

SBUV-2 (Solar Backscatter Ultraviolet instrument) satellite images from the NOAA-14 satellite show the variation in ozone concentration over the Antarctic continent from the beginning to the end of the 1994 cruise (Figures 3.2 and 3.3). The November 12 image shows a very distinct ozone hole which is centered over the Antarctic peninsula and the December 8 image indicates that ozone concentrations had greatly increased by this date. 1994 ozone concentrations varied between approximately 180 and 330 dobson units during the cruise. For the 1995 spring/summer, TOVS (TIROS Operational Vertical Sounder) images from the NOAA-10 satellite show the progression of ozone depletion

Table 3.1 : Average and integrated irradiances for RSP²94 determined by the model of Legendre et al. (1993) from mid-day irradiances.

Date	Stn #	PAR		308 nm		320 nm		340 nm		380 nm	
		Average (μEin $m^{-2} s^{-1}$)	Integrated (Ein $m^{-2} d^{-1}$)	Average (μW $cm^{-2} nm^{-1}$)	Integrated	Average (μW $cm^{-2} nm^{-1}$)	Integrated	Average (μW $cm^{-2} nm^{-1}$)	Integrated	Average (μW $cm^{-2} nm^{-1}$)	Integrated
14-Nov	7	511.28	44.17	0.564	4.87E+04	56.04	4.84E+06	211.35	1.83E+07	222.55	1.92E+07
15-Nov	9	529.26	45.73	0.871	7.52E+04	60.69	5.24E+06	220.48	1.90E+07	231.54	2.00E+07
16-Nov	13	380.28	32.86	0.618	5.34E+04	45.96	3.97E+06	168.54	1.46E+07	177.39	1.53E+07
17-Nov	18	669.37	57.83	1.041	8.99E+04	86.51	7.47E+06	314.94	2.72E+07	332.23	2.87E+07
18-Nov	19	417.99	36.11	0.745	6.44E+04	53.27	4.60E+06	195.89	1.69E+07	206.09	1.78E+07
21-Nov	26	660.57	57.07	1.218	1.05E+05	77.56	6.70E+06	274.59	2.37E+07	289.53	2.50E+07
22-Nov	31	590.32	51.00	1.476	1.27E+05	90.46	7.82E+06	321.92	2.78E+07	339.83	2.94E+07
23-Nov	36	427.70	36.95	1.114	9.63E+04	82.86	7.16E+06	300.09	2.59E+07	313.13	2.71E+07
25-Nov	38	557.53	48.17	1.282	1.11E+05	94.49	8.16E+06	351.19	3.03E+07	371.42	3.21E+07
26-Nov	39	489.75	42.31	1.130	9.77E+04	77.25	6.67E+06	276.26	2.39E+07	290.19	2.51E+07
27-Nov	44	546.20	47.19	1.282	1.11E+05	85.35	7.37E+06	305.53	2.64E+07	321.11	2.77E+07
28-Nov	47	708.97	61.25	1.299	1.12E+05	95.72	8.27E+06	354.09	3.06E+07	376.48	3.25E+07
30-Nov	53	873.00	75.43	1.725	1.49E+05	127.10	1.10E+07	470.37	4.06E+07	500.99	4.33E+07
1-Dec	57	786.39	67.94	2.101	1.82E+05	130.91	1.13E+07	476.44	4.12E+07	506.17	4.37E+07
2-Dec	60	897.85	77.57	2.952	2.55E+05	180.06	1.56E+07	634.29	5.48E+07	670.86	5.80E+07
3-Dec	65	310.74	26.85	1.016	8.77E+04	63.35	5.47E+06	224.66	1.94E+07	236.46	2.04E+07
4-Dec	70	349.66	30.21	1.270	1.10E+05	74.82	6.46E+06	265.26	2.29E+07	279.19	2.41E+07
6-Dec	75	689.17	59.54	2.081	1.80E+05	117.47	1.01E+07	423.70	3.66E+07	446.09	3.85E+07
Mean		577.56	49.90	1.321	1.14E+05	88.88	7.68E+06	321.64	2.78E+07	339.51	2.93E+07
St. deviation		172.26	14.88	0.589	5.09E+04	33.07	2857166.44	117.69	1.02E+07	125.34	1.08E+07

Table 3.2 : Average and integrated irradiances for RSP²95 determined by the model of Legendre et al. (1993) from mid-day irradiances.

Date	Stn #	PAR		308 nm		320 nm		340 nm		380 nm	
		Average (μEin m^{-2} s^{-1})	Integrated (Ein m^{-2} d^{-1})	Average (μW cm^{-2} nm^{-1})	Integrated	Average (μW cm^{-2} nm^{-1})	Integrated	Average (μW cm^{-2} nm^{-1})	Integrated	Average (μW cm^{-2} nm^{-1})	Integrated
22-Dec	7	198.64	17.16	1.369	1.18E+05	52.22	4.51E+06	94.91	8.20E+06	231.61	2.00E+07
23-Dec	12	853.02	73.70	5.321	4.60E+05	166.03	1.43E+07	313.23	2.71E+07	755.86	6.53E+07
24-Dec	16	882.56	76.25	4.065	3.51E+05	167.14	1.44E+07	326.29	2.82E+07	799.46	6.91E+07
26-Dec	17	354.03	30.59	2.072	1.79E+05	85.58	7.39E+06	159.54	1.38E+07	388.45	3.36E+07
27-Dec	21	890.01	76.90	2.974	2.57E+05	155.17	1.34E+07	315.09	2.72E+07	758.79	6.56E+07
28-Dec	24	483.76	41.80	2.224	1.92E+05	118.83	1.03E+07	227.22	1.96E+07	553.24	4.78E+07
29-Dec	27	915.12	79.07	3.119	2.69E+05	160.88	1.39E+07	325.98	2.82E+07	788.58	6.81E+07
30-Dec	29	809.52	69.94	3.590	3.10E+05	148.38	1.28E+07	291.86	2.52E+07	707.46	6.11E+07
1-Jan	36	889.66	76.87	3.902	3.37E+05	149.56	1.29E+07	300.27	2.59E+07	724.35	6.26E+07
3-Jan	41	288.97	24.97	1.415	1.22E+05	60.80	5.25E+06	115.43	9.97E+06	282.65	2.44E+07
5-Jan	48	484.73	41.88	2.643	2.28E+05	113.67	9.82E+06	211.54	1.83E+07	515.94	4.46E+07
5-Jan	56	1024.09	88.48	3.638	3.14E+05	155.57	1.34E+07	313.52	2.71E+07	753.77	6.51E+07
7-Jan	63	240.39	20.77	1.427	1.23E+05	60.06	5.19E+06	109.90	9.50E+06	268.62	2.32E+07
8-Jan	70	227.65	19.67	1.556	1.34E+05	58.57	5.06E+06	106.38	9.19E+06	259.76	2.24E+07
9-Jan	74	364.66	31.51	2.434	2.10E+05	81.07	7.00E+06	147.41	1.27E+07	360.25	3.11E+07
10-Jan	78	387.38	33.47	2.437	2.11E+05	88.05	7.61E+06	161.33	1.39E+07	393.83	3.40E+07
11-Jan	83	742.07	64.12	3.279	2.83E+05	127.41	1.10E+07	248.33	2.15E+07	602.35	5.20E+07
12-Jan	87	412.97	35.68	2.161	1.87E+05	87.60	7.57E+06	163.49	1.41E+07	399.46	3.45E+07
13-Jan	91	424.45	36.67	1.832	1.58E+05	82.30	7.11E+06	157.00	1.36E+07	384.44	3.32E+07
Mean		572.30	49.45	2.708	2.34E+05	111.52	9.64E+06	215.20	1.86E+07	522.57	4.52E+07
St. deviation		280.87	24.27	1.070	9.24E+04	41.22	3.56E+06	85.72	7.41E+06	206.06	1.78E+07

Table 3.3 Comparison of two PAR sensors and the Legendre et al. (1993) model approximation of integrated daily irradiance for RSP²95.

Date	PAR (Ein $m^{-2} s^{-1}$)		
	Model	PUV 511	QSR240
Dec-22	17.16		12.94
Dec-23	73.70	54.14	69.91
Dec-24	76.25	62.99	80.09
Dec-25		54.80	68.22
Dec-26	30.59	25.09	25.06
Dec-27	76.90	64.12	68.36
Dec-28	41.80	39.64	30.97
Dec-29	79.07	47.47	57.51
Dec-30	69.94	58.14	71.94
Dec-31		45.82	
Jan-1	76.87	45.65	48.29
Jan-2		41.53	43.00
Jan-3	24.97	29.10	30.34
Jan-4	41.88	44.36	50.53
Jan-5	88.48	35.55	41.72
Jan-6		36.37	50.51
Jan-7	20.77	19.17	17.74
Jan-8	19.67	33.58	37.92
Jan-9	31.51	23.49	24.09
Jan-10	33.47	39.24	
Jan-11	64.12	47.52	75.82
Jan-12	35.68	35.56	48.09
Jan-13	36.67	44.34	52.88
Jan-14		27.77	27.75
average	49.45	41.54	46.99

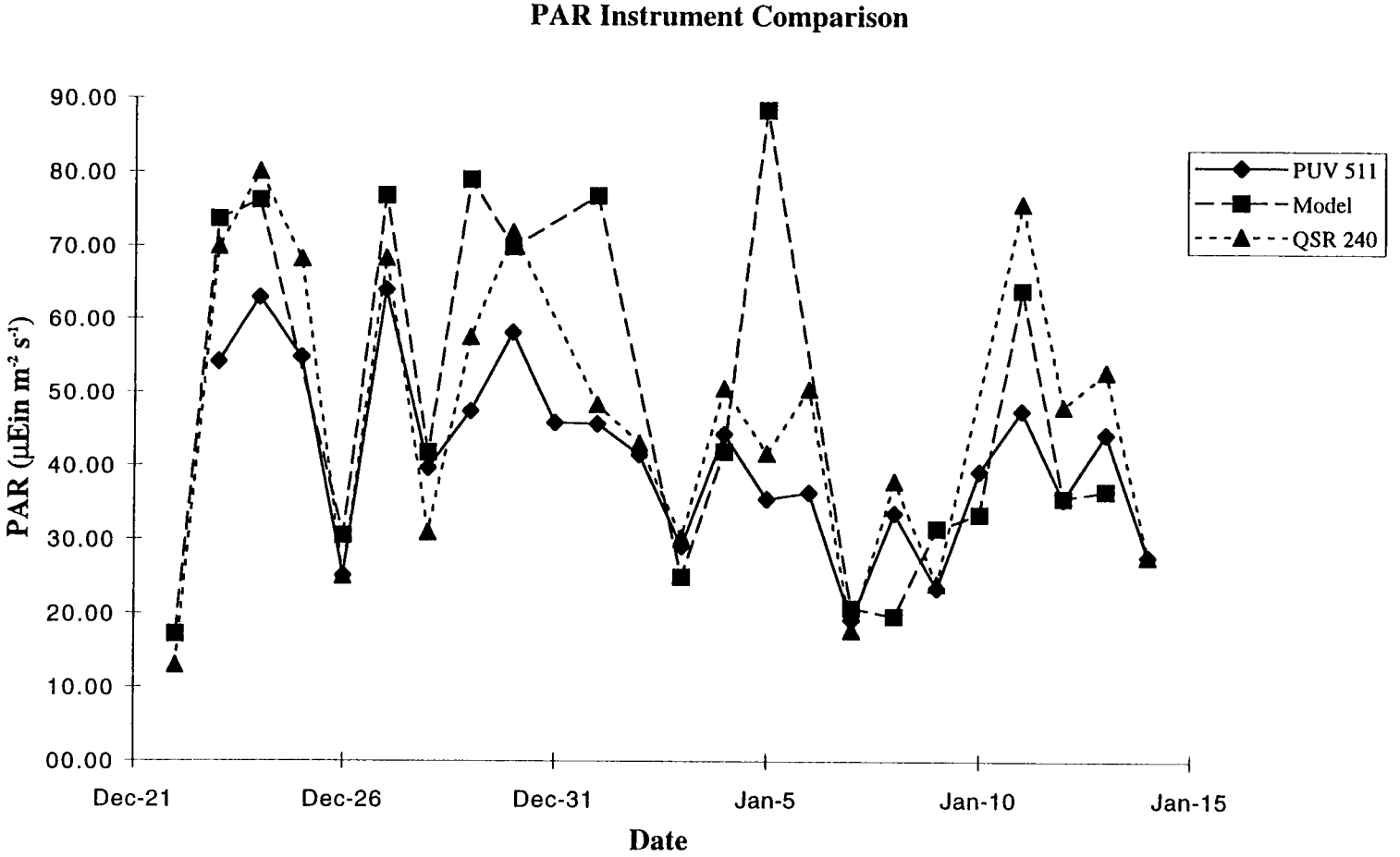

Figure 3.1 PAR as measured by two radiometers and approximated from midday irradiances by the Legendre et al. (1993) model. Note that the model displays the greatest variability.

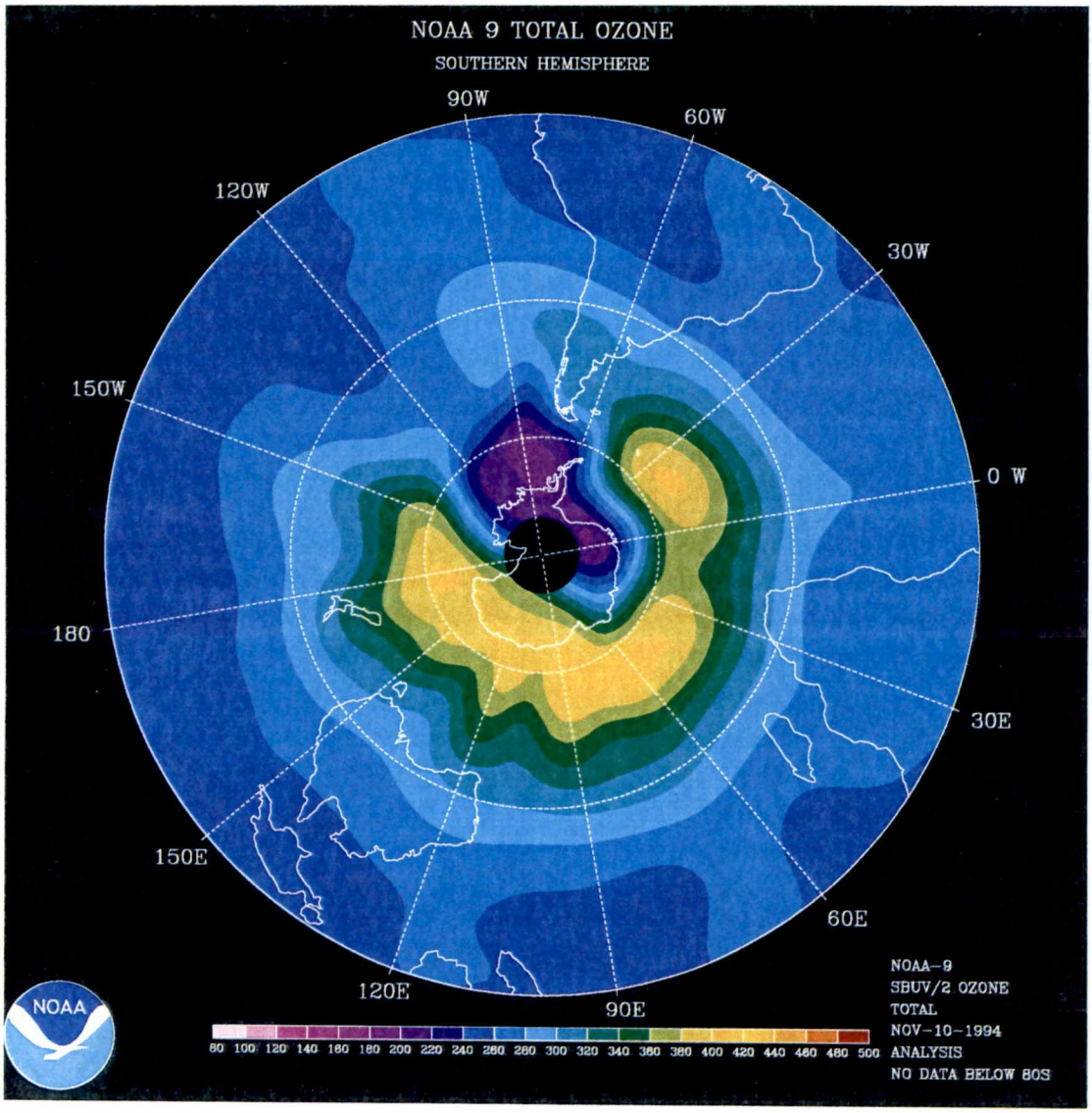

Figure 3.2 Ozone concentrations over the Antarctic continent on the 10th of November, 1994 (in dobson units).

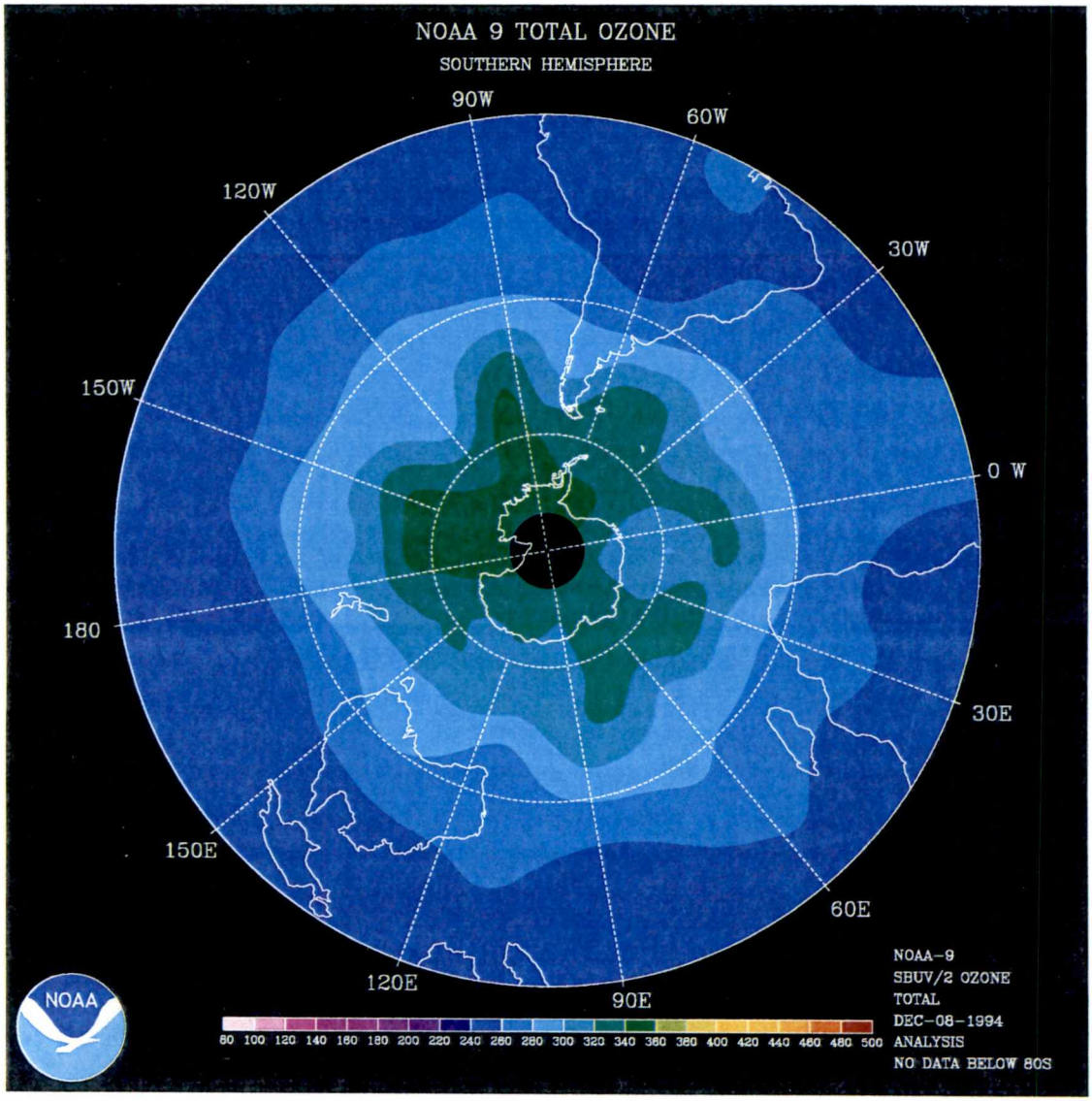

Figure 3.3 Ozone concentrations over the Antarctic continent on the 8th of December, 1994 (in dobson units).

over the Antarctic continent (Figures 3.4 - 3.7), with figures 3.6 and 3.7 marking the beginning and the end of the 1995 cruise, respectively. Dramatic increases in ozone concentrations can be seen from November to January. Ozone concentrations over the study area for the 1995 cruise varied between 275 and 330 dobson units (Figure 3.8). Ozone concentrations in 1995 spring/summer were much higher than in the spring of 1994.

3.3 PROFILING ULTRAVIOLET RADIOMETER PROFILES

Light profiles for PAR, two UV-A wavelengths (340 nm and 380 nm) and two UV-B wavelengths (308 nm and 320 nm) were measured at 18 stations in 1994 and 21 stations in 1995 (Figures 3.9 and 3.10 show these station locations). The penetration of all wavelengths of light into the water column showed great variation throughout the polynya for both years, with 308 nm penetrating to a maximum depth of 16 m in 1994 and 14 m in 1995/96, whereas the other UV-B waveband (320 nm) penetrated to 34 m and 27 m in 1994 and 1995/96, respectively (Figure 3.11). Vertical attenuation coefficients (K) were calculated for the five wavebands at all PUV profile stations using equation 10 :

$$K = \frac{1}{z} \times \ln\left(\frac{I_o}{I_d(z)}\right) \qquad (10)$$

where $I_d(z)$ and I_o are the values of downwelling irradiance at a depth of z meters and just below the surface (subsurface), respectively. Figures 3.12 and 3.13 show two extremes of light penetration, with figure 3.12 having high K values and figure 3.13 much lower

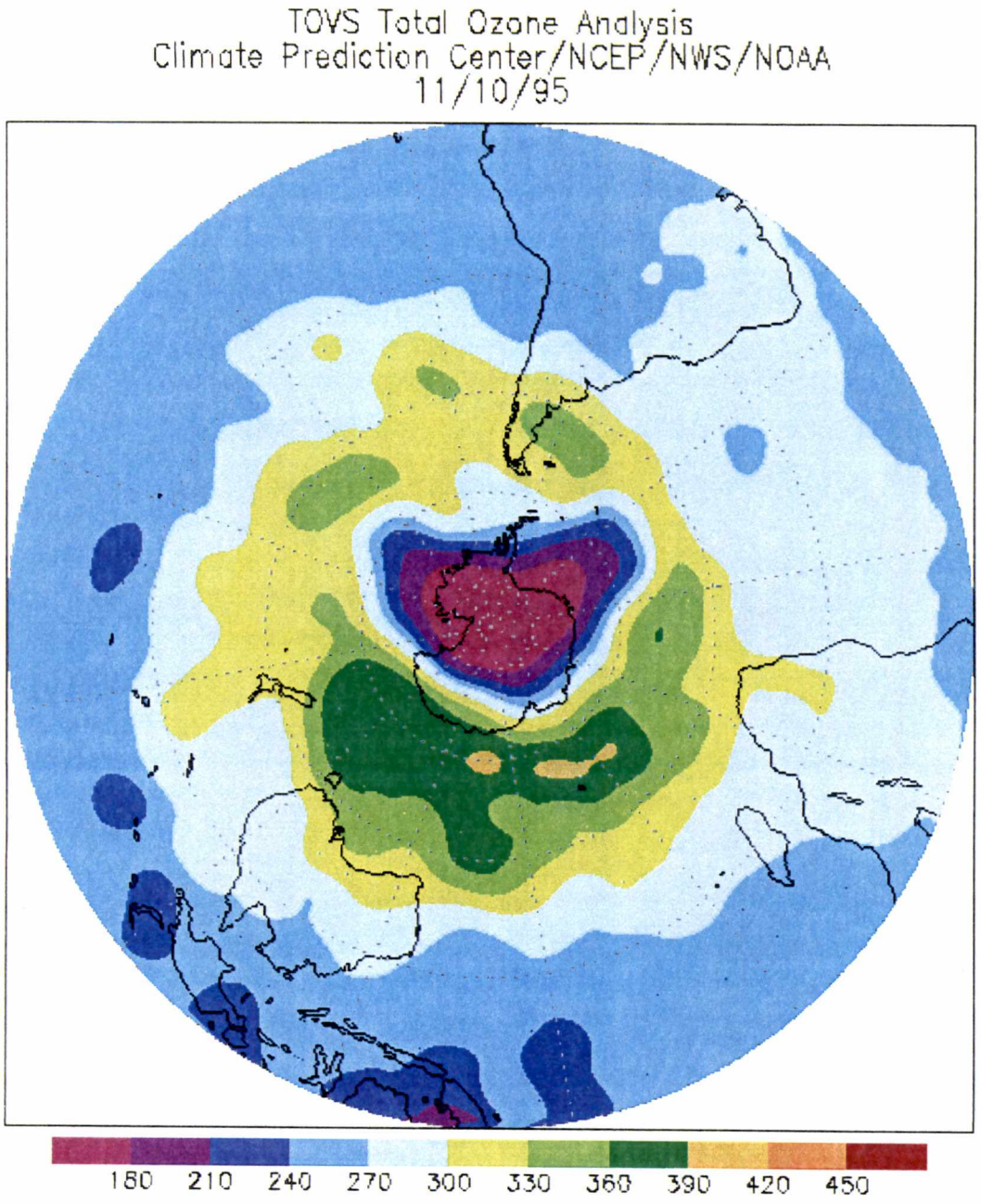

Figure 3.4 Ozone concentrations over the Antarctic continent on the 10th of November, 1995 (in dobson units).

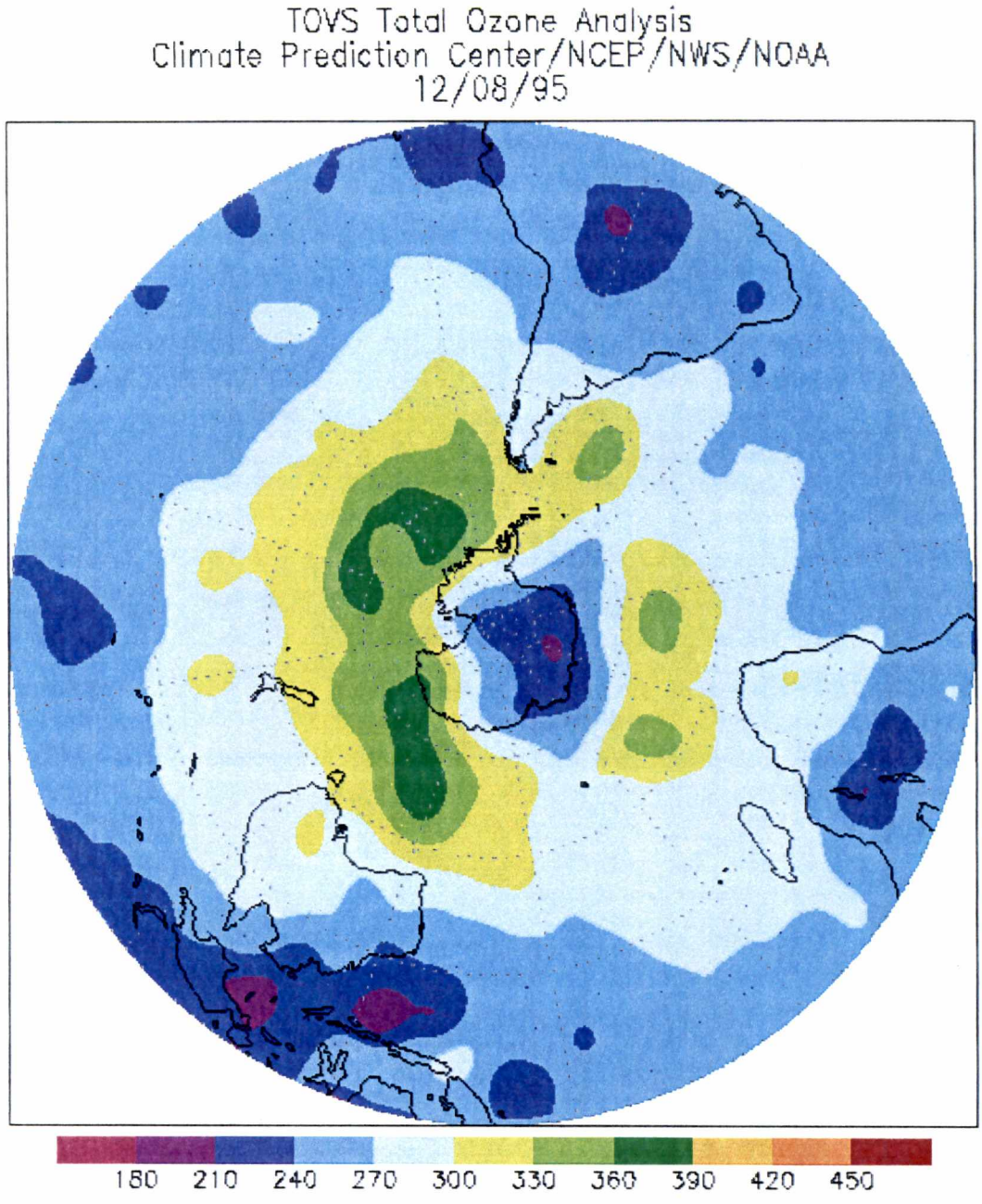

Figure 3.5 Ozone concentrations over the Antarctic continent on the 8th of December, 1995 (in dobson units).

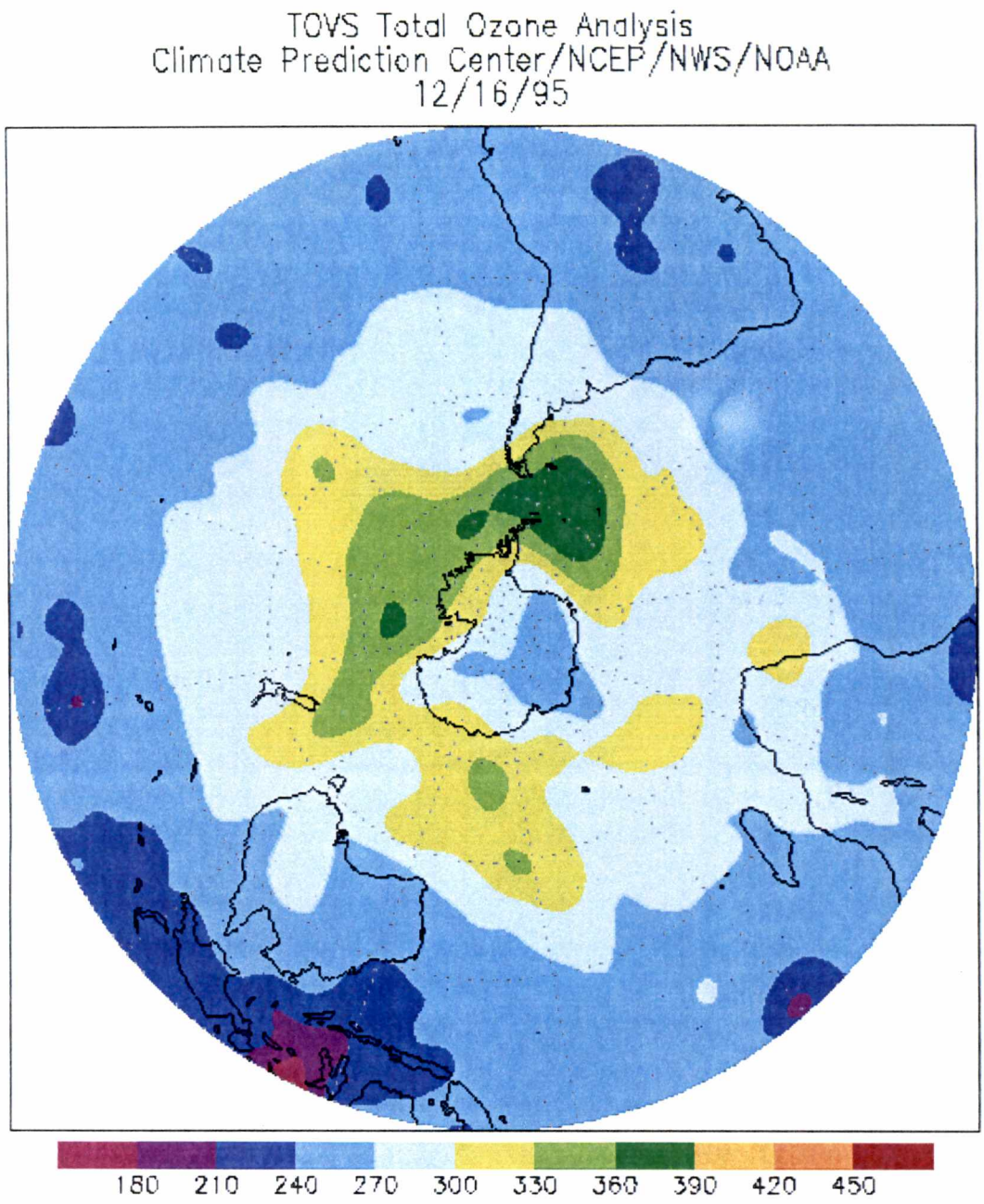

Figure 3.6 Ozone concentrations over the Antarctic continent on the 16th of December, 1995 (in dobson units).

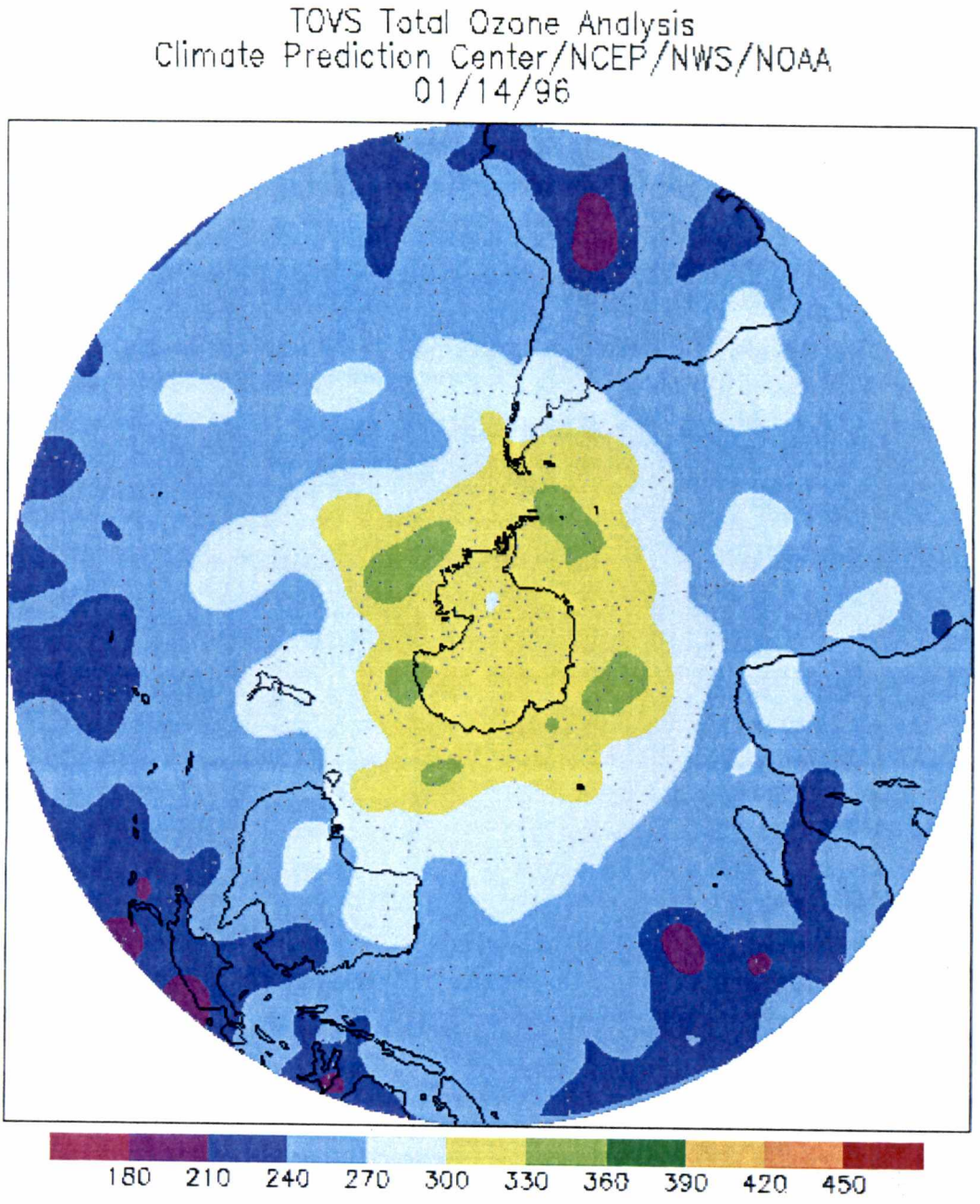

Figure 3.7 Ozone concentrations over the Antarctic continent on the 14th of January, 1996 (in dobson units).

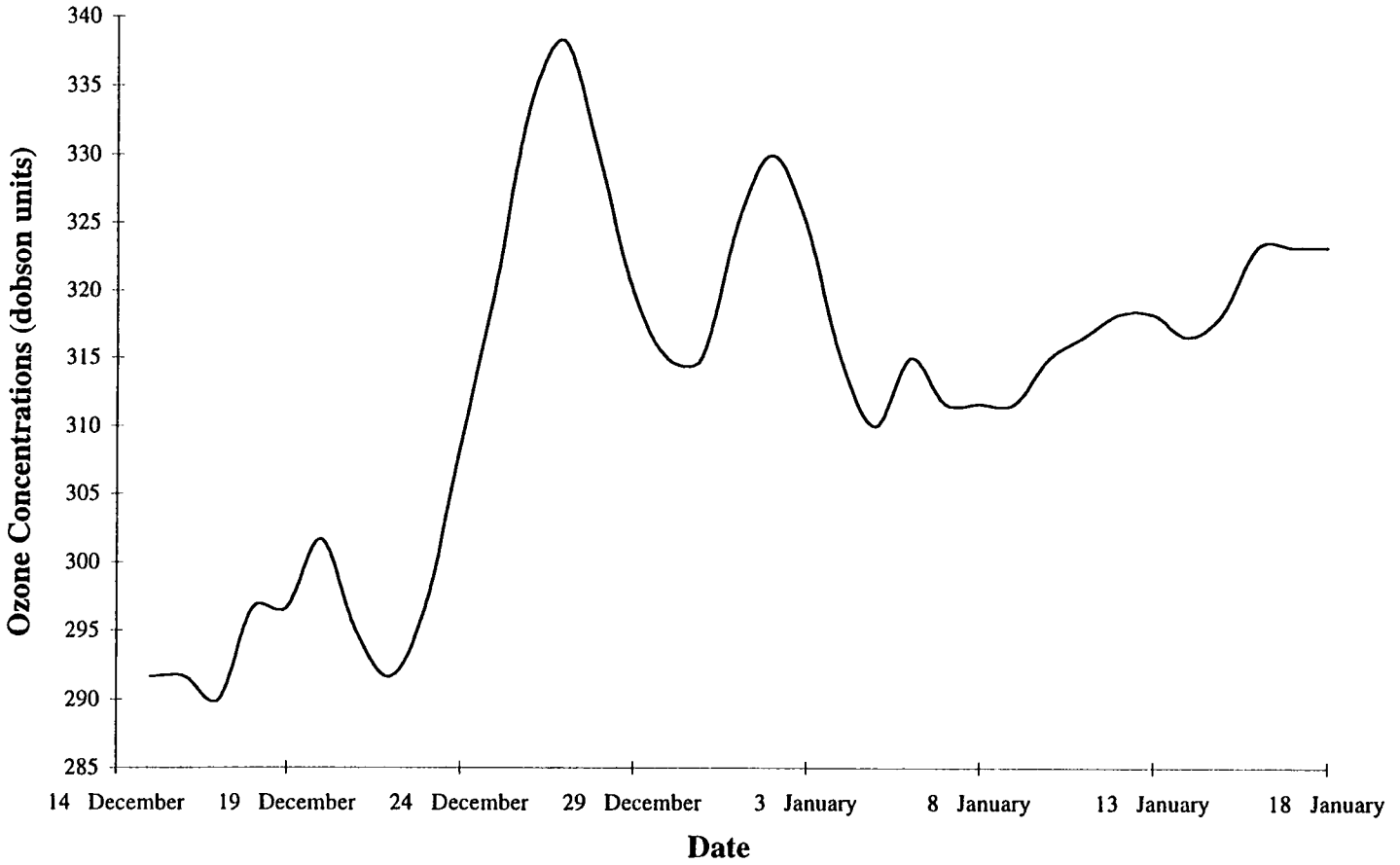

Figure 3.8 : Variation in stratospheric ozone concentrations over the Ross Sea polynya during RSP^{2}95.

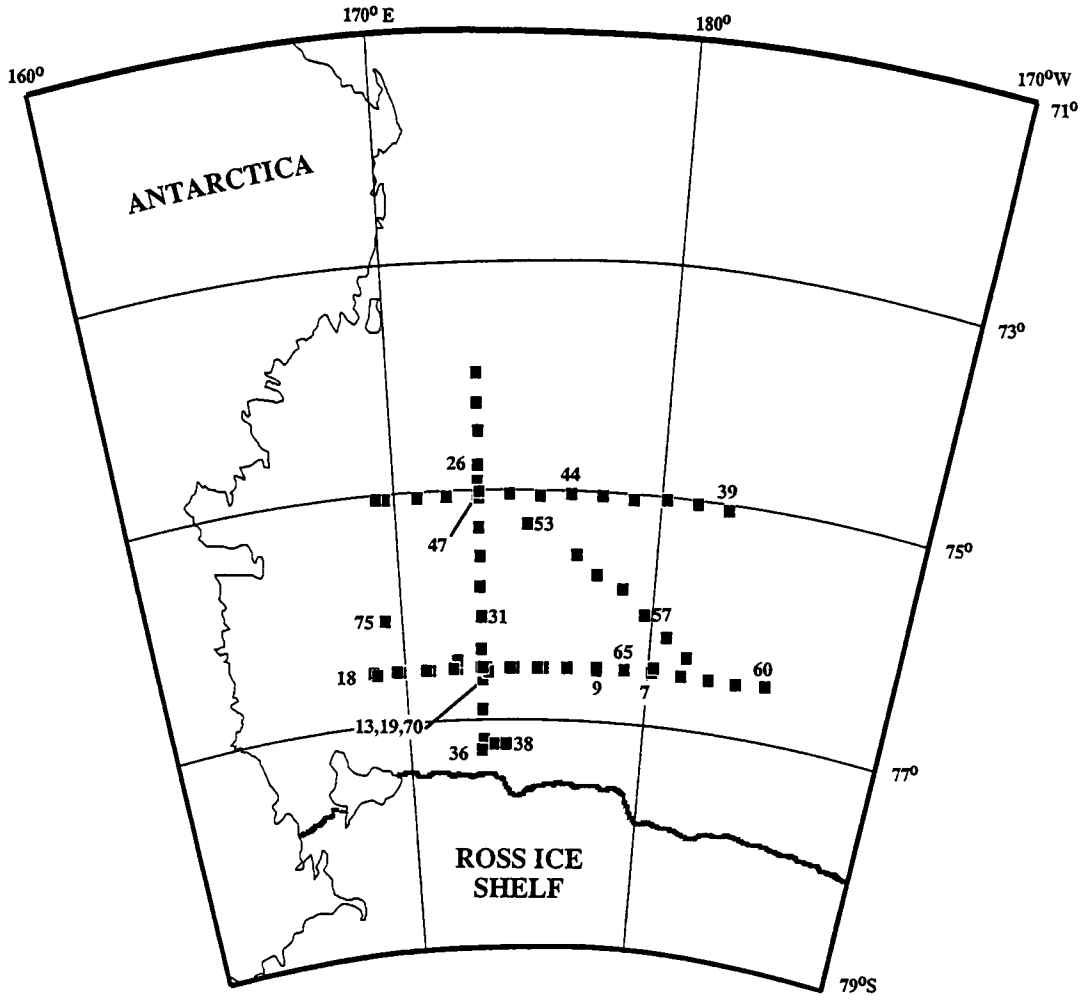

Figure 3.9 : Locations of PUV 500 profile stations for RSP2 94

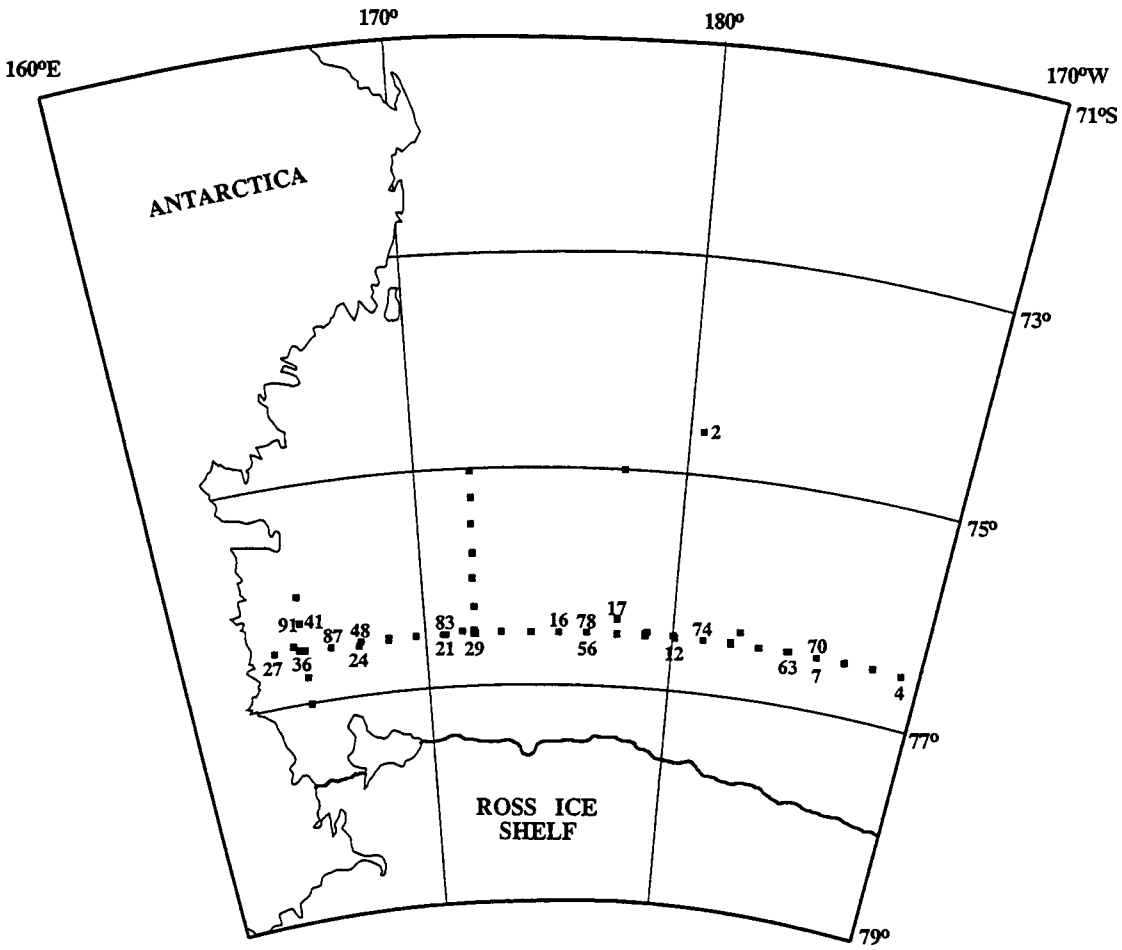

Figure 3.10 : Locations of PUV 500 profile stations for RSP295

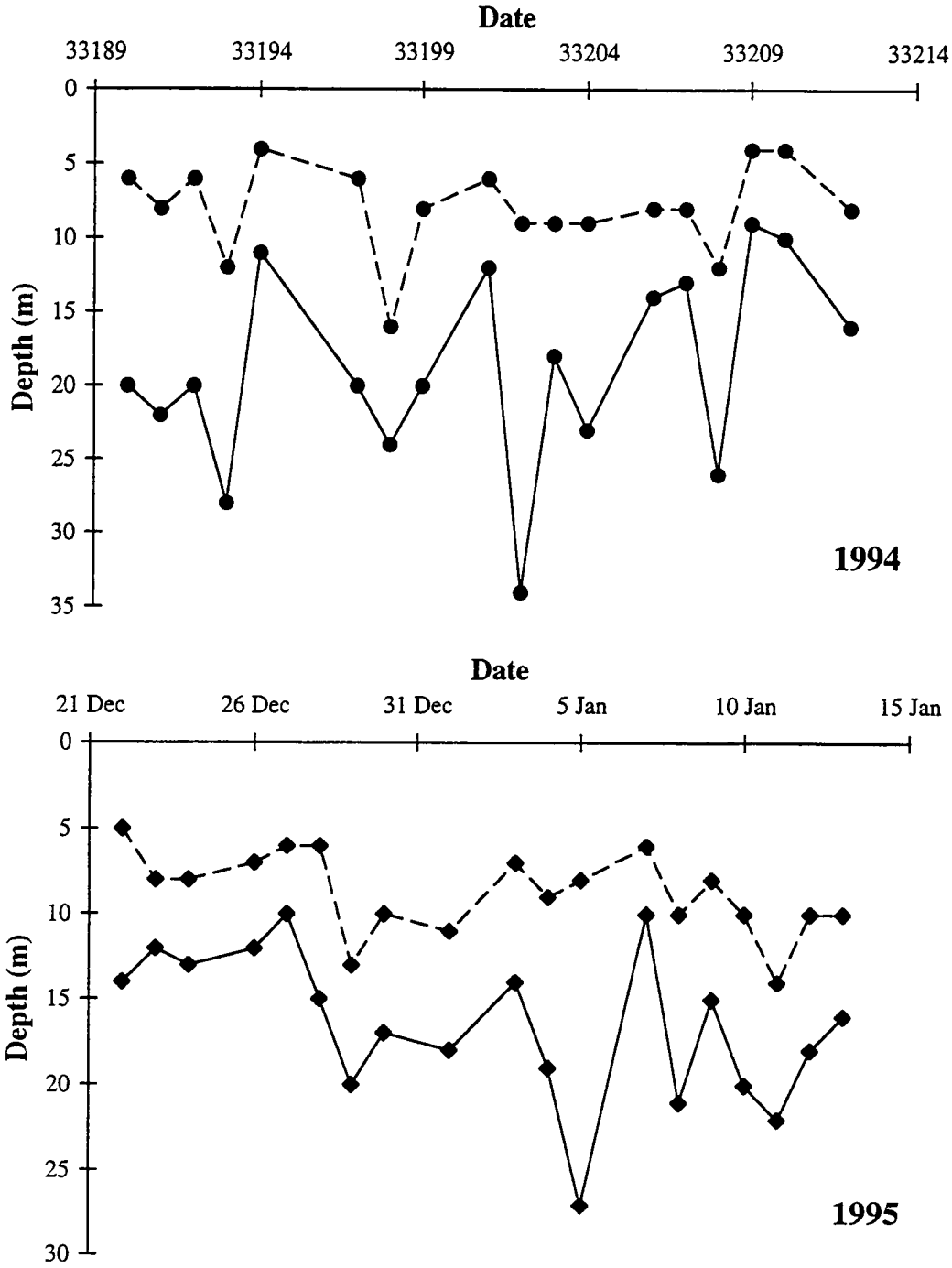

Figure 3.11 : Depth penetration of 1% of surface UV-B into the water column. Dashed lines indicate 308 nm and solid lines 320 nm.

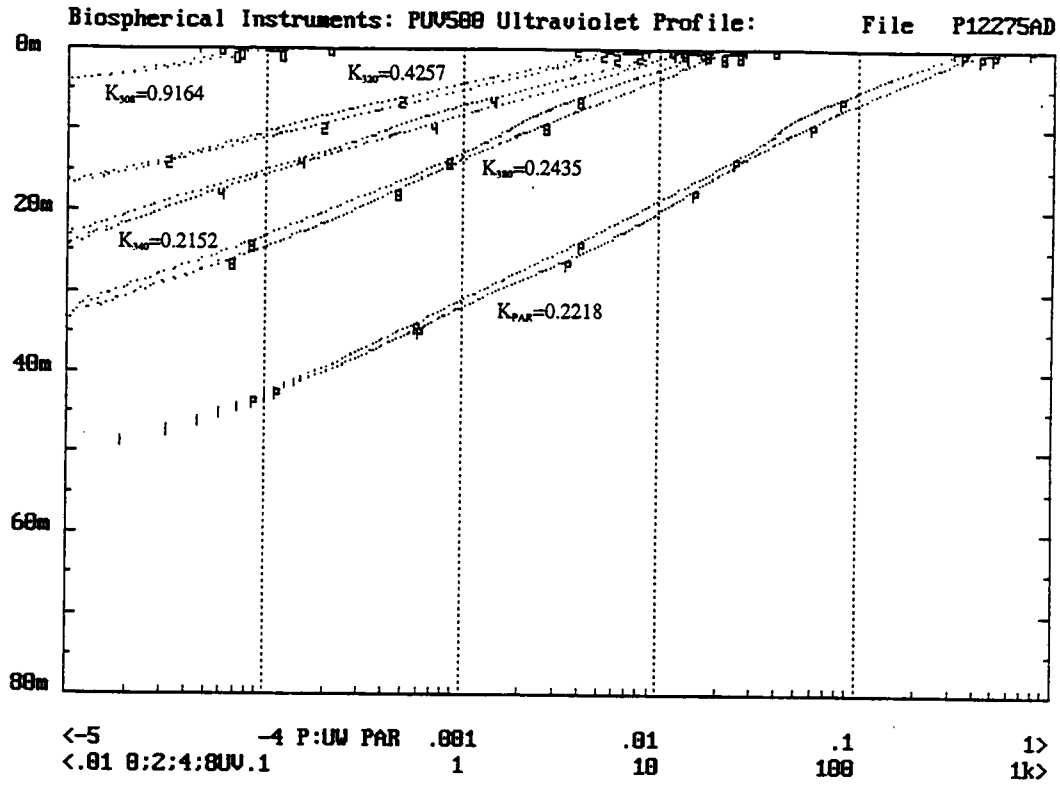

Figure 3.12 : Water column light profiles as measured by the PUV 500 ultraviolet radiometer - Station 24, 1995. 0 = 308 nm, 2 = 320 nm, 4 = 340 nm, 8 = 380 nm (all in $\mu W\ cm^{-2}\ nm^{-1}$) and P = PAR ($\mu Ein\ cm^{-2}\ s^{-1}$). Units of attenuation coefficients (K) are m^{-1}.

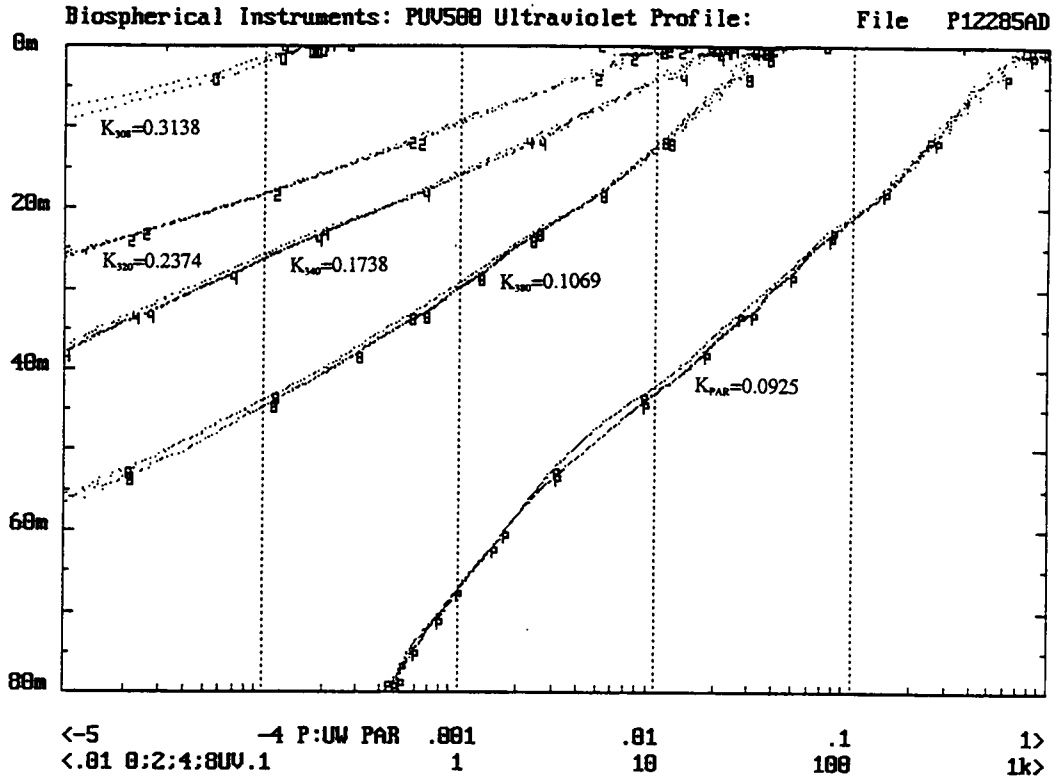

Figure 3.13 : Water column light profiles as measured by the PUV 500 ultraviolet radiometer - Station 27, 1995. 0 = 308 nm, 2 = 320 nm, 4 = 340 nm, 8 = 380 nm (all in $\mu W\ cm^{-2}\ nm^{-1}$) and P = PAR ($\mu Ein\ cm^{-2}\ s^{-1}$). Units of attenuation coefficients (K) are m^{-1}.

K values. Tables 3.4 and 3.5 summarise the attenuation coefficients calculated for the 1994 and 1995 PUV 500 profiles, respectively.

Simple correlation matrices were produced for the two field seasons, comparing the vertical attenuation of the 5 wavebands with the julian date (to see if a seasonal progression could be detected), latitude, longitude, integrated chlorophyll concentrations, integrated POC concentrations, integrated PON levels, and integrated primary production. The results from the correlations can be seen in Tables 3.6 and 3.7. Only 13 of the 18 stations were included in the matrix due to gaps in the other parameters. For 1994, correlations between vertical attenuation and julian date were not high, but all were positive except K_{308}, which was very slightly negative (-0.028). Chlorophyll, POC, PON, and production were all positively correlated with julian date. Correlations between the vertical attenuation coefficients and chlorophyll were always positive; however, only K_{PAR} and K_{380} were particularly high (0.517 and 0.418, respectively).

The correlation matrix for 1995 was considerably different than that of 1994. Eleven of the twenty one stations contained data for all the parameters. In contrast to 1994, all correlations between julian date and vertical attenuation coefficients, chlorophyll, POC, PON and production were negative, with all but K_{340} being strongly negative (> -0.5). All values of K were positively correlated with integrated chlorophyll (K_{308}=0.515, K_{320}=0.729, K_{340}=0.678, K_{380}=0.916, and K_{PAR}=0.914), and these correlations were much stronger than those for the 1994 cruise.

A second set of correlations was run for the *Phaeocystis* -dominated stations from 1994 and the diatom stations for 1995/6 to see if a) any major differences could be seen when compared with the matrix containing all stations and b) to determine whether a few of the

Table 3.4 : Vertical attenuation coefficients from PUV profiles - RSP²94.

Date	Station No.	Vertical Attenuation Coefficients (m^{-1})				
		PAR	308 nm	320 nm	340 nm	380 nm
14-Nov	7	0.1022	0.5201	0.2980	0.1664	0.1207
15-Nov	9	0.0718	0.3819	0.2087	0.1324	0.0877
16-Nov	13	0.0736	0.5638	0.3125	0.1544	0.1127
17-Nov	18	0.0617	0.2787	0.1904	0.1229	0.0775
18-Nov	19	0.1039	1.4621	0.5686	0.1528	0.1395
21-Nov	26	0.0813	1.1411	0.2106	0.1323	0.0956
23-Nov	36	0.1040	0.3340	0.2372	0.1664	0.1759
25-Nov	38	0.1182	0.2000	0.2910	0.1730	0.3298
26-Nov	39	0.0511	0.2646	0.1668	0.1054	0.0638
27-Nov	44	0.0982	0.3502	0.2810	0.1798	0.1288
28-Nov	47	0.1040	0.3289	0.2465	0.1774	0.1370
30-Nov	53	0.1297	0.4546	0.2839	0.1935	0.3065
1-Dec	57	0.1282	0.4668	0.2607	0.1869	0.4450
2-Dec	60	0.0827	0.3212	0.1925	0.1314	0.0933
3-Dec	65	0.1074	0.8283	0.2587	0.1589	0.6121
4-Dec	70	0.1112	1.2617	0.5083	0.1651	0.3745
6-Dec	75	0.1164	0.3583	0.2775	0.1181	0.1770
	Mean	0.0968	0.5598	0.2819	0.1539	0.2046
	St. deviation	0.0228	0.3801	0.1058	0.0259	0.1550

Table 3.5 : Vertical attenuation coefficients from PUV profiles - RSP²95.

Date	Station No.	Vertical Attenuation Coefficients (m^{-1})				
		PAR	308 nm	320 nm	340 nm	380 nm
22-Dec	7	0.1402	0.8770	0.4233	0.1726	0.1508
23-Dec	12	0.2208	0.4990	0.5000	0.2132	0.2998
24-Dec	16	0.2024	0.5005	0.4522	0.2263	0.2961
26-Dec	17	0.2393	0.7157	0.5514	0.2152	0.3528
27-Dec	21	0.2719	0.8359	0.6451	0.3338	0.3812
28-Dec	24	0.2218	0.9164	0.4257	0.2152	0.2435
29-Dec	27	0.0925	0.3138	0.2374	0.1738	0.1069
30-Dec	29	0.1504	0.4415	0.3533	0.2250	0.2530
1-Jan	36	0.1605	0.3292	0.3444	0.2134	0.1815
3-Jan	41	0.1296	0.5825	0.3869	0.1886	0.1817
4-Jan	48	0.1458	0.3571	0.3195	0.1986	0.1583
5-Jan	56	0.1107	0.3294	0.3593	0.1907	0.1443
7-Jan	63	0.0926	1.5454	0.7720	0.1799	0.1481
8-Jan	70	0.1277	0.3243	0.3188	0.1926	0.1506
9-Jan	74	0.1042	0.5332	0.5073	0.1956	0.1459
10-Jan	78	0.0828	0.3355	0.2999	0.1697	0.1103
11-Jan	83	0.0865	0.3090	0.2327	0.1791	0.1186
12-Jan	87	0.1150	0.3929	0.3467	0.1969	0.1577
13-Jan	91	0.1506	0.2792	0.4273	0.2185	0.2061
	Mean	0.1497	0.5483	0.4160	0.2052	0.1993
	St. deviation	0.0562	0.3165	0.1354	0.0360	0.0821

Table 3.6 : Vertical attenuation coefficient simple correlation matrix for RSP^{2}94

	Date	Latitude	Longitude	K_{PAR}	K_{308}	K_{320}	K_{340}	K_{380}	Chl (int)	POC (int)	PON (int)	Production.
Date	1.000											
Latitude	-0.318	1.000										
Longitude	-0.292	-0.118	1.000									
K_{PAR}	0.445	0.102	-0.139	1.000								
K_{308}	-0.028	0.154	-0.081	0.247	1.000							
K_{320}	0.031	0.235	-0.148	0.466	0.949	1.000						
K_{340}	0.016	0.075	0.123	0.729	0.200	0.365	1.000					
K_{380}	0.498	0.179	-0.135	0.772	0.293	0.484	0.636	1.000				
Chl a (int)	0.471	0.371	0.004	0.517	0.224	0.262	0.346	0.418	1.000			
POC (int)	0.551	-0.030	-0.114	0.711	0.432	0.458	0.494	0.544	0.756	1.000		
PON (int)	0.525	0.190	-0.090	0.669	0.248	0.296	0.469	0.499	0.847	0.926	1.000	
Production	0.584	-0.141	-0.456	0.399	0.046	0.127	-0.269	0.188	0.118	0.391	0.338	1.000

Note : Date=Julian date; K_x = vertical attenuation of light at wavelength x; Chl a=Chlorophyll a concentration; POC (int)=particulate organic carbon integrated through the top 150 m; PON (int)=particulate organic nitrogen integrated through the top 150 m; Production=Primary production integrated through the euphotic zone.

Table 3.7 : Vertical attenuation coefficient simple correlation matrix for RSP²95

	Date	Latitude	Longitude	K_{PAR}	K_{308}	K_{320}	K_{340}	K_{380}	Chl (int)	POC (int)	PON (int)	Production
Date	1.000											
Latitude	0.261	1.000										
Longitude	-0.221	-0.298	1.000									
K_{PAR}	-0.757	-0.419	0.031	1.000								
K_{308}	-0.670	-0.319	0.140	0.592	1.000							
K_{320}	-0.578	-0.384	0.271	0.806	0.768	1.000						
K_{340}	-0.355	-0.038	-0.230	0.787	0.455	0.744	1.000					
K_{380}	-0.684	-0.482	0.111	0.980	0.556	0.833	0.782	1.000				
Chl a (int)	-0.565	-0.626	0.045	0.914	0.515	0.729	0.678	0.916	1.000			
POC (int)	-0.599	-0.581	0.137	0.888	0.354	0.660	0.596	0.926	0.921	1.000		
PON (int)	-0.596	-0.549	0.164	0.884	0.381	0.681	0.609	0.916	0.936	0.990	1.000	
Production	-0.692	0.056	0.196	0.677	0.384	0.573	0.438	0.673	0.491	0.618	0.637	1.000

Note : Date=Julian date; K_x = vertical attenuation of light at wavelength x; Chl a=Chlorophyll a concentration; POC (int)=particulate organic carbon integrated through the top 150 m; PON (int)=particulate organic nitrogen integrated through the top 150 m; Production=Primary production integrated through the euphotic zone.

stations may be having a large impact on the correlations (Tables 3.8 and 3.9). Correlations between julian date and the other parameters were higher in all cases for the *Phaeocystis*-only stations in 1994. Correlations between chlorophyll and the attenuation coefficients were also higher. In contrast, the correlations for the 1995 diatom-dominated stations were less strong than the correlations for the whole data set, and the absolute changes were also smaller than in the 1994 correlations.

3.4 UV EXPERIMENTS

In 1994 six UV-B incubations were carried out at the station locations indicated in Figure 3.14. Four were of 24-h duration (1, 3, 4 and 5) and experiments 2 and 6 were of 8 and 7 days, respectively. On the 1995 cruise, eight UV-B experiments were carried out at the stations indicated in Figure 3.15. Experiments A, B, C, E, F and H lasted 24-hours, while D and G ran for 5 days.

3.4.1 CHLOROPHYLL

In 1994 chlorophyll concentrations decreased in all experiments (Table 3.10), despite the fact that cell numbers increased in the long-term studies. In experiments 1, 2, 5 and 6, the lowest chlorophyll levels were seen when samples were exposed to total UV-B irradiances. In experiment 3 the total light treatment displayed the least reduction in chlorophyll, but the reduction was similar to the no UV-B treatment (1.01 and 0.99 $\mu g\ L^{-1}$, respectively). In experiment 4 the lowest reduction in chlorophyll was seen in the partial UV-B treatment.

Table 3.8 : Vertical attenuation coefficient simple correlation matrix for RSP[2]94 (*Phaeocystis*- dominated stations only).

	Date	Latitude	Longitude	K_{PAR}	K_{308}	K_{320}	K_{340}	K_{380}	Chl (int)	POC (int)	PON (int)	Production
Date	1.000											
Latitude	-0.315	1.000										
Longitude	-0.421	0.030	1.000									
K_{PAR}	0.712	-0.256	0.105	1.000								
K_{308}	0.083	-0.058	0.005	0.152	1.000							
K_{320}	0.207	-0.002	-0.006	0.345	0.957	1.000						
K_{340}	0.128	-0.084	0.489	0.605	0.132	0.245	1.000					
K_{380}	0.744	-0.076	0.003	0.763	0.192	0.365	0.631	1.000				
Chl a (int)	0.575	0.040	0.045	0.785	0.322	0.437	0.671	0.673	1.000			
POC (int)	0.655	-0.461	-0.017	0.723	0.419	0.442	0.502	0.539	0.838	1.000		
PON (int)	0.631	-0.168	0.022	0.674	0.221	0.261	0.473	0.514	0.906	0.917	1.000	
Production	0.719	-0.395	-0.466	0.438	-0.013	0.058	-0.387	0.133	0.187	0.409	0.376	1.000

Note : Date=Julian date; K_x = vertical attenuation of light at wavelength x; Chl a=Chlorophyll a concentration; POC (int)=particulate organic carbon integrated through the top 150 m; PON (int)=particulate organic nitrogen integrated through the top 150 m; Production=Primary production integrated through the euphotic zone.

Table 3.9 : Vertical attenuation coefficient simple correlation matrix for RSP²95 (diatom-dominated stations only).

	Date	Latitude	Longitude	K_{PAR}	K_{308}	K_{320}	K_{340}	K_{380}	Chl (int)	POC (int)	PON (int)	Production
Date	1.000											
Latitude	0.100	1.000										
Longitude	-0.217	-0.921	1.000									
K_{PAR}	-0.769	-0.087	0.059	1.000								
K_{308}	-0.658	0.082	0.231	0.208	1.000							
K_{320}	-0.492	-0.452	0.533	0.486	0.566	1.000						
K_{340}	-0.150	0.005	-0.240	0.680	-0.337	0.327	1.000					
K_{380}	-0.629	-0.255	0.193	0.952	0.104	0.574	0.718	1.000				
Chl a (int)	-0.533	-0.056	0.015	0.887	-0.030	0.281	0.616	0.896	1.000			
POC (int)	-0.404	-0.203	0.087	0.785	-0.171	0.296	0.629	0.859	0.951	1.000		
PON (int)	-0.428	-0.259	0.167	0.759	-0.118	0.319	0.544	0.843	0.936	0.993	1.000	
Production	-0.659	-0.233	0.275	0.839	0.365	0.677	0.468	0.917	0.795	0.765	0.782	1.000

Note : Date=Julian date; K_x = vertical attenuation of light at wavelength x; Chl a=Chlorophyll a concentration; POC (int)=particulate organic carbon integrated through the top 150 m; PON (int)=particulate organic nitrogen integrated through the top 150 m; Production=Primary production integrated through the euphotic zone.

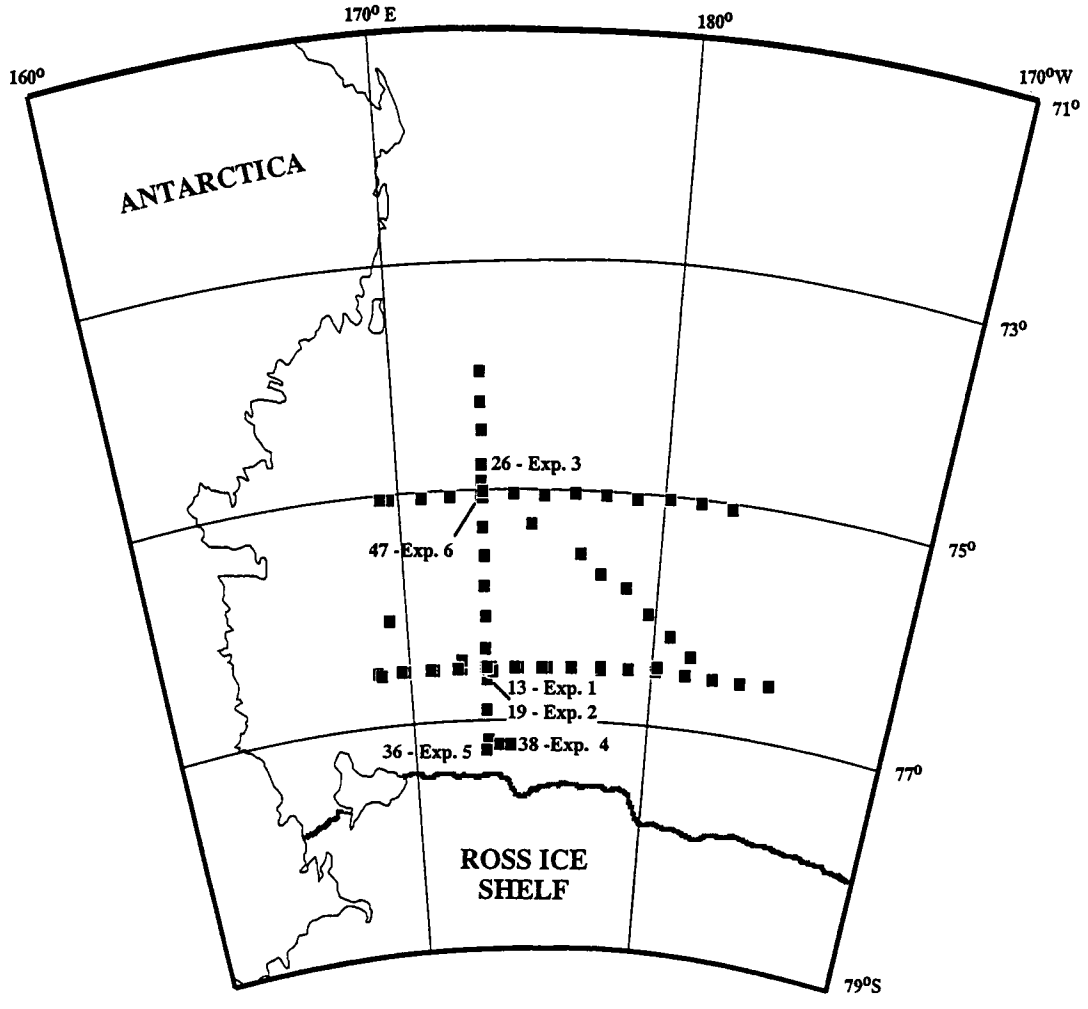

Figure 3.14 : Locations of stations where UV experiments were initiated for RSP^{2}94.

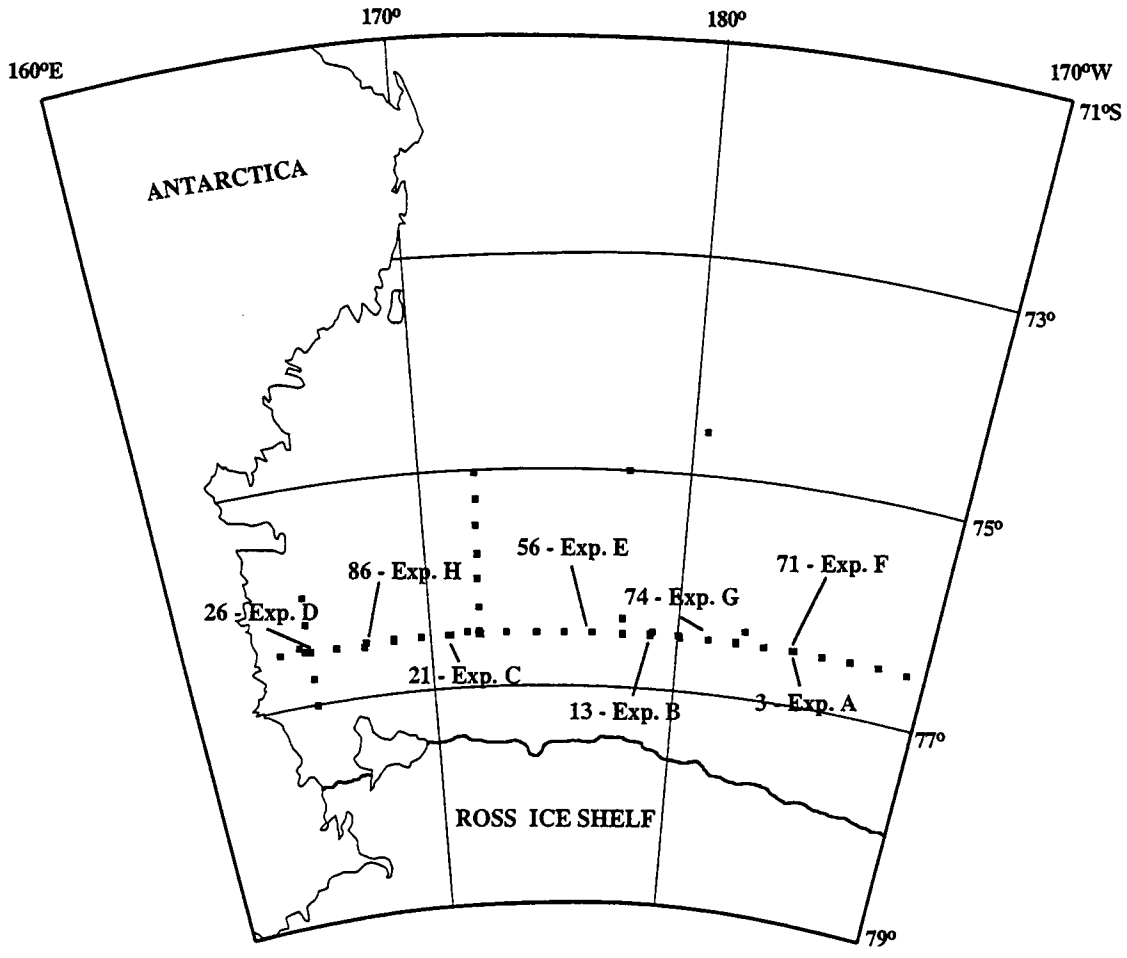

Figure 3.15 : Locations of stations where UV experiments were initiated for RSP^{2}95.

Table 3.10 : Chlorophyll *a* measurements from 1994 UV experiments.

Experiment	Time (h)	Chlorophyll ($\mu g\ L^{-1}$)		
		Total Light	Minus Partial UVB	Minus Total UVB
1	0	5.18		
	24	1.46	2.41	1.57
2	0	5.02		
	192	1.14	1.20	2.08
3	0	1.64		
	24	1.01	0.78	0.99
4	0	3.31		
	24	1.06	1.23	0.65
5	0	5.87		
	24	2.74	3.29	2.99
6	0	2.09		
	96	0.59	1.46	1.36

On the 1995 cruise chlorophyll concentrations in the 24-h experiments decreased, except in the case of the total light treatment of experiment C (Table 3.11). In both of the 5-day experiments, chlorophyll concentrations showed an initial decrease but reached a concentration higher than the initial level by the end of the experiment (Figure 3.17 - bottom and Figure 3.19 - top). There was no apparent differentiation between the responses of the phytoplankton under the different light regimes with respect to chlorophyll for any of the experiments (Figures 3.16 - 3.19).

3.4.2 PHYTOPLANKTON ASSEMBLAGES

Large numbers of *Phaeocystis* cells, both single cells and colonies, were observed in the 1994 experimental samples. The other main phytoplankter observed was a small pennate diatom, *Nitzschia subcurvata* . Some centric diatoms were present, although always in low numbers; similarly, dinoflagellates were seen in small concentrations. Cryptomonads were numerically important in experiment 3, although still much less common than the dominant species, *Nitzschia subcurvata.* (complete 1994 microscopy data are found in Appendix C). The phytoplankton assemblages for experiments 1, 2, 4 and 5 were dominated by *Phaeocystis*, although diatoms were present in low numbers (Table 3.12). Experiments 3 and 6 were dominated by diatoms, with background levels of *Phaeocystis* cells (and as mentioned above, *Cryptomonas* sp. in exp. 3). In experiment 3 there was a marked decrease in *Phaeocystis* cells after 24 hours whereas diatom numbers increased. The highest diatom concentrations for this experiment were observed under total UV-B exclusion (Figure 3.20). Experiments 4 and 5 also showed a drop in cell number for *Phaeocystis,* with the lowest reduction observed in the partial UV-B exclusion treatment for experiment 4 and the total UV-B exclusion treatment for experiment 5 (Figure 3.21). In both of these experiments diatoms increased from the experiment's start in all treatments (except for the partial exclusion in exp. 4 which was

Table 3.11 : Chlorophyll equivalent measurements from 1995/96 UV experiments.

Experiment	Time (h)	Chlorophyll *a* (equivalent) ($\mu g\ L^{-1}$)		
		Total Light	Minus Partial UVB	Minus Total UVB
A	12	4.39	4.49	4.08
	18	4.26	4.82	4.74
	24	3.14	3.64	
B	0	9.95		
	6	6.82	7.15	7.31
	12	5.40	6.43	5.28
	18	5.78	5.58	5.20
	24	4.07	4.79	4.96
C	0	4.05		
	6	2.44	2.25	3.22
	12	2.79	3.66	3.36
	18	2.07	4.08	3.37
	24	4.37	3.25	3.58
D	0	3.55		
	24	2.81	2.55	2.84
	48	2.24	3.00	2.77
	72	3.61	4.20	4.07
	96	5.10	5.95	5.70
	120	6.43	5.43	6.55
E	0	1.55		
	6	1.17	1.16	1.20
	12	1.12	1.14	0.97
	18	1.02	1.07	1.08
	24	1.06	0.94	0.97
F	0	2.23		
	6	2.52	2.75	2.45
	12	2.05	2.37	2.46
	18	1.94	1.82	1.82
	24	2.01	1.93	1.76
G	0	3.04		
	24	1.65	1.66	1.32
	48	2.28	1.81	1.87
	72	2.02	2.26	2.05
	96	2.26	1.74	2.32
	120	4.22	3.96	2.32
H	0	1.84		
	6	1.41	1.40	1.58
	12	1.06	1.10	1.10
	18	1.34	1.65	1.64
	24	0.92	0.88	0.81

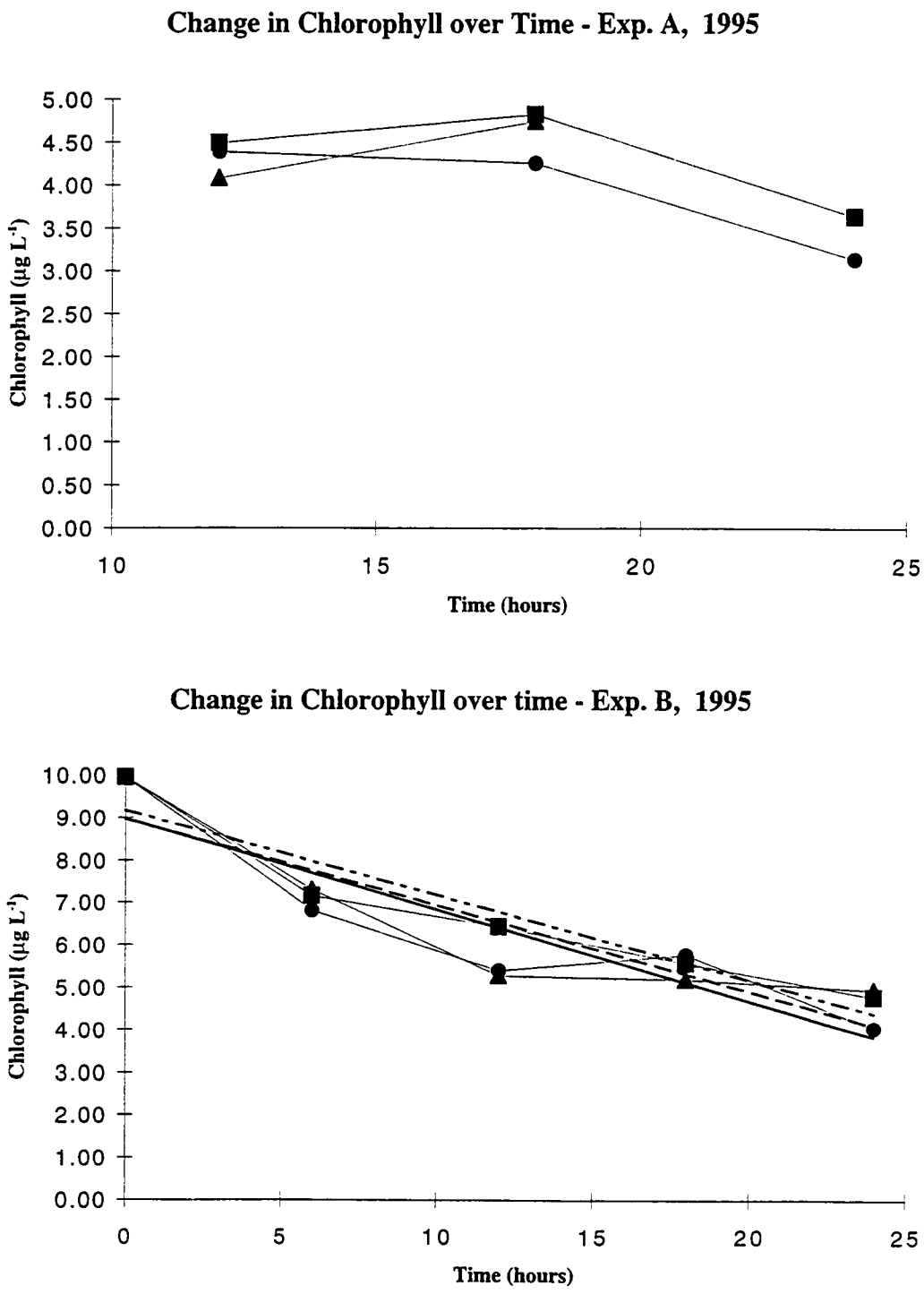

Figure 3.16 : Change in chlorophyll a over time in experiments A (top) and B (bottom). Dashed line and triangle=no UVB, mixed dash line and square= partial UVB solid line and circles= total UVB. Lines are linear regressions through the data

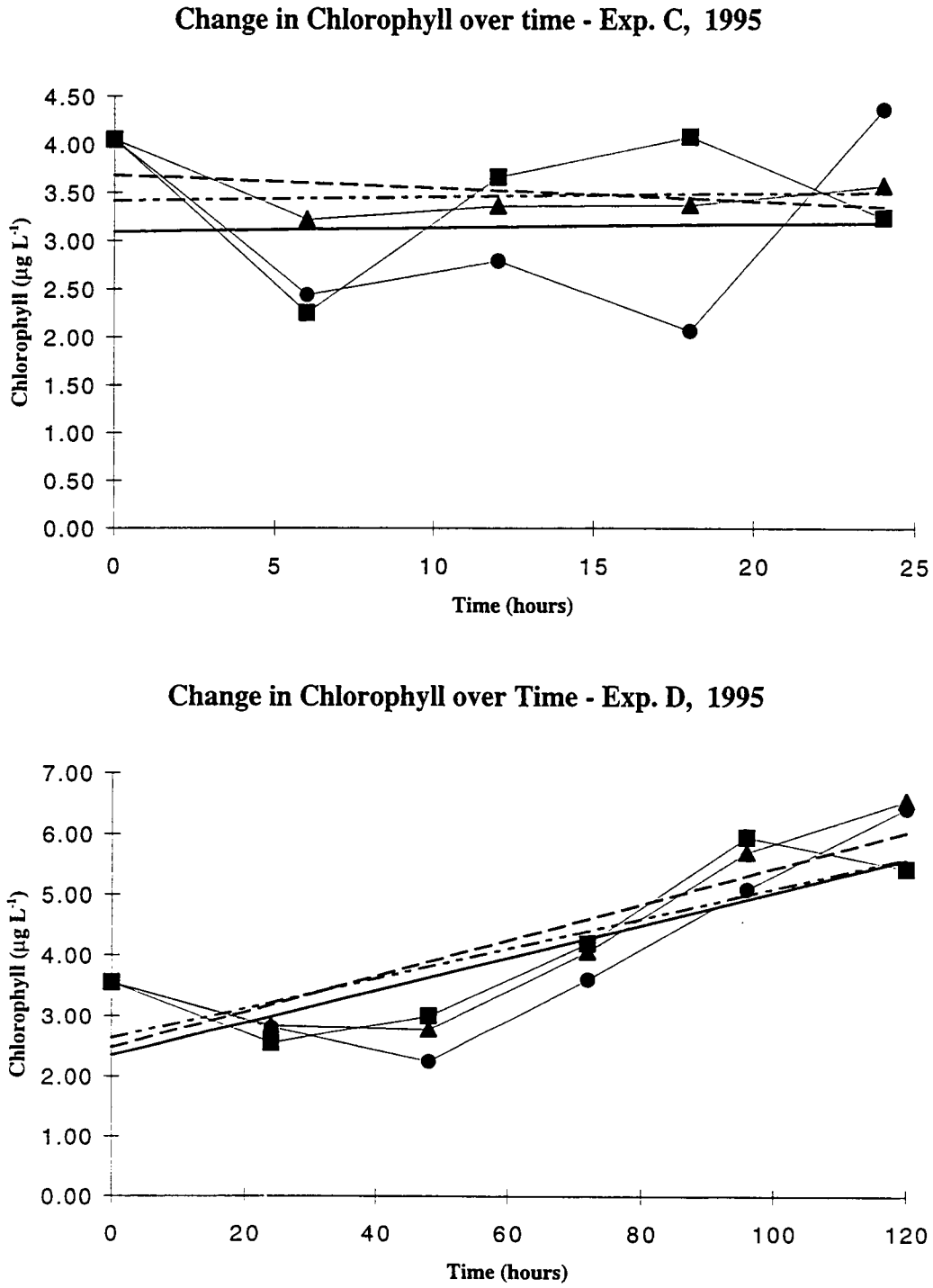

Figure 3.17 : Change in chlorophyll a over time in experiments C (top) and D (bottom). Dashed line and triangle=no UVB, mixed dash line and square= partial UVB solid line and circles= total UVB. Lines are linear regressions through the data.

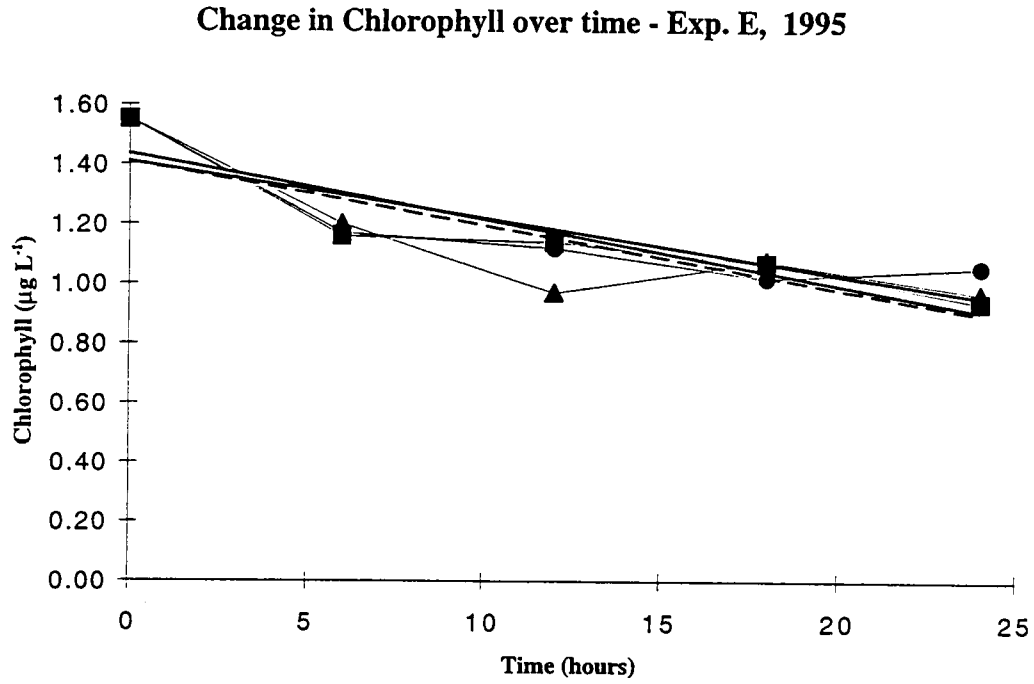

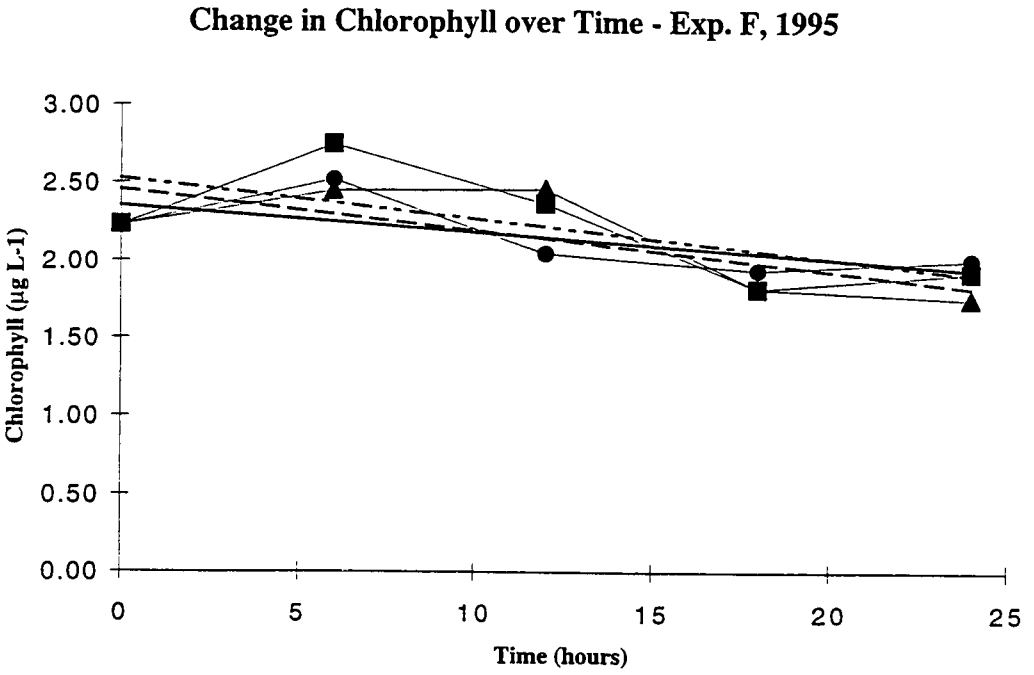

Figure 3.18 : Change in chlorophyll a over time in experiments E (top) and F (bottom). Dashed line and triangle=no UVB, mixed dash line and square= partial UVB solid line and circles= total UVB. Lines are linear regressions through the data.

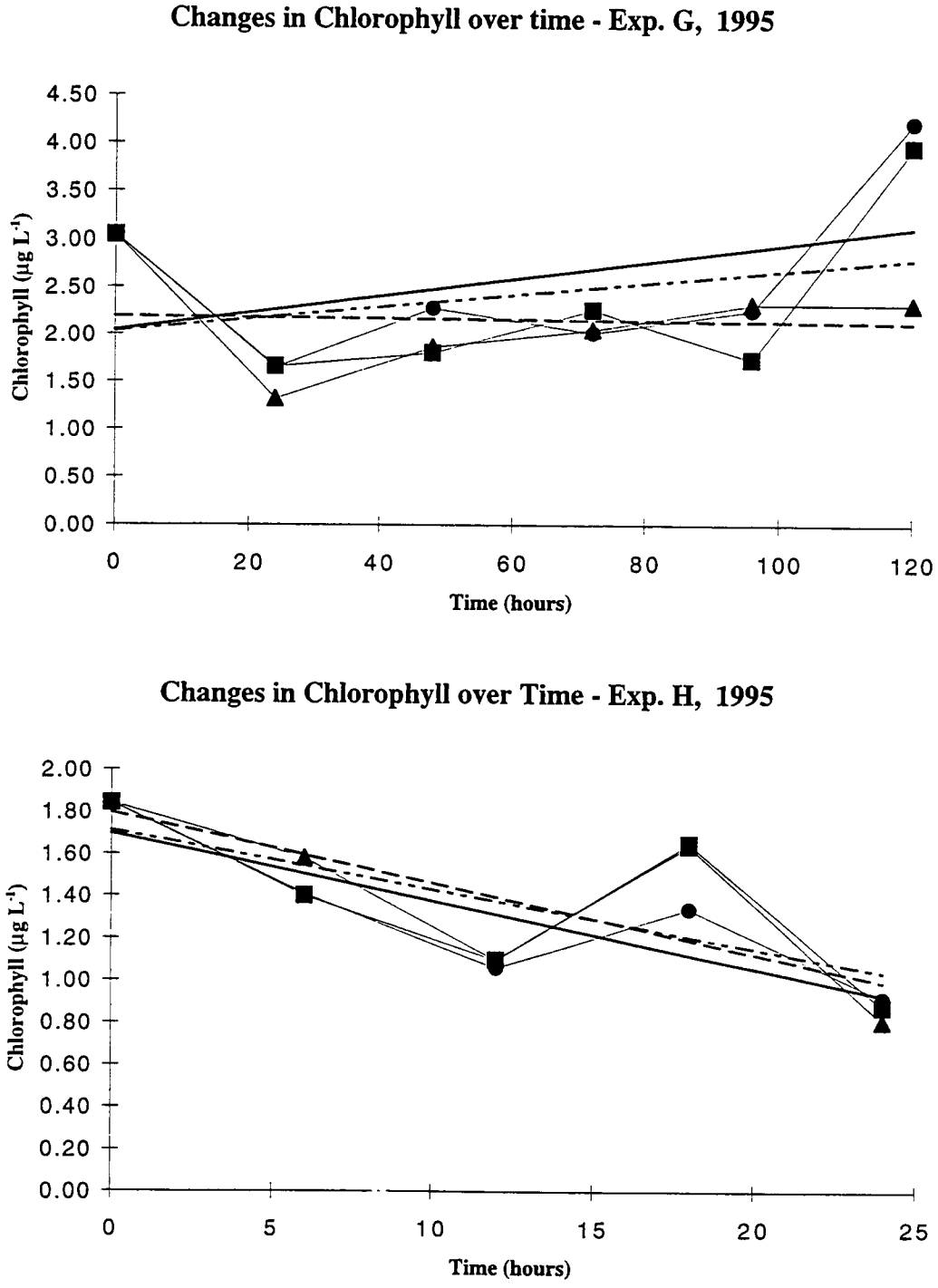

Figure 3.19 : Change in chlorophyll a over time in experiments G (top) and H (bottom). Dashed line and triangle=no UVB, mixed dash line and square= partial UVB solid line and circles= total UVB. Lines are linear regressions through the data.

Table 3.12 : Summary of changes in cell numbers for RSP²94 UV experiments.

Experiment	Time (h)	Total Light			Minus Partial UVB			Minus Total UVB		
		Phaeocystis (cells L^{-1})	Diatoms (cells L^{-1})	Ratio P : D (%)	*Phaeocystis* (cells L^{-1})	Diatoms (cells L^{-1})	Ratio P : D (%)	*Phaeocystis* (cells L^{-1})	Diatoms (cells L^{-1})	Ratio P : D (%)
1	24	3.39E+06	3.27E+04	99.0	6.73E+06	4.98E+04	99.3	5.95E+06	6.84E+04	98.9
2	48	8.39E+06	8.07E+04	99.0	1.10E+07	1.57E+05	98.6	9.59E+06	3.51E+04	99.6
	96	1.91E+07	1.18E+05	99.4	2.44E+07	3.27E+05	98.7	1.63E+07	3.81E+05	97.7
	144	3.05E+07	2.76E+05	99.1	4.28E+07	1.22E+05	99.7	2.80E+07	3.92E+05	98.6
	192	2.37E+07	3.41E+05	98.6	7.46E+07	6.40E+05	99.2	5.40E+07	8.53E+05	98.4
3	0	3.908E+05	6.586E+05	37.2						
	24	1.467E+05	9.198E+05	13.8	1.160E+05	1.392E+06	7.7	1.179E+05	1.709E+06	6.5
4	0	8.07E+06	1.83E+04	99.8						
	24	3.86E+06	2.31E+04	99.4	5.24E+06	0.00E+00	100	2.92E+06	4.02E+04	98.6
5	0	2.16E+07	3.85E+05	98.2						
	24	9.49E+06	4.18E+05	95.8	1.38E+07	5.56E+05	96.1	1.60E+07	6.44E+05	96.1
6	0	8.58E+05	7.79E+06	9.9						
	96	1.14E+06	6.29E+06	15.3	3.14E+05	1.07E+07	2.9	5.69E+05	1.01E+07	5.4
	168	6.59E+05	4.00E+06	14.1	2.26E+06	1.52E+07	13.0	1.52E+06	1.34E+07	10.2

Note : Ratio P:D=Ratio of *Phaeocystis* to diatoms as a percentage.

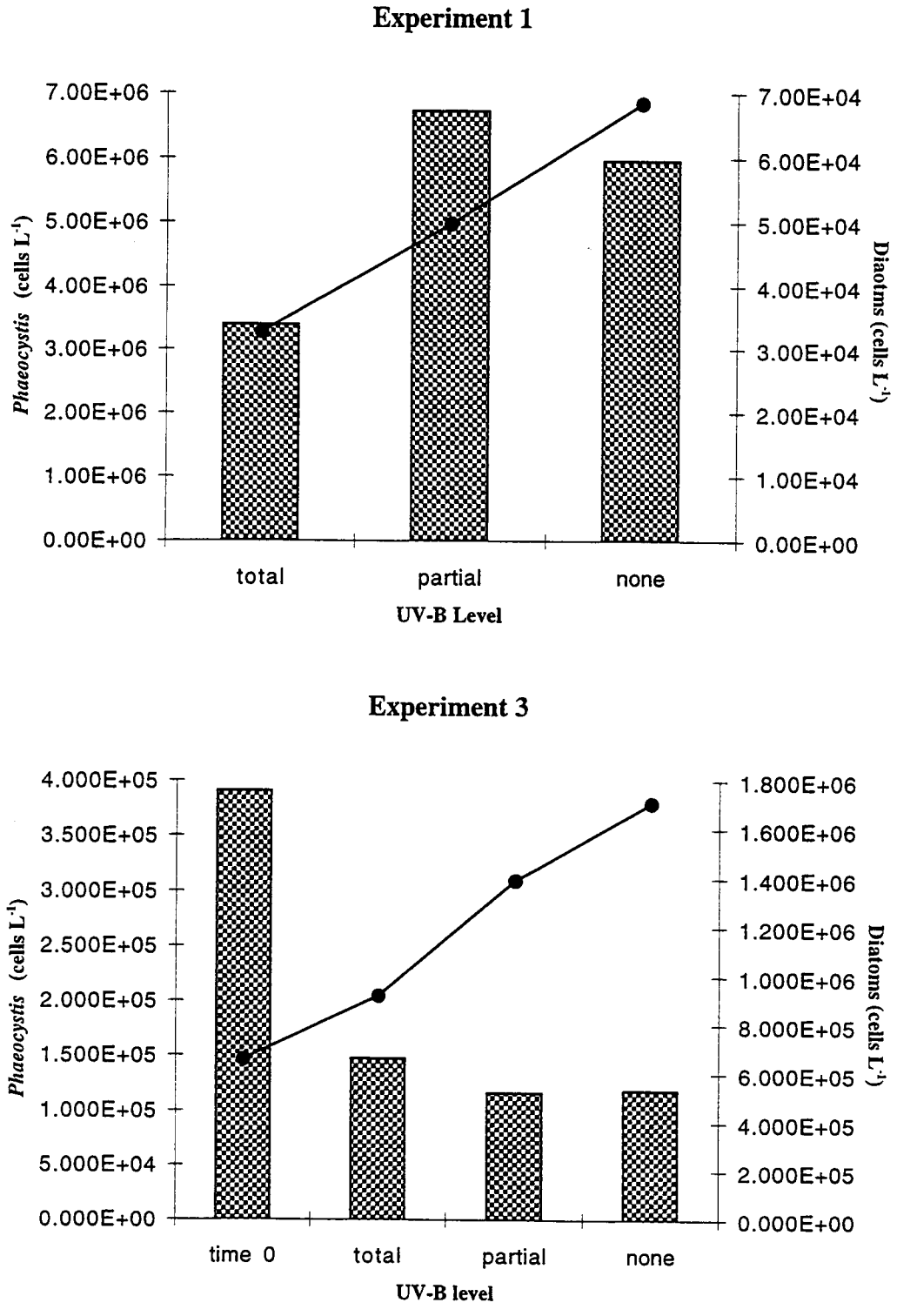

Figure 3.20 : Changes in cell concentration over time for experiments 1 and 3. Bars are *Phaeocystis* (cells L^{-1}) and lines are diatoms (cells L^{-1}).

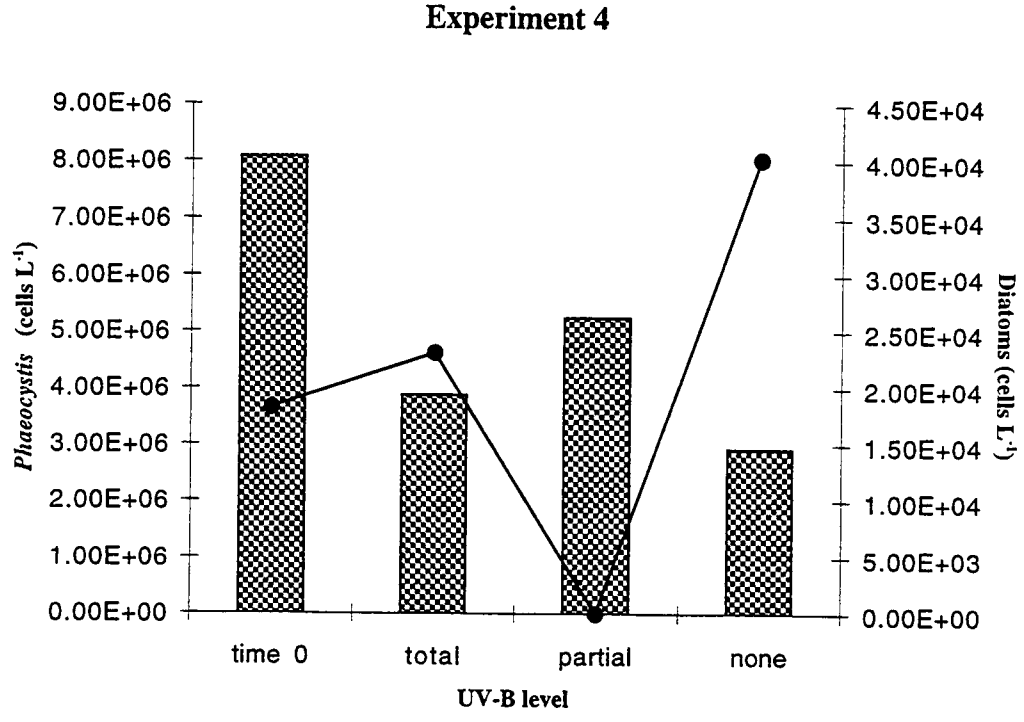

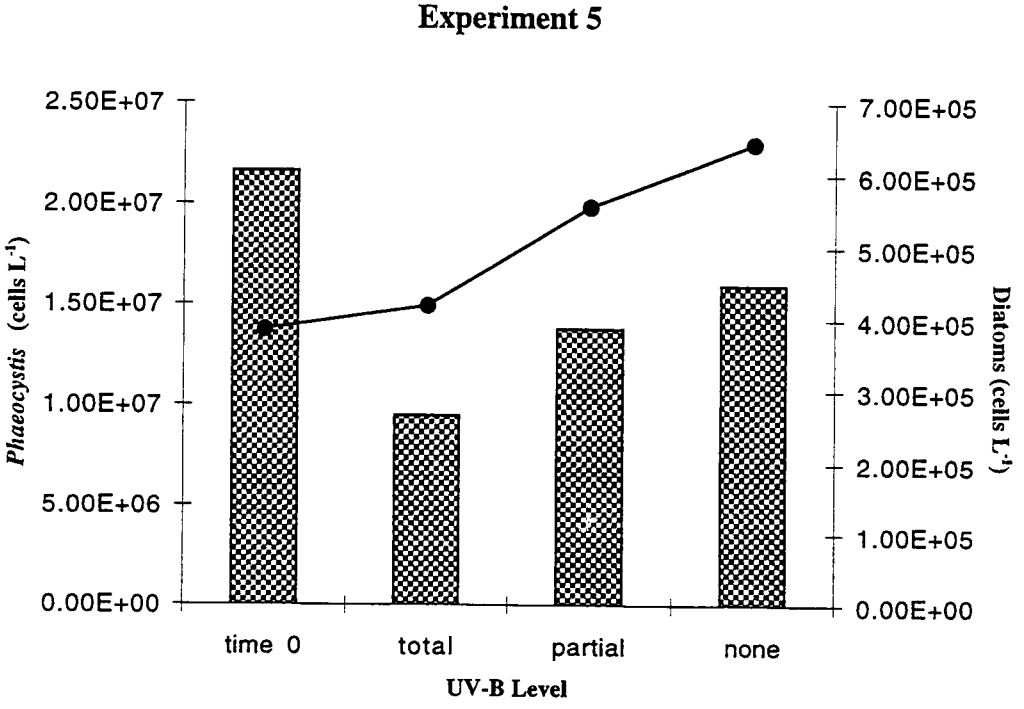

Figure 3.21 : Changes in cell concentration over time for experiments 4 and 5. Bars are *Phaeocystis* (cells L^{-1}) and the lines are diatoms (cells L^{-1}).

100% *Phaeocystis*), with the highest numbers being observed in the total UV-B exclusion treatment. In the first long-term experiment (experiment 2), an increase in cell numbers was observed. Greatest cell concentrations for both *Phaeocystis* and diatoms were seen when UV-B was either partially or completely excluded (Figure 3.22). Scatter in the diatom measurements was probably due to their being present in small numbers which, when converted to cells L^{-1} , increases error. Experiment 6, which was a diatom dominated assemblage, showed an increase of *Phaeocystis* cells under partial and complete UV-B exclusion while total UV-B resulted in a decrease in *Phaeocystis* abundance (Figure 3.23). Diatoms also increased significantly under partial and total exclusion of UV-B and decreased dramatically under total UV-B irradiances (P=0.09)

Ratios of *Phaeocystis* to diatom by cell numbers showed a decrease in all experiments (i.e., an increase in diatoms with respect to *Phaeocystis* - Table 3.12) with a decrease in the UV-B irradiance to which the samples were exposed. This was particularly clear for the diatom-dominated stations but could also be seen in the *Phaeocystis*-dominated stations. The partial UV-B treatment was the most variable.

For the 1995 cruise, experiments A, B, C, D, F, and G all had species assemblages dominated by diatoms but with a significant number of *Phaeocystis* cells (between 20 and 40 % by cell number). Experiments E and H were almost entirely diatomaceous (less than 3% *Phaeocystis*). The dominant diatom in all but experiment H was *Nitzschia subcurvata*, while experiment H was dominated by *Nitzschia seriata* (complete 1995 microscopy data are found in Appendix D). There were no clear trends in the 24-hour experiments, with some showing an increase in cell concentrations over time while others stayed the same or decreased (Table 3.13). In experiment A cell numbers decreased over the 24-hour period for *Phaeocystis* under all light regimes while diatoms remained at

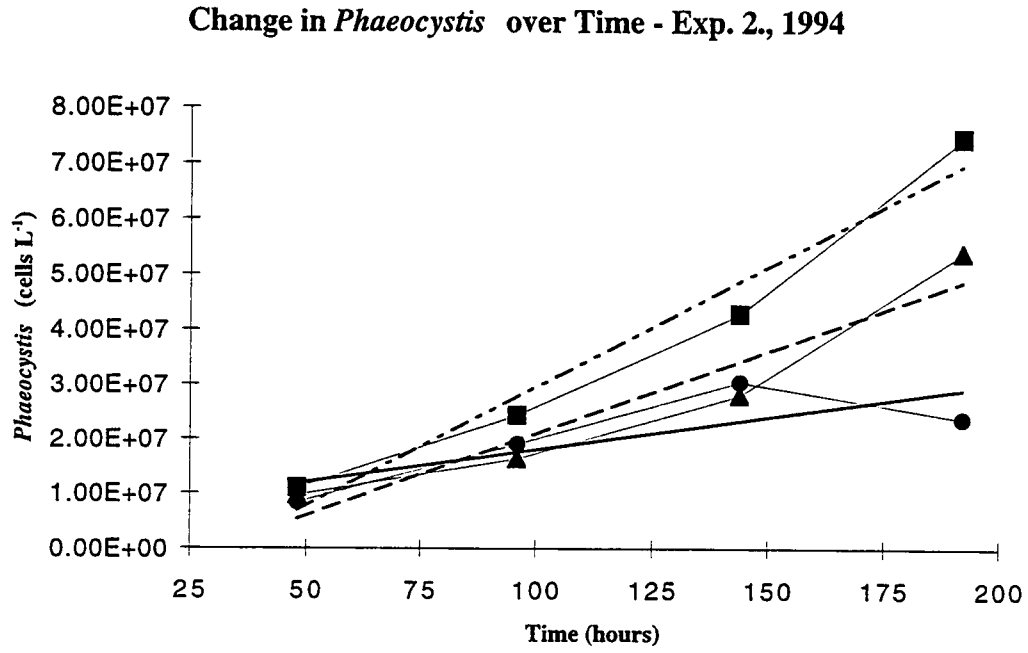

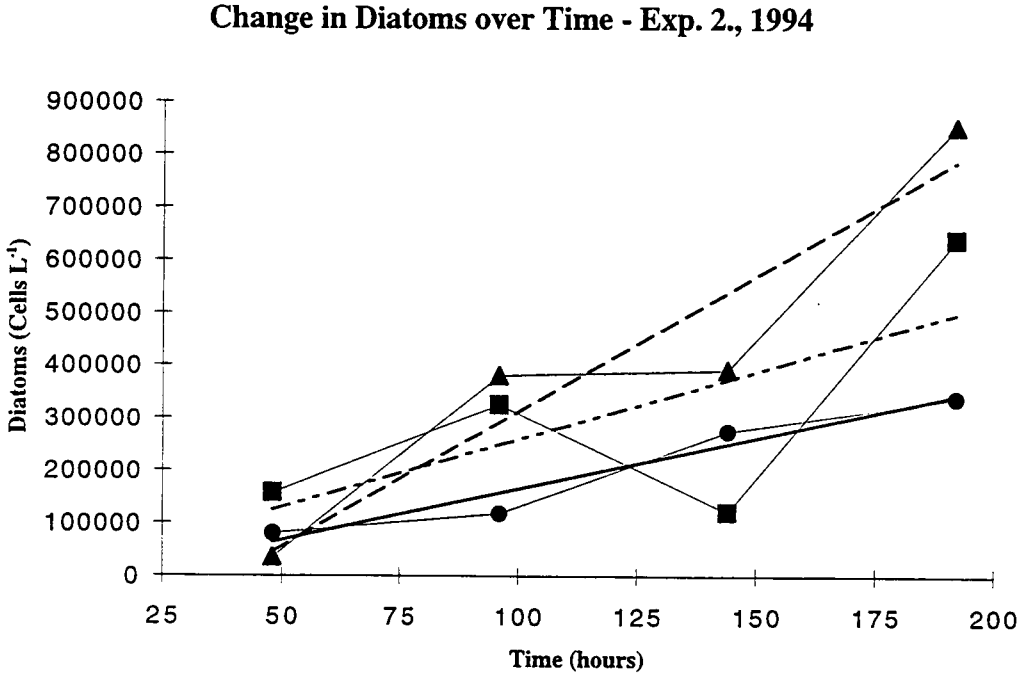

Figure 3.22 Change in cell numbers over time in experiment 2 for *Phaeocystis* (top) and diatoms (bottom). Dashed line and triangle=no-UVB, mixed dash line and square= partial UVB, solid line and circles= total UVB. Lines are linear regressions through the data.

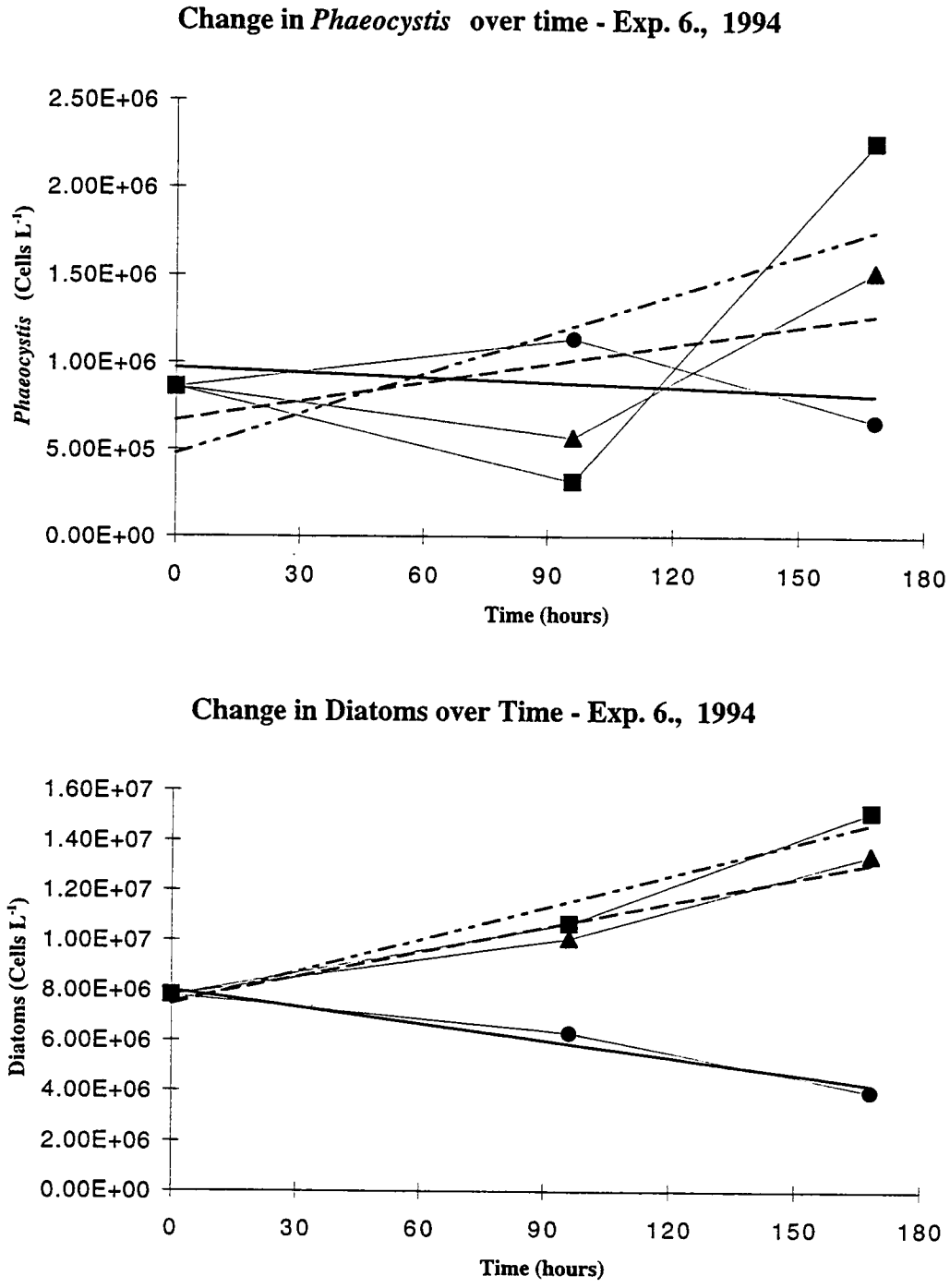

Figure 3.23: Change in cell numbers over time in Experiment 6 for *Phaeocystis* (top) and diatoms (bottom). Dashed line and triangle=no-UVB, mixed dash line and square= partial UVB, solid line and circles= total UVB. Lines are linear regressions through the data.

Table 3.13 : Summary of changes in cell numbers for RSP²95 UV experiments.

Experiment	Time (h)	Total Light			Minus Partial UVB			Minus Total UVB		
		Phaeocystis (cells L^{-1})	Diatoms (cells L^{-1})	Ratio P : D (%)	Phaeocystis (cells L^{-1})	Diatoms (cells L^{-1})	Ratio P : D (%)	Phaeocystis (cells L^{-1})	Diatoms (cells L^{-1})	Ratio P : D (%)
A	0	9.49E+06	2.15E+07	30.64						
	24	5.71E+06	2.28E+07	20.06	5.58E+06	2.03E+07	21.55	5.12E+06	2.21E+07	18.82
B	0	8.35E+06	2.62E+07	24.17						
	24	5.45E+06	1.75E+07	23.76	3.32E+06	1.43E+07	18.79	4.12E+06	1.96E+07	17.37
C	0	4.05E+06	1.11E+07	26.79						
	24	9.64E+06	1.11E+07	46.54	2.85E+06	1.16E+07	19.73	4.69E+06	1.08E+07	30.21
D	0	6.84E+06	1.91E+07	26.38						
	72	5.49E+06	3.39E+07	13.92	5.12E+06	3.59E+07	12.48	5.73E+06	3.27E+07	14.91
	120	1.04E+07	3.47E+07	23.09	9.86E+06	3.76E+07	20.80	9.87E+06	4.90E+07	16.75
E	0	3.26E+05	1.94E+07	1.66						
	24	2.95E+05	1.12E+07	2.56	3.97E+05	1.18E+07	3.26	2.07E+05	1.25E+07	1.62
F	0	4.52E+06	9.95E+06	31.26						
	24	1.47E+06	9.80E+06	13.08	5.03E+06	1.09E+07	31.59	3.58E+06	1.22E+07	22.67
G	0	3.36E+06	7.36E+06	31.34						
	72	1.62E+06	5.39E+06	23.07	7.73E+06	7.59E+06	50.46	8.46E+06	7.80E+06	52.03
	120	1.13E+07	7.86E+06	58.90	9.62E+06	8.04E+06	54.46	1.15E+07	9.02E+06	56.14
H	0	4.39E+04	2.31E+06	1.87						
	24	5.47E+04	2.83E+06	1.89	2.27E+04	2.66E+06	0.85	1.32E+04	2.34E+06	0.56

Note : Ratio P:D=Ratio of *Phaeocystis* to diatoms as a percentage.

similar concentrations. In experiment B a similar pattern was observed although diatoms also decreased in concentration. Experiment C showed an increase in *Phaeocystis* under total UV-B light, a decrease under partial UV-B exclusion and an increase under the total exclusion of UV-B. Diatoms in this experiment stayed at similar concentrations under total light, increased under partial UV-B exclusion and decreased under total UV-B exclusion. In experiment E both Phaeocystis and diatoms decreased in all treatments except *Phaeocystis* under partial UV-B exclusion. Experiment F *Phaeocystis* cell concentrations decreased under total light and under total exclusion of UV-B, and increased under partial UV-B exclusion while diatoms decreased under total light and increased in the other two light regimes. In experiment H *Phaeocystis* increased under total light and decreased under the other light regimes. Diatoms for this experiment increased in all cases.

The 5-day experiment D showed an initial decrease in *Phaeocystis* over time followed by an increase by day 5; there were no clear differences between light regimes (Figure 3.24 - top). Diatoms in experiment G increased over time with the total exclusion of UV-B yielding the highest cell concentrations on day 5 although the regressions were not significant (Figure 3.24 - bottom). In the second 5-day experiment (G) *Phaeocystis* increased over time with an initial decrease in the total light treatment (Figure 3.25 - top), while diatom cell concentrations changed little and there was also a small amount of variation between treatments.

The ratio of *Phaeocystis* to diatoms by cell number also showed a trend tc ,vard diatoms under UV-exclusion, with the exception of experiment F and experiment G after 3 days. The trend was much less clear than in 1994 and there was no clear differentiation between partial and total UV-B exclusion with respect to the ratio.

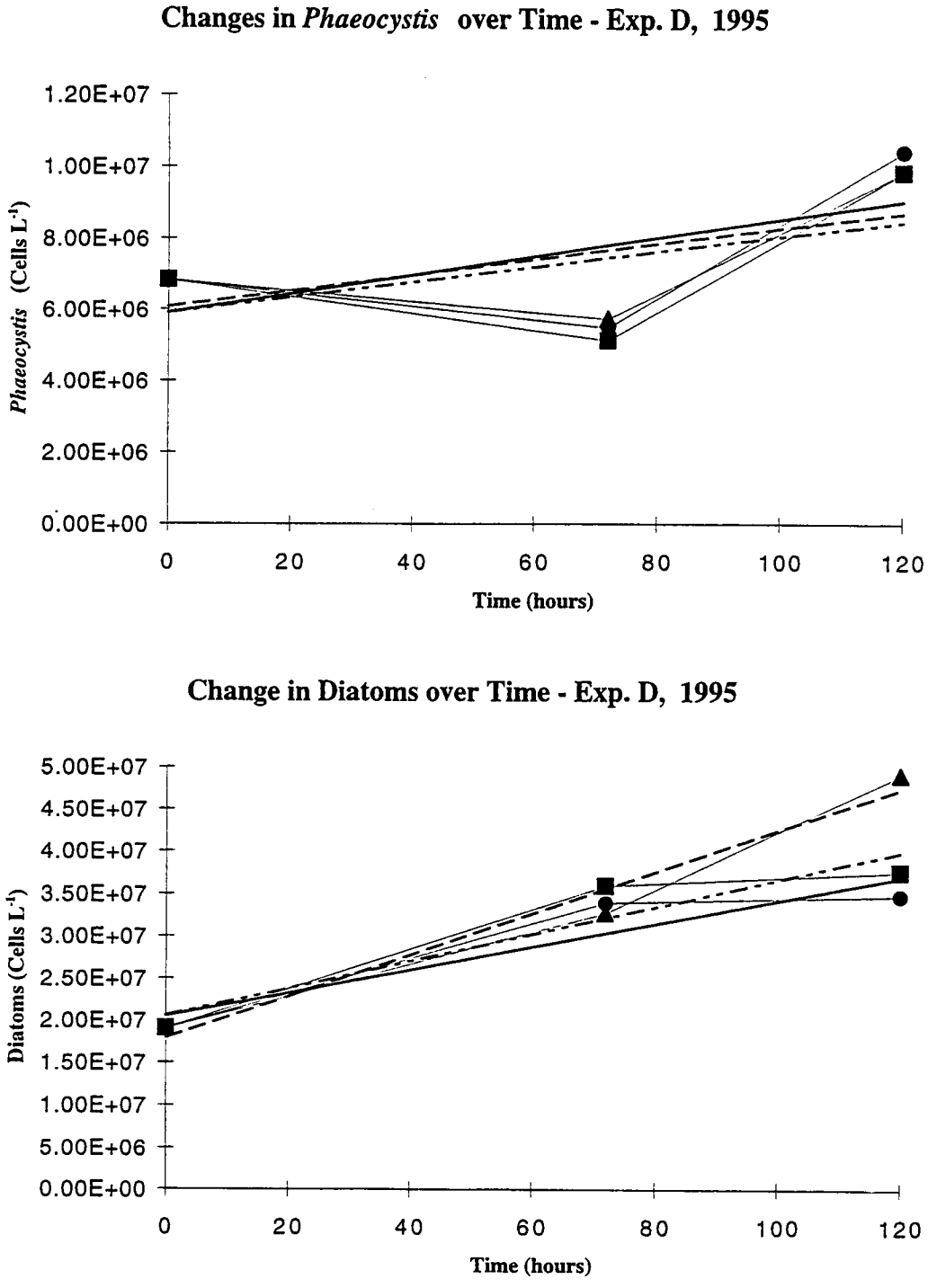

Figure 3.24 Change in cell numbers over time in experiment D for *Phaeocystis* (top) and diatoms (bottom). Dashed line and triangle=no-UVB, mixed dash line and square= partial UVB, solid line and circles= total UVB. Liines are linear regressions through the data

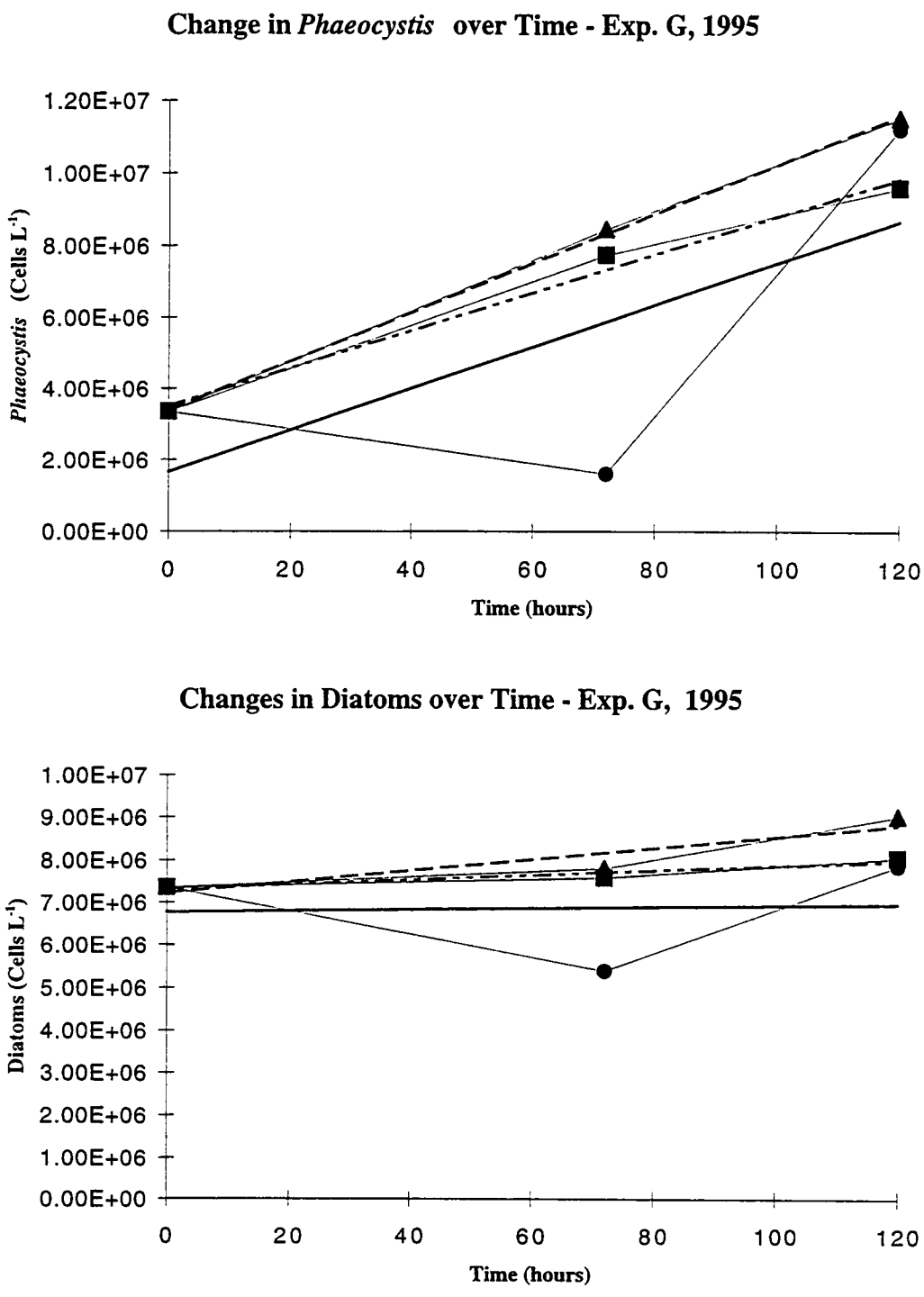

Figure 3.25 Change in cell numbers over time in experiment G for *Phaeocystis* (top) and diatoms (bottom). Dashed line and triangle=no-UVB, mixed dash line and square= partial UVB, solid line and circles= total UVB. Lines are linear regressions through the data

3.4.3 PIGMENT CONCENTRATIONS

Samples for HPLC pigments were not taken for experiment 2, but were collected at the beginning and end of all of the other 1994 experiments. 1994 pigment concentrations are summarized in Table 3.14. Hex-fucoxanthin can be considered a marker for *Phaeocystis* (Wright et al., 1991), while fucoxanthin is used as a marker for diatoms, although it is found in other phytoplankton as well (Wright et al., 1991). In the 24-hour experiments 1, 3, 4 and 5 all pigments decreased in concentration over time with no apparent differentiation between light regimes. In experiment 6, which ran for 7 days, there was also a decrease in all pigments. However, at the beginning of the experiment and under partial and total UV-B exclusion, concentrations of fucoxanthin were greater than hex-fucoxanthin while under total light, pigment concentrations were much lower overall, and the concentration of fucoxanthin was lower than the hex-fucoxanthin concentration.

Pigment concentrations in 1995 did not show the trends seen in the 1994 experiments (only experiments A, B, D and G were analyzed for pigments - see Table 3.15). Concentrations of fucoxanthin were much higher than in 1994, reflecting the increased contribution of diatoms in the algal assemblage, while hex-fucoxanthin concentrations were much lower. Experiment B, which was of 24-h duration, showed a decrease in pigment content over time, with hex-fucoxanthin decreasing to a greater extent than fucoxanthin (Figure 3.26); there was no differentiation between light regimes. Unlike the 1994 long term experiment there was little difference between light treatments for either experiment D or G with respect to the concentrations of fucoxanthin or hex-fucoxanthin (Figures 3.27 and 3.28). In both experiments there was an initial decrease in pigment content with a gradual increase by the end of the experiment (except in experiment D where fucoxanthin concentrations were greatest on day 3).

Table 3.14 : Concentrations of pigments from UV experiments as determined by HPLC for RSP²94.

Experiment	Treatment		Pigment Concentrations (μg L^{-1})						
	Time (h)	UV Regime	[C1+C2]	[Peridinin]	[19-But]	[Fucox]	[19 Hex]	[Chl B]	[Chl A]
1	0		1.188	0.000	0.036	0.107	1.658	0.124	1.001
	24	Total Light	0.518	0.000	0.012	0.039	0.599	0.000	0.483
	24	- Part UVB	0.505	0.000	0.019	0.038	0.566	0.067	0.457
	24	- Total UVB	0.439	0.000	0.010	0.052	0.545	0.047	0.407
3	0		0.890	0.011	0.061	0.311	1.226	0.089	0.631
	24	Total Light	0.504	0.005	0.013	0.190	0.747	0.042	0.390
	24	- Part UVB	0.410	0.000	0.006	0.169	0.408	0.035	0.046
	24	- Total UVB	0.352	0.003	0.011	0.151	0.427	0.039	0.319
4	0		0.924	0.000	0.022	0.096	0.803	0.000	0.910
	24	Total Light	0.527	0.000	0.011	0.054	0.510	0.026	0.479
	24	- Part UVB	0.550	0.000	0.011	0.037	0.468	0.066	0.459
	24	- Total UVB	0.219	0.000	0.006	0.022	0.204	0.021	0.250
5	0		2.666	0.000	0.049	0.295	3.754	0.061	2.289
	24	Total Light	1.003	0.000	0.012	0.087	1.205	0.064	0.976
	24	- Part UVB	1.170	0.000	0.016	0.119	1.298	0.125	1.178
	24	- Total UVB	1.200	0.000	0.017	0.133	1.309	0.000	1.089
6	0		0.718	0.000	0.012	0.479	0.342	0.016	0.770
	168	Total Light	0.147	0.000	0.000	0.067	0.117	0.000	0.154
	168	- Part UVB	0.657	0.022	0.000	0.399	0.221	0.000	0.638
	168	- Total UVB	0.489	0.015	0.000	0.309	0.206	0.000	0.587

Note : C1+C2 = chlorophyll C1 and C2; 19-But = 19'butanoyloxyfucoxanthin; Fucox = Fucoxanthin; 19-Hex = 19'hexanoyloxyfucoxanthin; Chl b = Chlorophyll b; Chl a = Chlorophyll a.

Table 3.15 : Concentrations of pigments from UV experiments as determined by HPLC for RSP²95.

Experiment	Treatment		Pigment Concentrations (μg L^{-1})				
	Time (h)	UV Regime	[C1+C2]	[Peridinin]	[Fucox]	[19 Hex]	[Chl A]
A	12	Total Light	0.0005	0.0000	0.4772	0.2634	0.7956
	12	- Part UVB	0.0005	0.0000	0.4844	0.3606	0.7630
	12	- Total UVB	0.0005	0.0000	0.4626	0.2590	0.8303
	24	Total Light	0.0003	0.0000	0.3765	0.1500	0.5623
	24	- Part UVB	0.0004	0.0000	0.3503	0.1595	0.5970
	24	- Total UVB	0.0004	0.0000	0.4904	0.1646	0.6730
B	0	-	0.0015	0.0148	1.0043	1.3987	1.9267
	12	Total Light	0.0006	0.0000	0.8170	0.3882	1.0605
	12	- Part UVB	0.0007	0.0000	0.8028	0.4723	0.9225
	12	- Total UVB	0.0007	0.0000	0.8232	0.4413	0.8895
	24	Total Light	0.0004	0.0000	0.5439	0.3220	0.7885
	24	- Part UVB	0.0005	0.0000	0.7703	0.4726	0.9831
	24	- Total UVB	0.0005	0.0000	0.7885	0.3646	0.9139
D	0		0.0003	0.0000	0.5841	0.3585	0.8045
	24	Total Light	0.0002	0.0000	0.4223	0.1321	0.5288
	24	- Part UVB	0.0002	0.0000	0.5253	0.1807	0.7178
	24	- Total UVB	0.0002	0.0000	0.4356	0.1142	0.5615
	72	Total Light	0.0002	0.0000	0.6802	0.0811	1.0193
	72	- Part UVB	0.0004	0.0000	0.5536	0.0855	0.8555
	72	- Total UVB	0.0002	0.0000	0.7539	0.0889	1.1406
	120	Total Light	0.0003	0.0044	0.5035	0.0755	0.8120
	120	- Part UVB	0.0004	0.0000	0.5790	0.1330	0.9614
	120	- Total UVB	0.0005	0.0000	0.5612	0.1126	0.9942
G	0		0.0006	0.0000	0.2662	0.7387	0.6683
	24	Total Light	0.0002	0.0000	0.1679	0.1280	0.3199
	24	- Part UVB	0.0002	0.0000	0.1636	0.1901	0.3271
	24	- Total UVB	0.0002	0.0000	0.1580	0.1415	0.2640
	72	Total Light	0.0002	0.0000	0.1316	0.1803	0.3521
	72	- Part UVB	0.0002	0.0000	0.1482	0.2240	0.4146
	72	- Total UVB	0.0002	0.0000	0.1550	0.1893	0.3758
	120	Total Light	0.0004	0.0000	0.1447	0.3349	0.6871
	120	- Part UVB	0.0005	0.0000	0.1915	0.4327	0.7983
	120	- Total UVB	0.0004	0.0000	0.1668	0.3033	0.6940

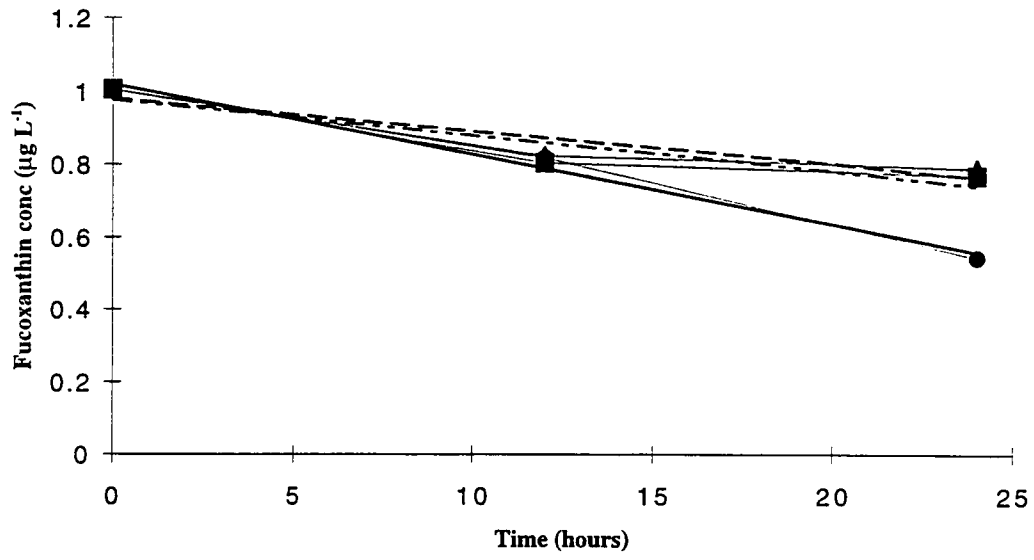

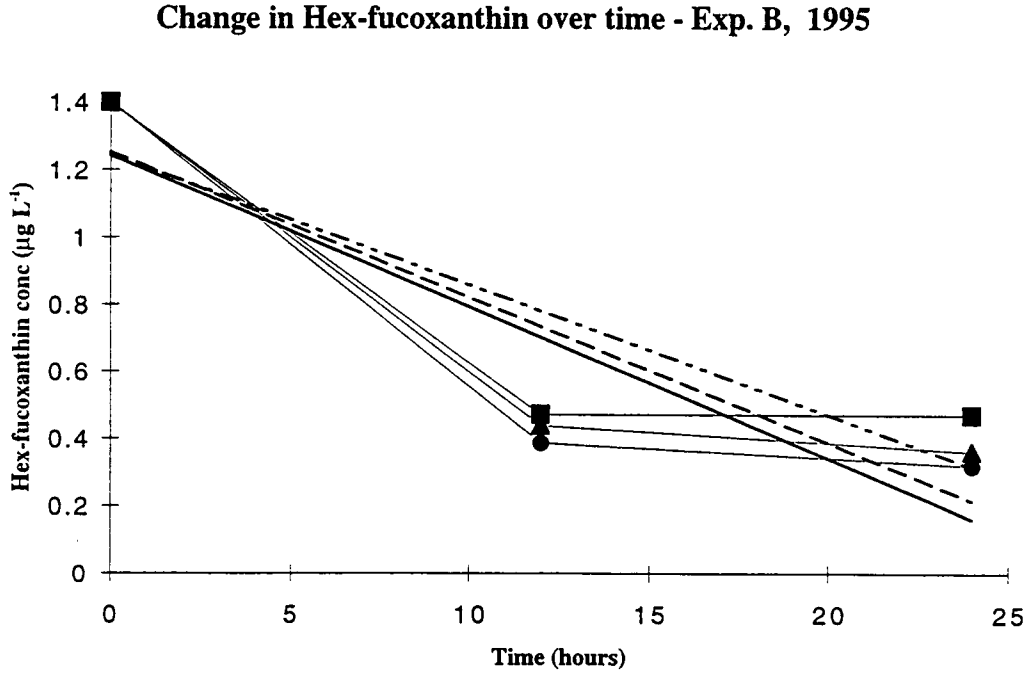

Figure 3.26 : Changes in concentrations of fucoxanthin (top) and hex-fucoxanthin (bottom) for experiment B. Lines are linear regressions through the data

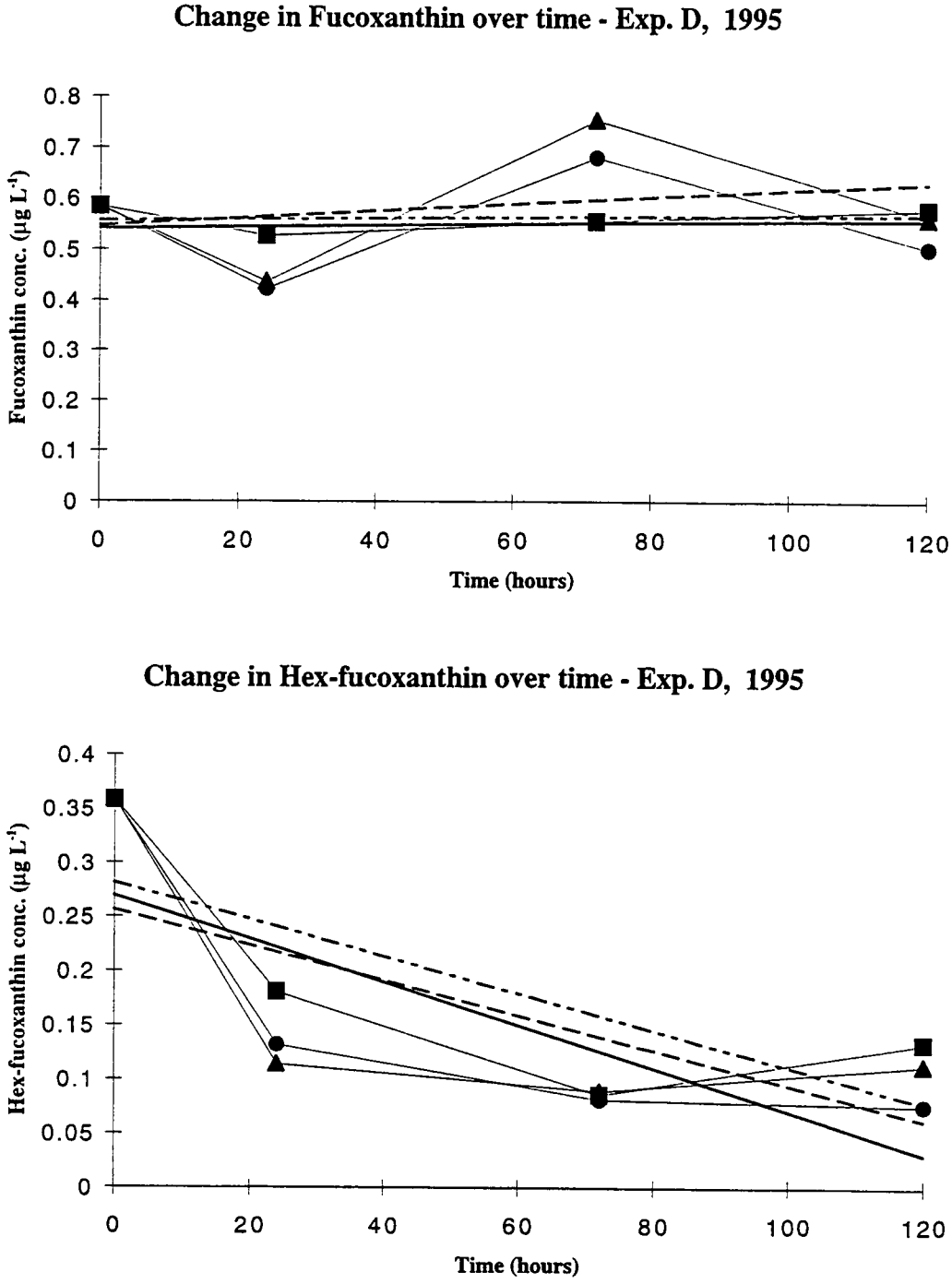

Figure 3.27 : Changes in concentrations of fucoxanthin (top) and hex-fucoxanthin (bottom) for experiment D. Lines are linear regressions through the data.

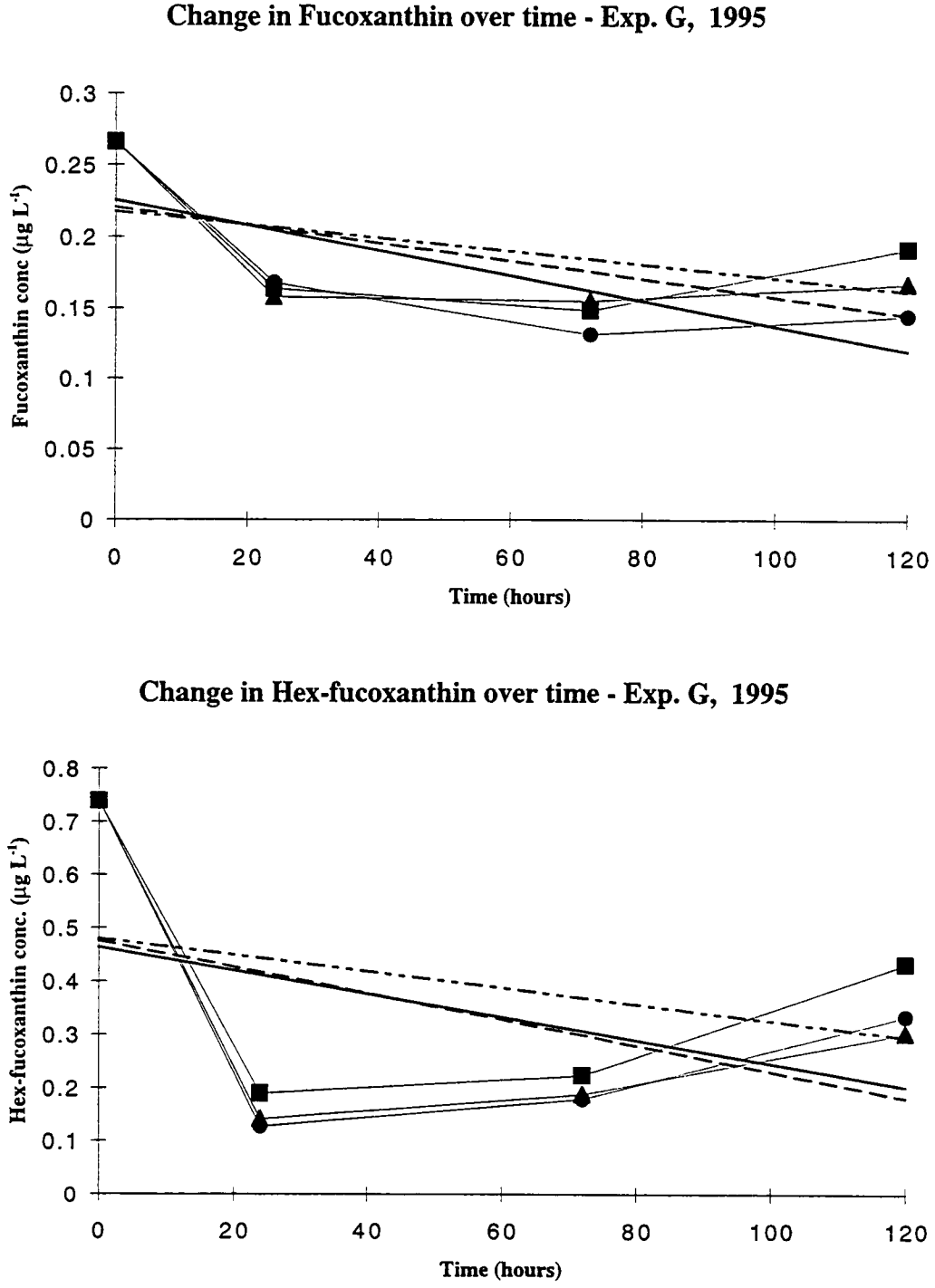

Figure 3.28 : Changes in concentrations of fucoxanthin (top) and hex-fucoxanthin (bottom) for experiment G. Lines are linear regressions through the data.

3.4.4 PRIMARY PRODUCTION

^{14}C-production measurements showed a large amount of variation between experiments in 1994 (Table 3.16). This parameter was only measured for the four 24-hour experiments (1, 3, 4, and 5). In three of four experiments there was an increase in production with the removal of partial UV-B wavelengths, and in two of four there was an increase in production with the total removal of UV-B. These variations did not correspond to a particular species assemblage. Average increases in production compared with total UV-B measures were 26 % and 37 % for partial and total UV-B exclusion, respectively.

Production rates on the 1995 cruise also showed a great deal of variation between the experiments (Table 3.17). There was an increase in production with the complete exclusion of UV-B in all but experiment F, and partial UV-B exclusion yielded higher production rates in all but E and F (E showed a very small decrease in production under partial UV-B exclusion). Average increases in production were 36 and 70% for partial and total UV-B exclusion, respectively. There was no clear difference between the light regimes in experiment D over the 120 hour period (Figure 3.29 - top). For experiment G the production rates at the end of the experiment for the UV-B excluded treatment were higher than those for the partial exclusion and total light treatments (Figure 3.29 - bottom).

3.4.5 PHOTOSYNTHETIC PARAMETERS (1995 ONLY)

The measurement of P/I parameters on days 3 and 5 of the two longer experiments (D and G) revealed that P_{max} was greater in all cases with partial UV-B exclusion (Table 3.18). For the total UV-B exclusion treatment (except day 3 of experiment G,) P_{max} was also higher (see Figures 3.30 and 3.31 for Exp. D, 3 and 5 day P/I curves). The index

Table 3.16 : Productivity measurements from UV Experiments for RSP²94.

Experiment	Time (h)	Total Light	Minus Partial UVB		Minus Total UVB	
		Chl-spec. Production mg C (mg Chl)$^{-1}$ day^{-1}	Chl-spec. Production mg C (mg Chl)$^{-1}$ day^{-}	Δ Production (%)	Chl-spec. Production mg C (mg Chl)$^{-1}$ day^{-}	Δ Production (%)
1	24	1.302	0.907	-30.314	0.973	-25.25
3	24	0.465	0.587	26.085	1.006	116.05
4	24	0.489	0.758	55.115	0.966	97.67
5	24	0.285	0.437	53.580	0.169	-40.81
	Sum	2.541	2.690	104.466	3.113	147.661
	Mean	0.635	0.672	26.117	0.778	36.915

Figure 3.17 Productivity measurements from UV experiments for RSP²95.

Experiment	Time (h)	Total Light	Minus Partial UVB		Minus Total UVB	
		Chl-spec. Production mg C (mg Chl)$^{-1}$ day^{-1}	Chl-spec. Production mg C (mg Chl)$^{-1}$ day^{-1}	Δ Production (%)	Chl-spec. Production mg C (mg Chl)$^{-1}$ day^{-1}	Δ Production (%)
A	24	0.248	0.392	58.322	0.437	76.418
B	24	0.182	0.259	42.424	0.338	85.413
C	24	0.219	0.325	48.693	0.324	48.172
D	24	0.497	0.473	-4.749	0.856	72.241
	72	0.334	0.433	29.605	0.393	17.554
	120	0.489	0.592	21.024	0.638	30.466
E	24	0.460	0.452	-1.777	0.526	14.317
F	24	0.805	0.474	-41.121	0.450	-44.081
G	24	-0.752	-0.924	-22.931	-0.963	-28.119
	72	0.098	0.295	201.554	0.166	70.147
	120	0.361	0.400	10.648	1.151	218.825
H	24	-0.602	-0.352	41.503	-0.595	1.107
	Sum	2.339	2.819	383.196	3.721	562.461
	Mean	0.195	0.235	31.933	0.310	46.872

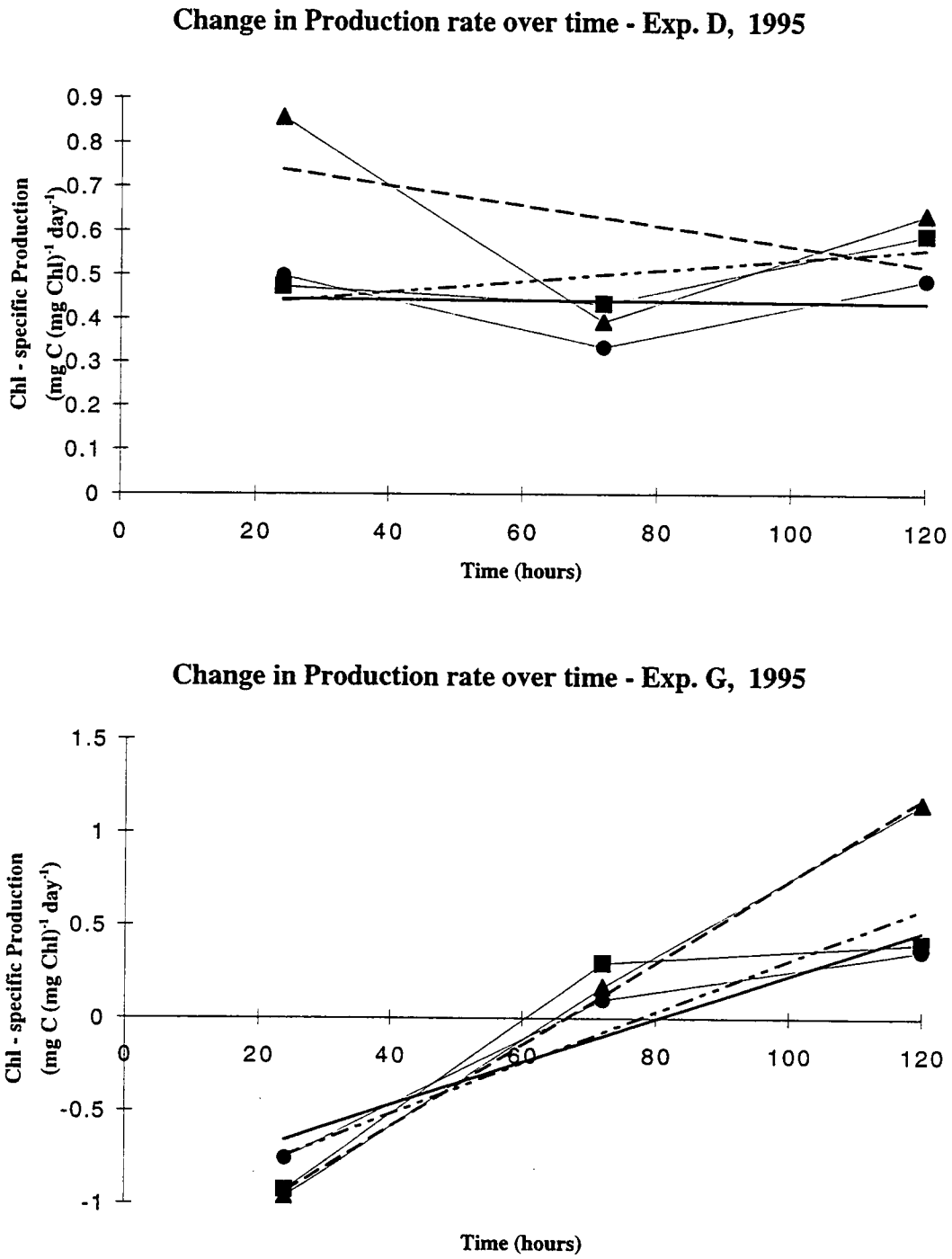

Figure 3.29 : Change in production rates over time for UV experiments D (top) and G (bottom). Lines are linear regressions through the data.

Table 3.18 : Summary of changes in P/I parameters over time for RSP²95 UV 5-day experiments.

Experiment	Time (days)	UV Regime	α	β	P_{max}	I_m	I_k
D	0		0.0651	0.0002	0.2714	24.639	4.169
	3	total light	0.0058	0.0000	0.5668	398.474	97.724
	3	-partial UVB	0.0174	0.0001	0.7516	231.139	43.196
	3	-total UVB	0.0086	0.0000	1.0858	563.847	126.256
	5	total light	0.0083	0.0009	0.7648	305.498	92.149
	5	-partial UVB	0.0311	0.0014	1.3744	167.320	44.193
	5	-total UVB	0.0141	0.0016	1.2012	280.712	85.194
G	3	total light	0.0090	0.0004	0.6034	254.349	67.040
	3	-partial UVB	0.0256	0.0002	0.9487	188.527	37.058
	3	-total UVB	0.0058	0.0000	0.5263	370.001	90.741
	5	total light	0.0231	0.0004	1.4101	271.447	61.045
	5	-partial UVB	0.0371	0.0006	1.8137	219.937	48.888
	5	-total UVB	0.0505	0.0025	2.8915	213.472	57.257

Note : Units - α, β: mg C (mg Chl)$^{-1}$ h^{-1} (μE m^{-2} s^{-1})$^{-1}$; P_{max}: mg C (mg Chl)$^{-1}$ h^{-1}; I_m, I_k: μE m^{-2} s^{-1}.

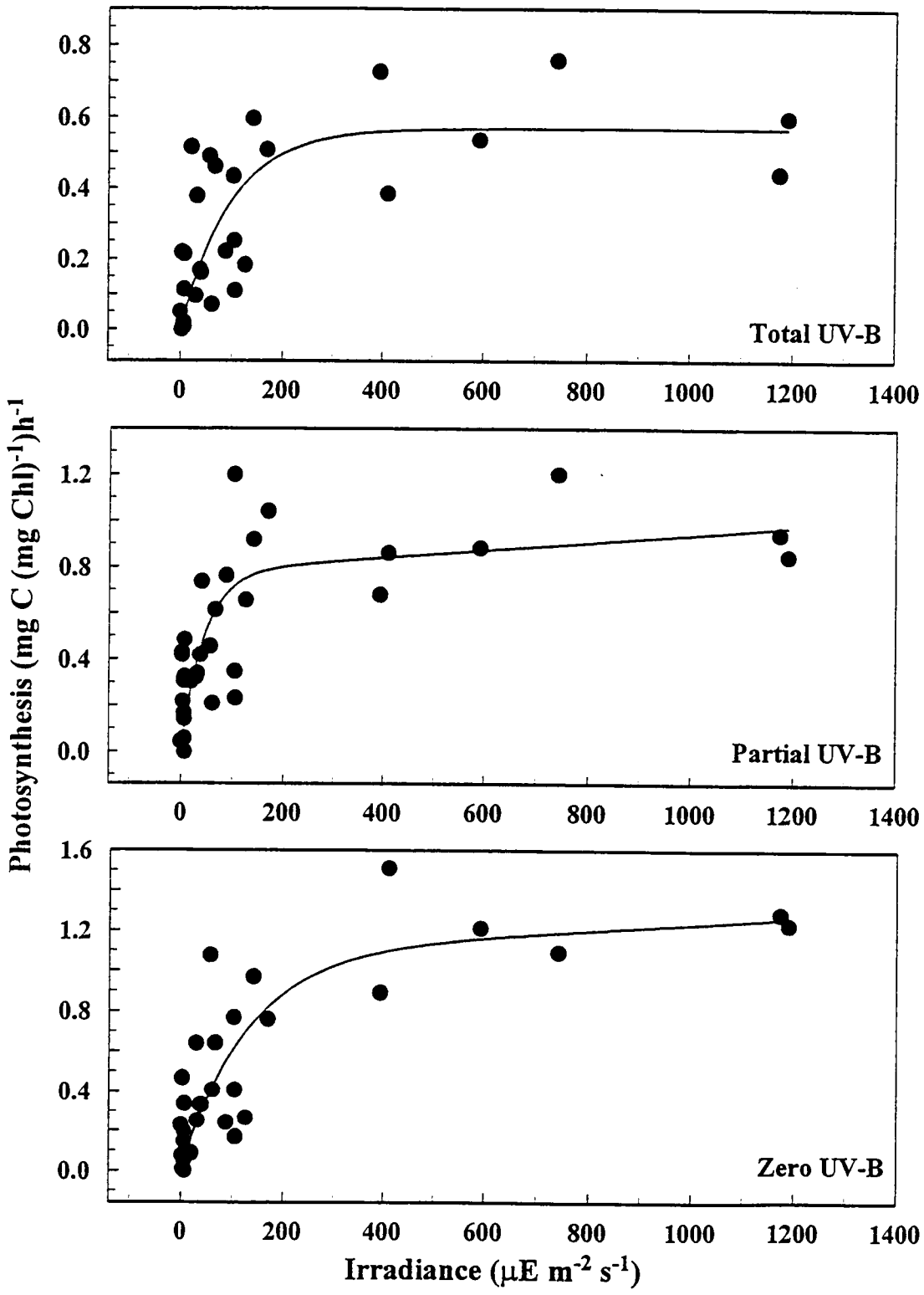

Figure 3.30 : Photosynthesis as a function of irradiance for experiment D after 3 days under the three different UV regimes.

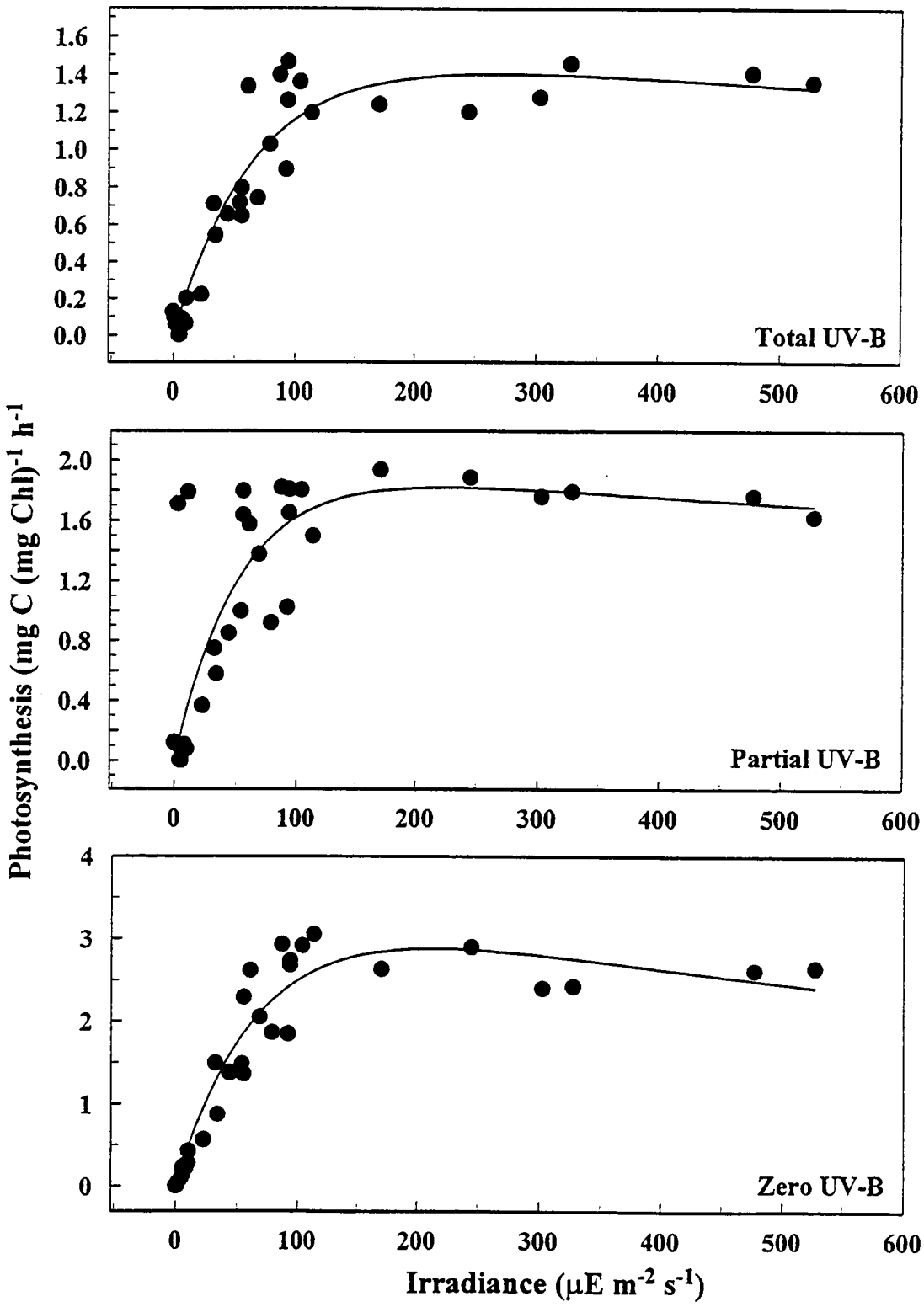

Figure 3.31 : Photosynthesis as a function of irradiance for experiment D after 5 days under the three different UV regimes.

of photoinhibition, β, increased over time in both experiments with no clear distinction with respect to light regime. The initial slope of the P/I curve, α, was higher under partial and total UV-B exclusion, except on day 3 of experiment G where the total UV-B exclusion sample had a lower α than the total light treatment. In all cases P_{max} and α for every light level increased from day 3 to day 5, (Figure 3.32) while β either increased or remained the same (see figures 3.33 and 3.34). There were no trends of variation in I_k, the light saturation onset parameter (Figure 3.32 - bottom).

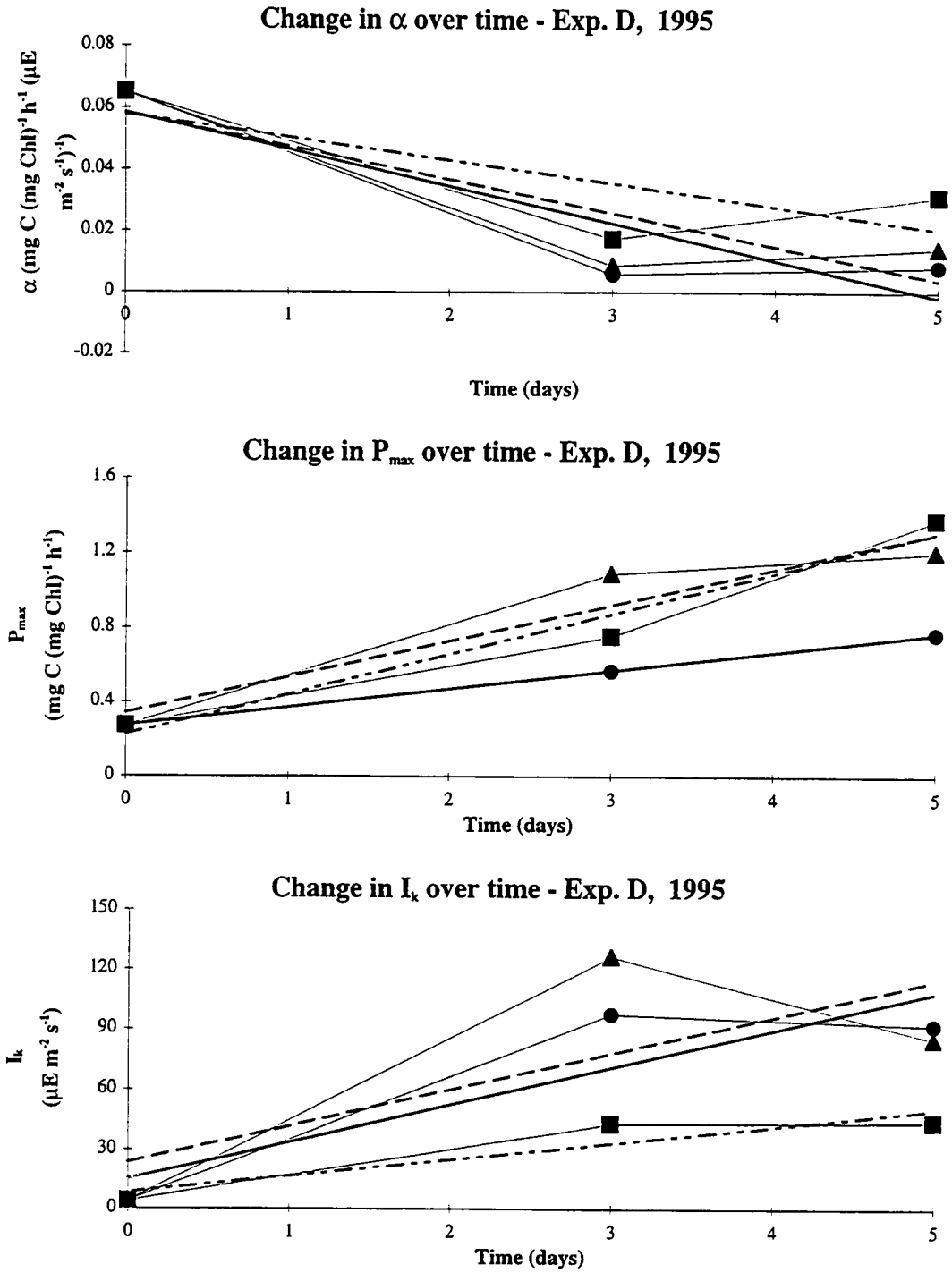

Figure 3.32 : Change in photosynthetic parameters over time for experiment D. α= initial slope of the P/I curve (top), P_{max}= maximum photosynthetic rate (middle) and I_k= the saturation onset parameter (bottom). Heavy lines are linear regressions through the data.

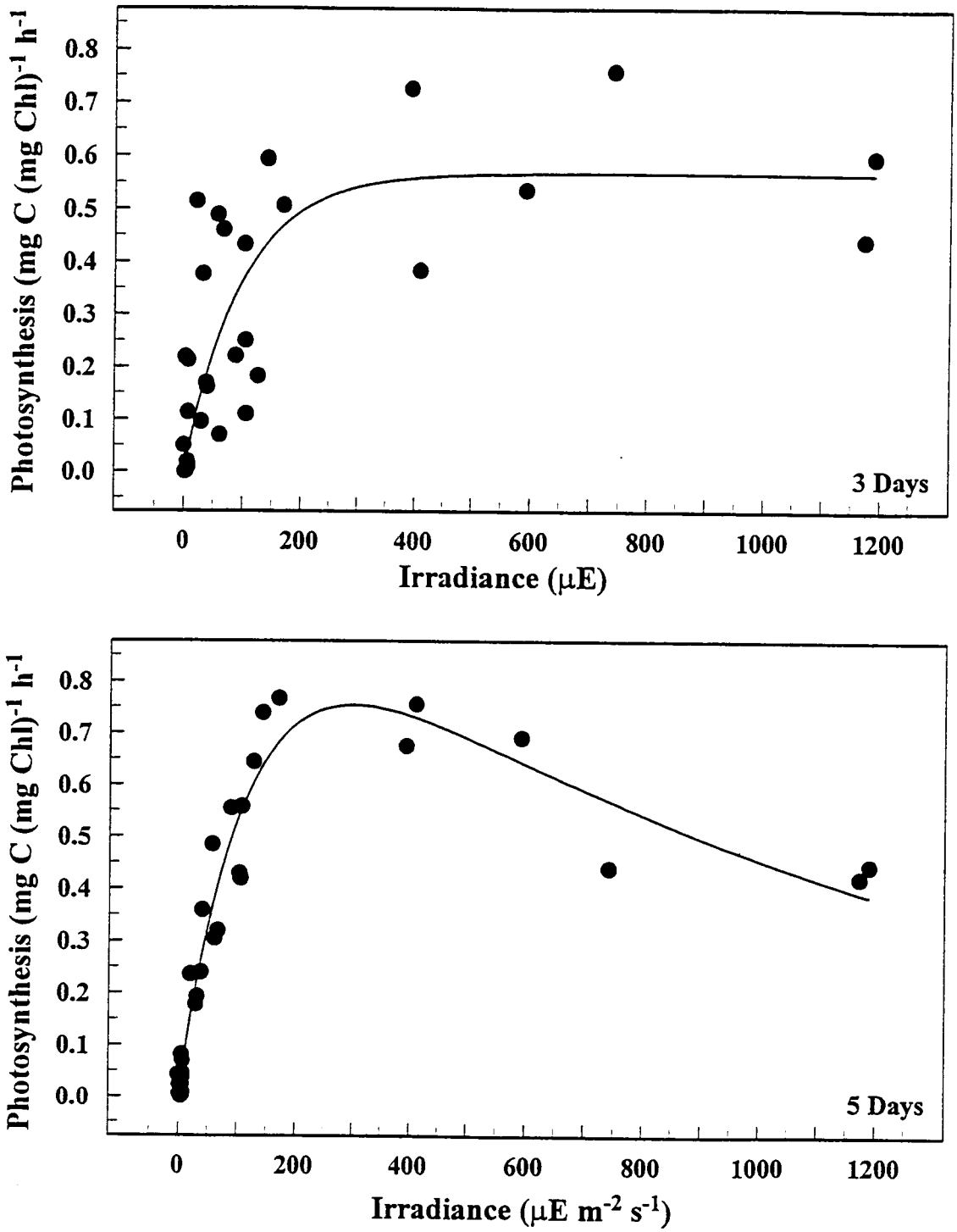

Figure 3.33 : Photosynthesis as a function of irradiance for experiment D after 3 (top) and 5 (bottom) days under total light conditions.

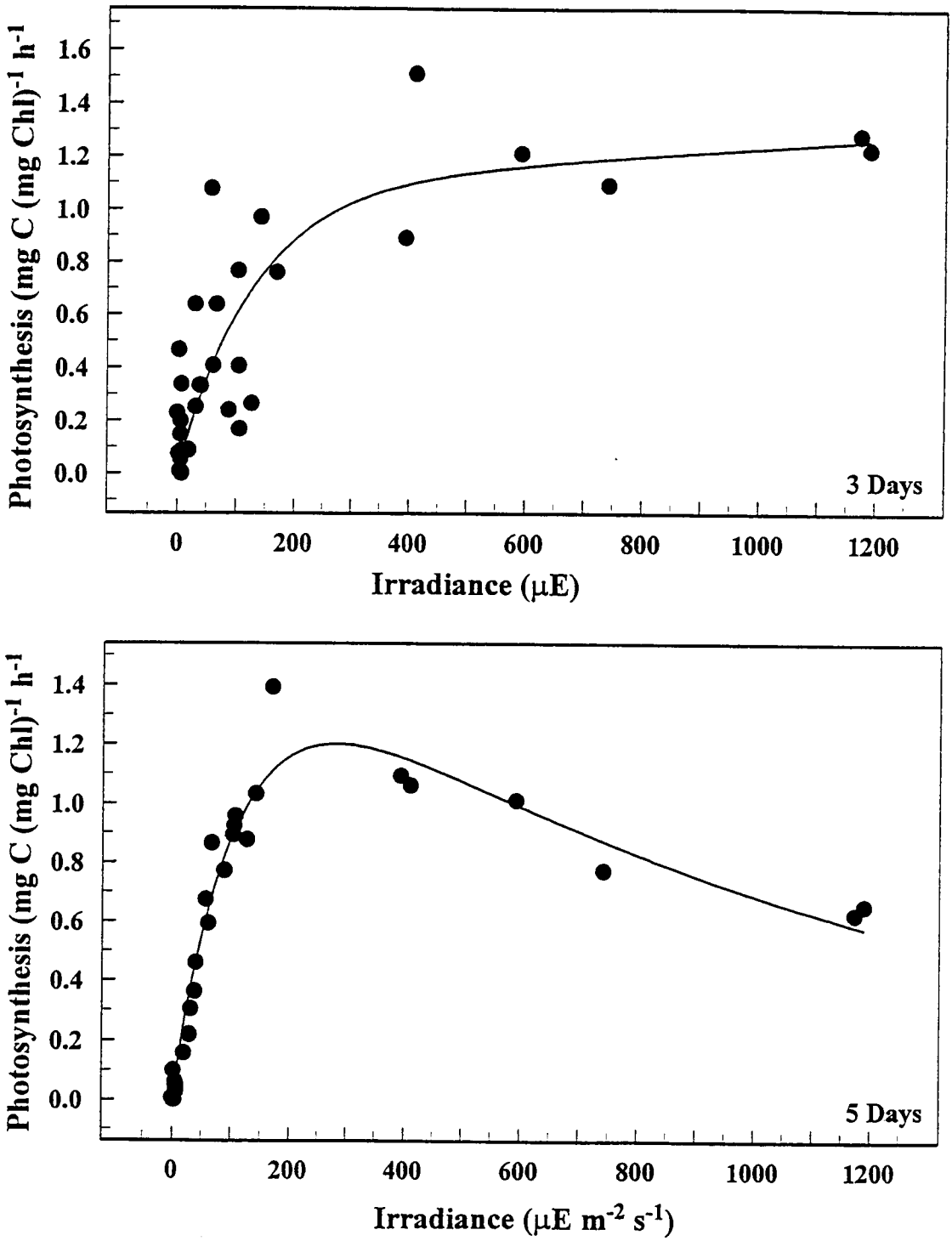

Figure 3.34 : Photosynthesis as a function of irradiance for experiment D after 3 (top) and 5 (bottom) days under total UV-B exclusion.

4. DISCUSSION AND CONCLUSIONS

4.1 DISCUSSION

A well developed region of depleted ozone concentrations or 'ozone hole' has been observed over the Antarctic continent for nearly two decades. This ozone depletion results in UV-B fluxes in spring comparable to those in summer, and phytoplankton are therefore exposed to a greatly extended period of elevated UV-B irradiances. In the austral spring when the ozone hole is present, extensive phytoplankton blooms occur in the Ross Sea polynya. These blooms are initially made up almost entirely of *Phaeocystis* sp. with diatoms becoming more abundant later in the year; *Nitzschia subcurvata* is the dominant diatom in the system. Measurements of daily irradiance (both photosynthetically active radiation (PAR) and UV wavelengths) from the two cruises on which data were collected showed a large amount of variation at all wavelengths. Similar UV fluxes were seen on both cruises, although the 1995/96 cruise had a higher average at all but 340 nm. These data are consistent with ozone depletion resulting in high spring UV-B irradiances similar to summer fluxes. Images of stratospheric ozone concentrations obtained from NOAA supported this finding, showing that a well developed ozone hole was present in the vicinity of the polynya for the first part of the 1994 cruise, gradually dissipating until normal ozone levels were re-established in mid-December.

Daily light profiles at local noon using a PUV 500 ultraviolet radiometer indicated that UV-B irradiances penetrated significantly into the water column. In 1994 a maximum observed penetration (to 1% of surface irradiance) of 16 m was observed for the 308 nm

waveband and 14 m in 1995/96. For the 320 nm waveband depths of 34 and 27 m were seen for 1994 and 1995/96, respectively. Mixed layer depths during both cruises averaged approximately 30 m (Smith and Gordon, 1997). Therefore, longer wavelength UV-B (320 nm) is penetrating at its deepest through most of the mixed layer and shorter wavelength UV-B (308 nm which is more harmful than the longer wavelengths of UV-B; Cullen et al., 1992; Lubin et al., 1992) through nearly half of the mixed layer. Even when light is more rapidly attenuated, minimum penetration depths of approximately 5 m for 308 nm and 10 m for 320 nm were seen.

The vertical attenuation coefficients calculated from the light profiles varied greatly. The correlation analysis of these coefficients with other parameters such as chlorophyll concentrations, particulate carbon (POC) and nitrogen (PON) concentrations, and primary productivity showed that chlorophyll was positively correlated with K (the vertical attenuation coefficient) at all wavelengths in both years, as were POC and PON. K_{PAR} and K_{380} were most closely correlated with chlorophyll, POC and PON. This may be because PAR and UV-A (380 nm) both penetrate further into the water column than the shorter UV-B wavelengths, and therefore may exert a stronger influence on phytoplankton throughout the euphotic zone. Also, the shorter wavelengths (308 and 320 nm) are absorbed more strongly by sea water itself rather than by the particles therein. These results indicate that phytoplankton are an important attenuator of light in these waters, particularly at the longer wavelengths. In open ocean waters phytoplankton are usually the major attenuators of light along with the sea water itself, while in coastal regions sediments play a much larger role (Kirk, 1994).

The physical data outlined above indicates that ozone depletion could potentially have an

ecological impact on the Ross Sea polynya phytoplankton assemblages with high UV-B fluxes in spring which penetrate through a large portion of the mixed layer. Experimental observations of the response of phytoplankton to variations in UV-B fluxes (ambient, partial UV-B exclusion and total UV-B exclusion) revealed that the biological effects of enhanced UV-B may decrease productivity and alter species composition of the phytoplankton assemblage in favor of *Phaeocystis*.

Chlorophyll levels decreased in all treatments in experiments on RSP^{2}94. There was no clear differentiation between the three light regimes, with four out of six experiments showing higher chlorophyll reduction under UV-B exclusion while the other two experiments showed greater decreases in the UV-B-excluded treatments. In 1995 these decreases of chlorophyll were again observed (except that in the long-term experiments chlorophyll increased after an initial decrease), but again there was no significant difference in this response under the different UV-B regimes. These results differ from those of El-Sayed et al. (1990), who found significantly less loss of chlorophyll under UV-B exclusion using similar methods and under similar conditions. The observed reduction in chlorophyll *a* seen in my experiments can be explained as a consequence of the phytoplankton being placed in a higher light environment than that from which they were sampled. Even though samples for the experiments were collected from surface waters, irradiances in the on-deck incubators were still higher than the in situ conditions, particularly if vertical mixing is taken into account. When phytoplankton are placed in a higher light environment they no longer require such high concentrations of pigments (including chlorophyll *a*) to absorb photons for photosynthesis, and as a result the number of photosynthetic units (composed of a complex of pigments) decreases (Kirk, 1994 and references therein). In these experiments it appears that this adaptation to high

light dwarfs any change in chlorophyll which might be seen as a result of exposure to the different UV-B regimes.

In contrast to the effects on chlorophyll, cell counts from 1994 experiments revealed a variable response of phytoplankton to the three experimental light regimes. Not only was there a difference in total cell concentrations under the different light regimes (with UV-B exclusion (partial or total) resulting in comparatively higher cell numbers), there was also a difference in the response to the light regimes between *Phaeocystis* and diatoms. The ratio of *Phaeocystis* to diatoms decreased when UV-B was completely excluded in eight out of ten observations and in five out of ten when UV-B was partially excluded. Absolute counts of *Phaeocystis* and diatoms showed that under UV-B exclusion diatoms nearly always increased, while *Phaeocystis* did not show this trend. These results imply that diatoms are more inhibited by UV-B fluxes than *Phaeocystis,* and therefore, when this negative impact is removed, diatoms are able to compete more successfully with *Phaeocystis*. In 1995, the results were more equivocal with five out of eight of the experiments decreasing in *Phaeocystis* cell numbers with respect to diatoms under UV-B exclusion, while in two out of eight this ratio increased under partial UV-B exclusion and decreased under total UV-B exclusion.

The different responses of *Phaeocystis* and diatoms to changes in UV-B could also be seen in the changes in pigment concentrations, although the response was not as clear. The pigment fucoxanthin can be considered a diatom marker, while hex-fucoxanthin is an indicator of *Phaeocystis* (Wright et al., 1991). In the 24 hour experiments all pigments (including chlorophyll *a*) were seen to decrease, remaining in similar proportions to one another. This would appear to be a response of the whole

photosynthetic complex to a higher light regime. Experiment 6, which ran for seven days, initially had fucoxanthin concentrations which were greater than the hex-fucoxanthin concentrations. Under total light this was still the case at the end of the experiment (although the concentrations were lower). However, under partial and total UV-B exclusion, fucoxanthin concentrations were higher than hex-fucoxanthin concentrations and total pigment concentrations were also higher than under total light indicating again that diatoms seem to benefit more from UV-B exclusion than *Phaeocystis* (although higher total pigment concentrations indicate that both groups benefit to a certain extent from UV-B exclusion). HPLC samples were unfortunately not taken for the other long-term experiment 2, but cell numbers suggest that a similar relationship would have been seen. The difference between 24 and 120-hour experiments is important, as it indicates that the time of exposure to enhanced UV-B determines the extent of UV-B damage. As such, mixed layer depths, mixing rates and depths of UV-B penetration strongly influence the impact of UV-B on pigment concentrations and on phytoplankton as a whole. In 1995 there was little variation in pigment concentrations under the different light regimes, and there was also no observable difference in the response of fucoxanthin compared to hex-fucoxanthin. This would seem to suggest that the phytoplankton assemblage in the summer is adapted to the ambient UV-B levels. Since summer UV-B levels are unaffected by the ozone hole, which has dissipated by this time, this is not unexpected. Alternatively this response may be due to the larger proportion of solitary *Phaeocystis* cells which are present later in the year and have been found to be more UV-B sensitive than *Phaeocystis* cells in colonies (Davidson and Marchant, 1994). This may result in diatoms and *Phaeocystis* being similarly UV-B sensitive. The actual summer response is probably a combination of both adaptation and changes in the morphology of *Phaeocystis*.

Production levels increased on average in both years under UV-B exclusion. However, 1994 results were somewhat equivocal, with production actually decreasing in two out of four of the experiments under either partial or total UV-B exclusion. In 1995 six out of eight experiments showed increases in production under total UV-B exclusion. These results may reflect the increased proportion of diatoms in the assemblage in 1995 which, as is evident from cell counts and pigment concentrations, appear to be more UV-B sensitive. It may also be due to the increased proportion of the more UV-B sensitive solitary *Phaeocystis* cells. Many studies have previously shown that the current standard method of measuring primary production (through ^{14}C incorporation into cells incubated in UV-B-opaque vessels) results in a production overestimate (Lorenzen, 1979; Smith and Baker, 1979; Smith and Baker, 1980). The increased production rates seen in my experiments with UV-B exclusion indicate that current measurements of primary production in the Ross Sea polynya are probably also overestimated. This is particularly the case for surface waters where UV-B effects are felt most strongly. The differential response of *Phaeocystis* and diatoms to increased UV-B may also cause the late spring diatom-dominated production measurements to be more spurious than the *Phaeocystis*-dominated assemblage, which is less UV-B sensitive, although there does seem to be some adaptation by diatoms to the UV-B levels in the summer.

Photosynthetic parameters were only determined in the longer experiments in 1995/96, and as such the results can not be said to signify any seasonal or species variations, but are simply a response of photosynthetic parameters to variation in 'normal' levels of UV-B. In most cases P_{max} increased when UV-B was either partially or totally removed. Thus it appears that with the removal of UV-B radiation the phytoplankton are able to

make more efficient use of the available light. Surprisingly β, the index of photoinhibition, increased when UV-B was excluded suggesting that PAR and UV-A may play a larger role in photoinhibition than does UV-B.

The greater sensitivity of diatoms to enhanced UV-B compared with *Phaeocystis* seen in my experiments is a different response to what has been found in other studies. In other parts of the Southern Ocean (Smith et al., 1992; Karentz and Spero, 1995) and in laboratory studies (Karentz et al., 1991; Davidson and Marchant, 1994), it has been found that *Phaeocystis*, while containing greater concentrations of UV-B absorbing compounds than diatoms, is nevertheless more susceptible to increases in UV-B. My findings suggest that diatoms may have other UV-B tolerance mechanisms. Possibly the silica frustule of the diatoms gives some UV-B resistance or the MeTHF insoluble material of many diatom species may contribute to the survival of diatom cells at UV-B irradiances which damage *Phaeocystis* (Davidson and Marchant, 1994). A possible explanation for the discrepancy between my study and others cited above is that most of the diatoms investigated in previous studies were larger than those which are dominant in the polynya or were small centric diatoms occurring in chains (such as *Chaetoceros socialis* and *Chaetoceros neglectum*). These forms may be shaded by each other, thereby increasing their effective size with respect to UV-B damage. Karentz et al. (1991a) found a significant relationship between cell size and UV-B tolerance, with smaller species which have a greater surface area to volume ratio being more sensitive to UV-B exposure. Although *Phaeocystis* cells are small (8-10 μm), their occurrence in colonies may result in 'self-shading', which could act as a UV-B protective mechanism, or the mucus itself may have some UV-B protective properties. In support of this, Marchant et al. (1991) and Davidson and Marchant (1994) found that solitary

Phaeocystis cells were less UV-B tolerant than colonial forms.

The diatom species that is most numerically dominant in the Ross Sea polynya is a small solitary pennate diatom, *Nitzschia subcurvata*. Figure 4.1 shows micrographs of both *Nitzschia subcurvata* and *Phaeocystis* cells. The effective area of *N. subcurvata* (that part of the cell where the cellular material is centered) is at most one and a half to two times that of a *Phaeocystis* cell and much smaller than even a small colony. This cellular geometry may cause this particular diatom to be less tolerant of changes in UV-B in the spring than *Phaeocystis*, hence giving *Phaeocystis* an ecological advantage. There are no pre-ozone hole data available for the Ross Sea with respect to bloom dynamics, and as such it is impossible to suggest that the dynamics of the system were any different before ozone depletion. It is unlikely that this is the case, as *Phaeocystis* has been found to be an early blooming species in other systems and has physiological characteristics which enable it to thrive in the early spring. *Phaeocystis* is a very efficient phytoplankter with high relative growth rates (Weisse and Scheffel-Moser, 1990; Smith and Gordon, 1997) and is adapted to the low light environment of the early spring. The mucus which binds *Phaeocystis* cells together in colonies has also been found to sequester trace metals from the water (Davidson and Marchant, 1987; Lubbers et al., 1990) providing another potential ecological advantage. If trace metals are limiting in this region (Martin et al., 1990a; Sedwick and DiTullio, 1996) and the *Phaeocystis* cells are able to utilize the trace metals present in the mucus, this would make them more competitive with *Phaeocystis* and even if they are not able to utilize the trace metals the diatoms do not have access to that micronutrient pool either. Even with these other advantages it is possible that the *Phaeocystis* blooms in the Ross Sea are even more successful in competition with the

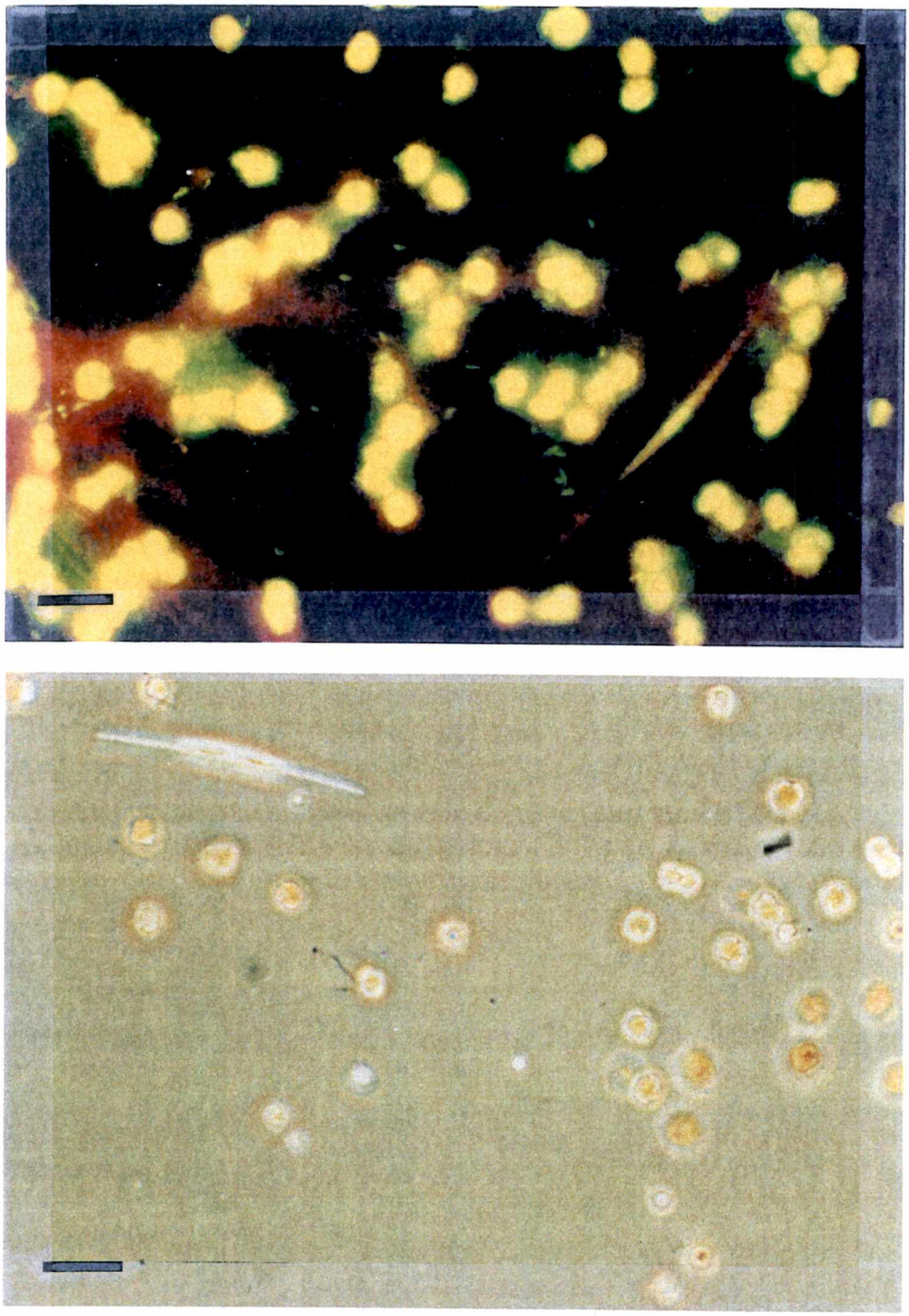

Figure 4.1 Micrographs of *Phaeocystis* (small round cells) and *Nitzschia subcurvata* (long thin cells). Scale bars in lower left corners are 10 μm. In the top micrograph cells have been stained with acridine orange and viewed through an epifluorescence microscope. In the lower micrograph cells have been fixed with Lugols iodine solution and viewed with an inverted microscope. Photographs courtesy of S. Mathot.

diatoms present as a result of anthropogenic ozone depletion.

If there has been a shift in species abundance away from diatoms and toward *Phaeocystis,* this could have many impacts on the ecosystem. *Phaeocystis* as a food source is generally thought to be less beneficial than diatoms. One of the factors which effects the value of a phytoplankton as food is the polyunsaturated fatty acid content (PUFAs; the greater the PUFA content, the more nutritionally advantageous), and these lipids are absent in *Phaeocystis* (Al-Hasan et al., 1990). *Phaeocystis* is generally considered to be less palatable to grazers than diatoms, although there is evidence of it being significantly grazed by some copepod species (Huntley et al., 1987) while being rejected by others (Verity and Smayda, 1983). Kamermans (1994) suggests that colonial *Phaeocystis* is nutritionally unimportant in the diet of the coastal North Sea bivalve *Macoma balthica*, because the colonies are simply too large to be taken in the siphon of the organism. This size factor could pose a problem for Antarctic bivalves and other heterotrophs as well. Because *Phaeocystis* appears to be of less value than diatoms as food, any shift toward *Phaeocystis* caused by ozone depletion may result in a reduction in the energy transferred to higher trophic levels.

A further potential consequence of a shift towards *Phaeocystis*-dominated assemblages is through two potential impacts on the benthic community. Firstly, the nutritional quality of *Phaeocystis* as opposed to diatoms is relevant to benthic communities. As mentioned above at least some species of bivalves are unable to ingest colonial *Phaeocystis* (Kamermans, 1994), and therefore if particles predominantly composed of *Phaeocystis* provide food for the benthic community, it may not be as productive as if the pelagic assemblage were diatom-dominated. Secondly, there is circumstantial

evidence to suggest that sinking rates of particles are faster in a diatom-dominated assemblage as sinking rates are greater later in the season (Asper et al., 1996). This may be a result of diatoms being more readily incorporated into fecal pellets than *Phaeocystis,* hastening their flux to the sediments (Smith and Dunbar, 1997). It has also been found that total fluxes in diatom-dominated assemblages are greater than in *Phaeocystis*-dominated assemblages (Smith and Dunbar, 1997). If UV-B gives *Phaeocystis* a greater competitive advantage in the early spring, the influx of nutrients into the benthic community may be decreased until diatoms increase in numbers later in the year, and thus the net production for the growing season would also be lower.

As mentioned previously I do not think that ozone depletion has dramatically altered the Ross Sea polynya phytoplankton assemblage because *Phaeocystis* is able to thrive under early spring conditions. However, to my knowledge this is the only area where the dominant diatoms have been found to be less UV-B tolerant than the nutritionally poorer *Phaeocystis*. This raises interesting ecological questions for the Ross Sea system if the ozone hole persists. It is likely that any changes which may occur in the system have already occurred with two decades of ozone depletion. However, *Phaeocystis* could potentially become more dominant with blooms lasting longer, or alternatively diatom species which have a greater UV-B tolerance may fill the niche now occupied by *Nitzschia subcurvata.*

Whatever the future implications of ozone depletion for this system I think that the following four areas should be investigated to better understand the impact of enhanced UV-B: 1) Because of the time dependence of UV-B damage, it is important to determine mixing rates and therefore the extent of UV-B exposure. This could either be approached through modeling of the mixing processes or through the development of

biological weighting functions for the Ross Sea polynya phytoplankton using methods such as those used by Cullen et al. (1992), and coupling this information with detailed UV-B profiles taken throughout the day. 2) More frequent long-term experiments should be carried out under ozone-depleted conditions to test the reproducibility of these results and to test how bloom progression effects UV-B susceptibility. 3) Related to 2, experiments should be modified to simulate more closely the actual light field experienced by the phytoplankton in situ. The ideal way to do this would be by using an in situ array to position the phytoplankton samples at the exact depth from which they were sampled. This method would require that the ship be stationary for the duration of the experiment, and as such may be logistically impractical for long term studies. Neutral density screens may be a more practical solution. For short term experiments in situ incubations would remove the problem of photoadaptation dwarfing any detectable UV-B effect. 4) Detailed investigations of UV-B tolerance of Ross Sea strains of *Phaeocystis* and *N. subcurvata* in culture should be conducted to determine the magnitude of the difference in the responses of these two species to UV-B under controlled conditions.

4.2 CONCLUSIONS

- Ozone depletion occurs over the Ross Sea polynya during bloom initiation and development resulting in UV-B levels similar to those experienced in summer under normal ozone concentrations.
- UV-B penetrates to biologically significant depths with the longer wavelengths of UV-B extending throughout the mixed layer and the shorter wavelengths occurring through half of the mixed layer.

- Light penetration at all wavelengths decreases with increased phytoplankton concentrations in the water column as evidenced by positive correlations between vertical attenuation coefficients and chlorophyll, POC and PON.
- Species assemblages and their responses to changes in UV-B vary greatly from spring to summer. Results of 1994 UV-B experiments show a shift toward diatoms under UV-B exclusion, indicating that diatoms are less UV-B resistant than *Phaeocystis* in this system.
- In short term experiments UV-B effects are masked by photoadaptive responses to high light.
- Long term experiments reveal variable responses of phytoplankton assemblages as a whole and between *Phaeocystis* and diatoms, with phytoplankton benefiting from UV-B exclusion under ozone depletion.
- *Phaeocystis* appears to be more UV-B tolerant than the dominant diatom, *Nitzschia subcurvata* in the spring, giving it an added ecological advantage. In the summer there seems to be little variation in the response of these phytoplankton to UV-B exclusion.
- The small size and high surface area to volume ratio of *N. subcurvata* compared to colonial *Phaeocystis* may explain its greater UV-B sensitivity.
- Any competitive advantage that favors *Phaeocystis* over diatoms could have wide-reaching ecosystem effects on both pelagic and benthic communities due to its poorer nutritional value.
- Primary production increases on average under UV-B exclusion. Consequently, enhanced UV-B in the Ross Sea polynya results in reduced productivity, particularly in surface waters.
- More work needs to be done to be able to understand clearly the way in which enhanced UV-B has and will effect phytoplankton blooms in the Ross Sea polynya.

REFERENCES CITED

REFERENCES CITED

Al-Hasan, R.H., Ali, A.M., Radwan, S.S. (1990). Lipids, and their constituent fatty acids, of Phaeocystis sp. from the Arabian Gulf. **Marine Biology** 105 : 9-14.

Anonymous (1994). Sun. In: **The astronomical almanac 1994**. U.S. Government Printing Office, Washington, DC, C1-C25.

Anonymous (1995). Sun. In: **The astronomical almanac 1995**. U.S. Government Printing Office, Washington, DC, C1-C25.

Anonymous (1996). Sun. In: **The astronomical almanac 1996**. U.S. Government Printing Office, Washington, DC, C1-C25.

Arrigo, K.R. (1994). Impact of ozone depletion on phytoplankton growth in the Southern Ocean : large-scale spatial and temporal variability. **Marine Ecology Progress Series** 114 : 1-12.

Arrigo, K.R., and McClain, C.R. (1994). Spring phytoplankton in the Western Ross Sea. **Science** 266 : 261-263.

Arrigo, K.R., Weiss, A.M., and Smith, W.O.Jr. (1997) Physical forcing of phytoplankton dynamics in the western Ross Sea. **Journal of Geophysical Research** (submitted).

Asper, V.L., Diercks, A-R., Lee, J.J. (1996a). Large aggregate dynamics in the Ross Sea polynya. Proceedings of the International Workshop on Ross Sea Ecology, Taormina, Italy, 14-16 May, 1996. Pp 8-9.

Asper,V.L., Diercks, A-R., and Tuel, M.D. (1996b). Fluxes of carbon and total mass in the Ross Sea polynya during the early austral spring, 1994. (Abstract). **Eos** 76(3) : OS137.

Azzali, M., and Kalinowski, J. (1996). Spatial and temporal distribution of krill *Euphausia superba* in the Ross Sea (1989-90, 1994). Proceedings of the International Workshop on Ross Sea Ecology, Taormina, Italy, 14-16 May, 1996. Pp. 96-97.

Barber, R.T., and Smith, R.L. (1991). Coastal upwelling ecosystems. In : **Analysis of Marine Ecosytems**. Ed. by Longhurst, A.R. Academic Press, New York. Pp. 31-68.

Becquevort, S., Mathot, S., and Lancelot, C. (1992). Interactions in the microbial community of the marginal ice zone of the northwestern Weddell Sea through size distribution analysis. **Polar Biology** 12 : 211-218.

Bidigare, R.R. (1989). Potential effects of UV-B radiation on marine organisms of the Southern Ocean : distributions of phytoplankton and krill during austral spring. **Photochemistry and Photobiology** 50 : 469-477.

Buma, A.G.J., de Baar, H.J.W., Nolting, R.F., van Bennekom, A.J. (1991). Metal enrichment experiments in the Weddell-Scotia Seas : effects of iron and manganese on various plankton communities. **Limnology and Oceanography** 36 : 1865-1878.

Burkill, P.H., Edwards, E.S., and Sleigh, M.A. (1995). Microzooplankton and their role in controlling phytoplankton growth in the marginal ice zone of the Bellingshausen Sea. **Deep-Sea Research II** 42 : 1277-1290.

Calkins, J., and Thordardottir, T. (1980). The ecological significance of solar radiation on aquatic organisms. **Nature** 283 : 563-566.

Carlson, C.A., Ducklow, H.W., Hansell, D.A., and Smith, W.O. Jr. (1997) Carbon dynamics during spring blooms in the Ross Sea polynya and the Sargasso Sea: Contrasts in dissolved and particulate organic carbon partitioning. **Limnology and Oceanography** In press.

Carreto, J.I., Carignan, M.O., Daleo, G. and De Marco, S.G. (1990). Occurrence of mycosporine-like amino acids in the red tide dinoflagellate *Alexandrium excavatum* : UV-

protective compounds. **Journal of Plankton Research** 12 : 909-921.

Cleaver, J.E., and Kraemer, K.H. (1989). Xeroderma pigmentosum. In **The metabolic basis of inherited disease, 6th edition**. Ed. by Scriver, C.R. et al. McGraw-Hill. Pp. 2949-2971.

Coale, K.H., Johnsom, K.S., Fitzwater, S.E., Tanner, S., Chavez, F.P., Ferioli, L., Sakamoto, C., Rogers, P., Millero, F., Steinberg, P., Nightingale, P., Cooper, D., Cochlan, W.P., Landry, M.R., Constantinou, J., Rollwagen, G., Trasvina, A., and Kudela, R. (1996). A massive phytoplankton bloom induced by an ecosystem-scale iron fertilization experiment in the equatorial Pacific Ocean. **Nature**. 383 : 495-501.

Comiso, J.C., McClain, C.R., Sullivan, C.W., Ryan, J.P. and Leonard, C.L. (1993). Coastal zone color scanner pigment concentrations in the Southern Ocean and relationships to geophysical surface features. **Journal of Geophysical Research** 98 : 2419-2451.

Cullen, J.J. (1991). Hypotheses to explain high-nutrient conditions in the open sea. **Limnology and Oceanography** 36(8) : 1578-1599.

Cullen, J.J., Neale, P.J. and Lesser, M.P. (1992). Biological weighting function for the inhibition of phytoplankton photosynthesis by ultraviolet radiation. **Science** 258 : 646-650.

Cushing, D.H. (1959). The seasonal variations in oceanic production as a problem in population dynamics. **Journal du Conseil International pour L'Exploration de la Mer** 24 : 455-464.

Davidson, A.T., and Marchant, H.J. (1987). Binding of manganese by Antarctic Phaeocystis pouchetii and the role of bacteria in its release. **Marine Biology** 95 : 481-487.

Davidson, A.T., and Marchant, H.J. (1994). The impact of ultraviolet radiation on Phaeocystis and selected species of Antarctic marine diatoms. In : **Ultraviolet**

radiation in Antarctica : Measurements and biological Effects. Antarctic Research Series Volume 62. Ed. by Weiler, C.S. and Penhale, P. American Geophysical Union, Washington DC. Pp. 187-205. 257 pp.

DiTullio, G.R., and Sedwick, P. (1996). Phaeocystis antarctica and the cycling of carbon, iron and sulfur in the Southern Ocean. Proceedings of the International Workshop on Ross Sea Ecology, Taormina, Italy, 14-16 May, 1996. p. 51.

DiTullio, G.R., and Smith, W.O., Jr. (1996). Spatial patterns in phytoplankton biomass and pigment distributions in the Ross Sea. **Journal of Geophysical Research**. 101 : 18467 - 18477.

Dohler, G., (1984). Effect of UV-B radiation on the marine diatoms *Lauderia annulata* and *Thalassiosira rotula* grown in different salinities. **Marine Biology** 83 : 247-253.

Duce, R.A. (1986). The impact of atmospheric nitrogen, phosphorus, and iron species on marine biological productivity. In **: The Role of Air-Sea exchange in Geochemical Cycling**. Ed. by Buat-Menard, P. D. Reidel Publishing company. Pp. 497-529

Duce, R.A., and Tindale, N.W. (1991). Atmospheric transport of iron and its deposition in the ocean. **Limnology and Oceanography** 36 : 1715-1726.

Ducklow, H.W., and Carlson, C.A. (1992).Oceanic bacterial production. **Advances in Marine Biology** 12 : 113-181.

Dunlap, W.C., Chalker, B.E., Oliver, J.K. (1986). Bathymetric adaptations of reef-building corals at Davies Reef, Great Barrier Reef, Australia. III. UV-B absorbing compounds. **Journal of Experimental Marine Biology and Ecology** 104 : 1-10.

Dunlap, W.C., Williams, D.M., Chalker, B.E.and Banaszak. (1989). Biochemical photoadaptation in vision : UV-absorbing pigments in fish eye tissues. **Comparative Biochemistry and Physiology B, Comparative Biochemistry** 93 : 601-607.

El-Sayed, S.Z., Stephens, F.C., Bidigare, R.R. and Ondrusek, M.E. (1990). Effect of ultraviolet radiation on Antarctic marine phytoplankton. In **: Antarctic ecosystems : Ecological change and conservation.** Ed. by Kerry, K.R., and Hempel, G. Springer-Verlag, New York. Pp. 379-385.

Farman, J.C., Gardiner, B.G., and Shanklin, J.D. (1985). Large losses of total ozone in Antarctica reveal seasonal ClO_x/NO_x interaction. **Nature** 315 : 207-210.

Frederick, J.E., and Lubin, D. (1994). Solar ultraviolet irradiance at Palmer Station, Antarctica. In : **Ultraviolet radiation in Antarctica : Measurements and biological Effects. Antarctic Research Series Volume 62.** Ed. by Weiler, C.S. and Penhale, P. American Geophysical Union, Washington DC. Pp. 43-52. 257 pp.

Frederick, J.E., and Snell, H.E. (1988). Ultraviolet radiation levels during the Antarctic spring. **Science** 241 : 438-440.

Frost, B.W. (1991). The role of grazing in nutrient-rich areas of the open sea. **Limnology and Oceanography** 36 : 1616-1630.

Gloersen, P., Campbell, W.J., Cavalieri, D.J., Comiso, J.C., Parkinson, C.L., Zwally, H.J. (1992). **Arctic and Antarctic Sea Ice, 1978 - 1987, satellite passive-microwave observations and analysis. NASA SP - 511.** National Aeronautics and Space Administration. Washington DC, USA. 290 pp.

Goldman, G.A., and Dennett, M.R. (1985). Susceptibility of some marine phytoplankton species to cell breakage during filtration and post-filtration rinsing. **Journal of Experimental Marine Biology and Ecology** 86 : 47-58.

Graneli, E., Graneli, W., Rabbani, M.M., Daugbjerg, N., Fransz, G., Cuzin-Roudy, J., and Alder, V.A. (1993). The influence of copepod and krill grazing on the species composition of phytoplankton communities from the Scotia-Weddell Sea An experimental approach. **Polar Biology** 13 : 201-213.

Hart, T.J. (1934). On the phytoplankton on the south-west Atlantic and Bellingshausen Sea, 1929-31. **Discovery Reports** 8 : 1-268.

Hofmann, D.J. (1996). Recovery of Antarctic ozone hole. **Nature** 384 : 222-223.

Holm-Hansen, O., Mitchell, B.G., and Vernet, M. (1989a). Ultraviolet radiation in Antarctic waters : Effect on rates of primary production. **Antarctic Journal of the United States** 24 : 177-178.

Holm-Hansen, O., Mitchell, B.G., Hewes, C.D. and Karl, D.M. (1989b). Phytoplankton blooms in the vicinity of Palmer station, Antarctica. **Polar Biology** 10 : 49-57.

Honjo, S. (1990) Particle fluxes and modern sedimentation in the polar oceans. In. **Polar Oceanography** Part B : Chemistry, Biology, and Geology. Ed by Smith, W.O., Jr. Academic Press, San Diego, California. Pp. 687-739.

Huntley, M., Tande, K., and Eilertsen, H.C. (1987). On the trophic fate of Phaeocystis pouchetii (Hariot). II. Grazing rates *of Calanus hyperboreus* (Kroyer) on diatoms and different size categories of *Phaeocystis pouchetii.* **Journal of Experimental Marine Biology and Ecology** 110 : 197-212.

Ito, S., and Hirata, Y. (1977). Isolation and structure of a mycosporine from the zoanthid *Palythoa tuberculosa.* **Tetrahedron Letters** 28 : 2429-2430.

Jacques, G. (1989). Primary production in the open Antarctic Ocean during the austral summer. A Review. **Vie Milieu** 39 : 1-17.

Jaeger, J.M., Nittrouer, C.A., DeMaster, D.J., Kelchner, C., and Dunbar, R.B. (1996). Lateral transport of settling particles in the Ross Sea and implications for the fate of biogenic material. **Journal of Geophysical Research** 101 : 18479-18488.

Jerlov, N.G. (1976). **Marine Optics**. Elsevier, Amsterdam. 231 pp.

Kamermans, P. (1994). Nutritional value of solitary cells and colonies of Phaeocystis sp. for the bivalve Macoma balthica (L.) **Ophelia** 1 : 35-44.

Karentz, D. (1991). Ecological considerations of ozone depletion. **Antarctic Science** 3 : 3-11.

Karentz, D. (1994). Ultraviolet tolerance mechanisms in Antarctic marine organisms. In : **Ultraviolet radiation in Antarctica : Measurements and biological Effects. Antarctic Research Series Volume 62.** Ed. by Weiler, C.S. and Penhale, P. American Geophysical Union, Washington DC. Pp. 93-110. 257 pp.

Karentz, D., and Lutze, L.H. (1990). Evaluation of biologically harmful ultraviolet radiation in Antarctica with a biological dosimeter designed for aquatic environments. **Limnology and Oceanography** 35 : 549-561.

Karentz, D., and Spero, H.J. (1995). Response of a natural Phaeocystis population to ambient fluctuations of UVB radiation caused by Antarctic ozone depletion. **Journal of Plankton Research**. 17 : 1771-1789.

Karentz, D., Cleaver, J.E., and Mitchell, D.L. (1991a). Cell survival characteristics and molecular responses of Antarctic phytoplankton to ultraviolet-b radiation. **Journal of Phycology** 27 : 326-341.

Karentz, D., McEuen, F.S., Land, M.C., and Dunlap, W.C. (1991b). Survey of mycosporine-like amino acid compounds in Antarctic marine organisms : potential protection from ultraviolet exposure. **Marine Biology** 109 : 157-166.

Kirchman, D. (1996). Microbial ferrous wheel. **Nature** 383 : 303-304.
Kirk, J.T.O. (1994). **Light and Photosynthesis in Aquatic Ecosystems** 2nd Ed. Cambridge University Press, Cambridge. 509 pp.

Kobayashi, J., Nakamura, H., and Hirata, Y. (1981). Isolation and structure of a UV-absorbing substance 337 from the ascidian *Halocynthia roretzi*. **Tetrahedron Letters**. 22 : 3001-3002.

Kurylo, M.J. (1990). The chemistry of stratospheric ozone : its response to natural and anthropogenic influences. **International Journal of Refrigeration** 13 : 62-72.

Lancelot, C., Mathot, S., Veth, C., and de Baar, H. (1993). Factors controlling phytoplankton ice-edge blooms in the marginal ice-zone of the northwestern Weddell Sea during sea ice retreat 1988 : field observations and mathematical modelling. **Polar Biology** 13 : 377-387.

Lancelot, C., Rousseau, V., Keller, M., Smith, W.O., Jr. and Mathot, S. (1997). Auto-ecology of *Phaeocystis* sp. blooms. **NATO series on harmful algal blooms** In press.

Legendre, L., Gosselin, M., Hirche, H-J., Kattner, G. and Rosenberg, G. (1993). Environmental control and potential fate of size-fractionated phytoplankton production in the Greenland Sea (75°N). **Marine Ecology Progress Series** 98 : 297-313.

Leventer, A., and Dunbar, R.B. (1996). Factors influencing the distribution of diatoms and other algae in the Ross Sea. **Journal of Geophysical Research** 101 : 18489-18500.

Lewis, M.R., and Smith, J.C. (1983). A small volume, short incubation-time method for measurement of photosynthesis as a function of incident irradiance. **Marine Ecology Progress Series** 13 : 99-102.

Lorenzen, C.J. (1979). Ultraviolet radiation and phytoplankton photosynthesis. **Limnology and Oceanography** 24 : 1117-1120.

Lubbers, G.W., Gieskes, W.W.C., Del Castilho, P., Salomon, W., and Bril, J. (1990). Manganese accumulation in the high pH microenvironment of Phaeocystis (Haptophyceae) colonies of the North Sea. **Marine Ecology Progress Series** 59 : 285-293.

Lubin, D., Mitchell, B.G., Frederick, J.E., Alberts, A.D., Booth, C.R., Lucas, T., and Neuschuler, D. (1992). A contribution toward understanding the biospherical

significance of Antarctic ozone depletion. **Journal of Geophysical Research** 97 : 7817-7828.

Marchant, H.J., Davidson, A.T., and Kelly, G.J. (1991) UV-B protecting pigments in the marine alga Phaeocystis pouchetii from Antarctica. **Marine Biology** 109 : 391-395.

Martin, J.H., and Fitzwater, S.E. (1988). Iron deficiency limits phytoplankton growth in the north-east Pacific subarctic. **Nature** 331 : 341-343.

Martin, J.H., Fitzwater, S.E. and Gordon, R.M. (1990a). Iron deficiency limits phytoplankton growth in Antarctic waters. **Global Biogeochemical Cycles** 4 : 5-12.

Martin, J.H., Gordon, R.M., and Fitzwater, S.E. (1990b). Iron in Antarctic waters. **Nature** 345 : 156-158.

Martin, J.H., Gordon, R.M., and Fitzwater, S.E. (1991). The case for iron. **Limnology and Oceanography** 36 : 1793-1802.

Martin, J.H., Coale, K.H., Johnson, K.S., Fitzwater, S.E., Gordon, R.M., Tanner, S.J., Hunter, C.N., Elrod, V.A., Nowicki, J.L., Coley, T.L., Barber, R.T., Lindley, S., Watson, A.J., Van Scoy, K., Law, C.S., Liddicoat, M.I., Ling, R., Stanton, T., Stockel, J., Collins, C., Anderson, A., Bidigare, R., Ondrusek, M., Latasa, M., Millero, F.J., Lee, K., Yao, W., Zhang, J.Z., Friedrich, G., Sakamoto, C., Chavez, F., Buck, K., Kolber, Z., Greene, R., Falkowski, P., Chisholm, S.W., Hoge, F., Swift, R., Yungel, J., Turner, S., Nightingale, P., Hatton, A., Liss, P., and Tindale, N.W. (1994). Testing the iron hypothesis in ecosystems of the equatorial Pacific Ocean. **Nature** 371 : 123-129.

Mathot, S., Dandois, J-M., Lancelot, C. (1992). Gross and net primary production in the Scotia-Weddell Sea sector of the Southern Ocean during spring 1988. **Polar Biology** 12 : 321-332.

Maykut, G.A. and Grenfell, T.C. (1975). The spectral distribution of light beneath

first-year sea ice in the Arctic Ocean. **Limnology and Oceanography** 20 : 554-563.

Mitchell, B.G., and Holm-Hansen, O. (1991). Observations and modeling of the Antarctic phytoplankton crop in relation to mixing depth. **Deep-Sea Research** 38 : 981-1007.

Mobley, C.D. (1994). **Light and water : radiative transfer in natural waters**. Academic Press, San Diego. 591 pp.

Morel, F.M.M., Hudson, R.J.M., and Price, N.M. (1991a). Limitation of productivity by trace metals in the sea. **Limnology and Oceanography** 36 : 1742-1775.

Morel, F.M.M., Rueter, J.G., and Price, N.M. (1991b). Iron nutrition of phytoplankton and its possible importance in the ecology of ocean regions with high nutrient and low biomass. **Oceanography** 4 : 56-61

Muench, R.D., (1990). Mesoscale phenomena in the polar oceans. In**: Polar Oceanography** Part A, Physical Science. Ed. by W. O. Smith Jr. Academic Press, Inc. San Diego, USA. pp. 223-285. (406 pp)

Nakamura, H., Kobayashi, J., and Hirata, Y. (1981). Isolation of a 320 nm UV-absorbing substance, asterina-330 from the starfish Asterina pectinifera. **Chemy Letters** (Chemistry Society of Japan, Tokyo) 1981 : 1413-1414.

Nelson, D.M. and Smith, W.O., Jr. (1986). Phytoplankton bloom dynamics of the western Ross Sea ice edge-II. Mesoscale cycling of nitrogen and silicon. **Deep-Sea Research** 33 : 1389-1412.

Nelson, D.M. and Smith, W.O., Jr. (1991). Sverdrup revisited: Critical depths, maximum chlorophyll levels, and the control of Southern Ocean productivity by the irradiance-mixing regime. **Limnology and Oceanography** 36 : 1650-1661.

Nelson, D.M., Smith, W.O., Jr., Muench, R.D., Gordon, L.I., Sullivan, C.W., and Husby, D.M. (1989). Particulate matter and nutrient distributions in the ice-edge zone

of the Weddell Sea: relationship to hydrography during late summer. **Deep-Sea Research** 36 : 191-209.

Normile, D. (1996). New satellite puts Japan in top tier of remote sensing. **Science** 273 : 1038.

Pakulski, J.D., Coffin, R.B., Kelley, C.A., Holder, S.L., Downer, R., Aas, P., Lyons, M.M., and Jeffrey, W.H. (1996). Iron stimulation of Antarctic bacteria. **Nature** 383 : 133-134.

Platt, T., Harrison, W.G., Irwin, B., Horne, E.P. and Gallegos, C.L. (1982). Photosynthesis and photoadaptation of marine phytoplankton in the Arctic. **Deep-Sea Research** 29 : 1159-1170.

Prezelin, B.B., Boucher, N.P., and Smith, R.C. (1994). Marine primary production under the influence of the Antarctic ozone hole: ICECOLORS '90. In : **Ultraviolet radiation in Antarctica : Measurements and biological effects. Antarctic research series Volume 62.** Ed. by Weiler, C.S. and Penhale, P. American Geophysical Union, Washington DC. Pp. 159-186. 257 pp.

Price, H.J., Boyd, K.R., and Boyd, C.M. (1988). Omnivorous feeding behavior of the Antarctic krill *Euphausia superba*. **Marine Biology** 97 : 67-77.

Putt, M., Miceli, G., and Stoecker, D.K. (1994). Association of bacteria with *Phaeocystis* sp. in McMurdo Sound, Antarctica. **Marine Ecology Progress Series** 105 : 179-189.

Rousseau, V., Mathot, S., and Lancelot, C. (1990). Calculating carbon biomass of *Phaeocystis* sp. from microscopic observations. **Marine Biology** 107 : 305-314.

Sakshaug, E., Slagstad, D., and Holm-Hansen, O. (1991). Factors controlling the development of phytoplankton blooms in the Antarctic Ocean - a mathematical model. **Marine Chemistry** 35 : 259-271.

Sherr, E.B., and Sherr, B.F. (1993). Preservation and storage of samples for enumeration of heterotrophic protists. In **: Handbook of methods in aquatic microbial ecology**. Ed. by Kemp, P.F., Sherr, B.F., Sherr, E.B. and Cole, J.J. Lewis Publishers, Boca Raton, Florida. Pp. 207-212. 777 pp.

Shick, J.M., Dunlap, W.C., Chalker, B.C., Banaszak, A.T., and Rosenzweig, T.K. (1992). Survey of ultraviolet radiation-absorbing mycosporine-like amino acids in organs of coral reef holothuroids. **Marine Ecology Progress Series** 90 : 139-148.

Sivalingham, P.M., Ikawa, T., and Nisizawa, K. (1974a). Possible physiological roles of a substance showing characteristic UV-absorbing patterns in some marine algae. **Plant Cell Physiology** 15 : 583-586.

Sivalingham, P.M., Ikawa, T., Yokohama, Y., and Nisizawa, K. (1974b). Distribution of a 334 UV-absorbing-substance in algae with special regard of its possible physiological roles. **Botanica Marina** 17 : 23-29.

Smith, R.C., and Baker, K.S. (1979). Penetration of UV-B and biologically effective dose-rates in natural waters. **Photochemistry and Photobiology** 29 : 311-323.

Smith, R.C., and Baker, K.S. (1980). Stratospheric ozone, middle ultraviolet radiation, and carbon-14 measurements of marine productivity. **Science** 208 : 592-593.

Smith, R.C., Prezelin, B.B., Baker, K.S., Bidigare, R.R., Boucher, N.P., Coley, T., Karentz, D., MacIntyre, S., Matlick, H.A., Menzies, D., Ondrusek, M., Wan, Z., and Waters, K.J. (1992). Ozone depletion : Ultraviolet radiation and phytoplankton biology in Antarctic waters. **Science** 255 : 952-959.

Smith, S.D., Muench, R.D., and Pease, C.H. (1990). Polynyas and leads: an overview of physical processes and environment. **Journal of Geophysical Research** 95 : 9461-9479.

Smith, W.O., Jr., and Dunbar, R.B. (1997). The relationship between new production and vertical flux on the Ross Sea continental shelf. **Journal of Marine Systems** In

press.

Smith, W.O., Jr., and Gordon, L.I. (1997). Hyperproductivity of the Ross Sea (Antarctica) polynya during austral spring. **Geophysical Research Letters** In press.

Smith, W.O., Jr., and Nelson, D.M. (1990). Phytoplankton growth and new production in the Weddell Sea marginal ice zone in the austral spring and autumn. **Limnology and Oceanography** 35 : 809-821.

Smith, W.O., Jr., and Sakshaug, E. (1990). Polar Phytoplankton. In. **Polar Oceanography,** Part B : Chemistry, Biology, and Geology. Ed. by Smith, W.O., Jr. Academic Press Inc., San Diego, California 477-525. 760 pp.

Smith, W.O., Keene, N.K., and Comiso, J.C. (1988). Interannual variability in estimated primary productivity of the Antarctic marginal ice edge zone. In. **Antarctic Ocean and Resources Variability**. Ed. by Sahrage, D. Springer-Verlag, Berlin Heidelberg. Pp. 131-139.

Sommer, U. (1994). The impact of light intensity and daylength on silicate and nitrate competition among marine phytoplankton. **Limnology and Oceanography** 39 : 1680-1688.

Sverdrup, H.U. (1953). On conditions for the vernal blooming of phytoplankton. **Journal du Conseil International pour L'Exploration de la Mer** 18 : 287-295.

Tomas, C.R., (1996). **Identifying marine diatoms and dinoflagellates.** Academic Press, San Diego. 598 pp.

Tortell, P.D., Maldonado, M.T. and Price, N.M. (1996). The role of heterotrophic bacteria in iron-limited ocean ecosystems. **Nature** 383 : 330-332

Utermohl, H. (1958). Zur Vervollkommnung der quantitaven Phytoplankton-Methodik. **Mitteilungen. internationale Vereinigung fuer theoretische und angewandte Limnologie** 9 : 1-38.

Verity, P.G., and Smayda, T.J. Nutritional value of *Phaeocystis pouchetii* (Prymnesiophyceae) and other phytoplankton for *Acartia* spp. (Copepoda) : ingestion, egg production, and growth of nauplii. **Marine Biology** 100 : 161-171.

Vincent, W.F., and Roy, S. (1993). Solar ultraviolet-B radiation and aquatic primary production: Damage, protection and recovery. **Environmental Review** 1 : 1-12.

Weisse, T., and Scheffel-Moser, U. (1990). Growth and grazing loss rates in single-celled *Phaeocystis* sp. (Prymnesiophyceae). **Marine Biology** 106 : 153-158.

Wood, W.F. (1987). Effect of solar ultraviolet-B radiation on the kelp *Ecklonia radiata*. **Marine Biology** 96 : 143-150.

Worrest, R.C., Van Dyke, H., and Thomson, B.E. (1978). Impact of enhanced simulated solar ultraviolet radiation upon a marine community. **Photochemistry and Photobiology** 27 : 471-478.

Worrest, R.C., Wolniakowski, K.U., Scott, J.D., Brooker, D.L., Thomson, B.E., and Van Dyke, H. (1981). Sensitivity of marine phytoplankton to UV-B radiation : Impact upon a model ecosystem. **Photochemistry and Photobiology** 33 : 223-227.

Yoder, J.A., Ackleson, S.G., Barber, R.T., Flament, P., and Balch, W.M. (1994). A line in the sea. **Nature** 371 : 689-692.

APPENDICES

APPENDIX A

Date: Thu, 20 Jul 1995 16:58:03 -0400
From: NASA HQ Public Affairs Office <NASANews@luna.osf.hq.nasa.gov>
To: press-release-edu@mercury.hq.nasa.gov
Subject: NASA-Funded Research Sees Fall of Ozone-Depleting Chemical

Brian Dunbar
Headquarters, Washington, DC
(Phone: 202/358-1547)

July 20, 1995

RELEASE: 95-115

NASA-FUNDED RESEARCH SEES FALL OF OZONE-DEPLETING CHEMICAL

NASA-sponsored university research has indicated that levels of an ozone-depleting chemical are falling, the first decrease ever measured of a substance restricted by the Montreal Protocol, an international treaty limiting the production of ozone-depleting chemicals.

The research, led by Dr. Ronald Prinn of the Massachusetts Institute of Technology, Cambridge, MA, showed that concentrations of methyl chloroform have decreased at approximately two percent a year since mid-1990. Until that point, levels had increased approximately four percent a year since 1978.

Concentrations of methyl chloroform are measured from four ground stations around the globe. NASA funded this research through its Upper Atmosphere Research Program, part of its Mission to Planet Earth (MTPE). Results of the study were published in the journal Science last week.

"This is a very important measurement," said Dr. Robert Harriss, head of the Science Division of NASA's Office of Mission to Planet Earth. "We've already seen slowing increases in chlorofluorocarbons and other ozone-depleting chemicals. Now, for the first time, we've actually measured a decrease in one of these chemicals.

"What we're seeing are the effects of the Montreal Protocol and its amendments. Continued monitoring of ozone and the chemicals involved in ozone depletion will be crucial over the next several decades to ensure that the treaties continue to work, so that ozone levels ultimately recover," Harriss said. Scientists believe that under the Montreal Protocol, ozone levels will begin to return to their pre-1980s concentrations early in the next century. The Antarctic "ozone hole" is not expected to subside until at least the middle of the 21st century.

Monitoring ozone depletion is one of the ongoing programs of MTPE, which studies the Earth as a single global environment. MTPE scientists study how the Earth changes and how human activities contribute to those changes.

-end-

NASA press releases and other information are available automatically by sending an Internet electronic mail message to domo@hq.nasa.gov. In the body of the message (not the subject line) users should type the words "subscribe press-release" (no quotes). The system will reply with a confirmation via E-mail of each subscription. A second automatic message will include additional information on the service. Questions should be directed to (202) 358-4043.

APPENDIX B

Comparison between the model and the PUV 511

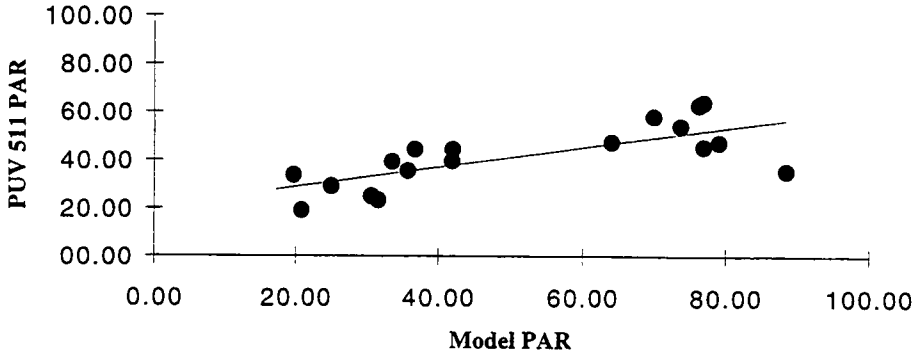

Comparison between the model and the QSR 240

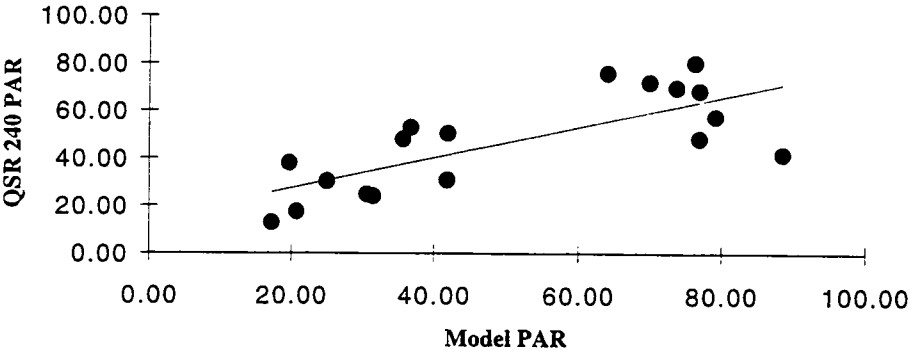

Comparison between the QSR 240 and the PUV 511

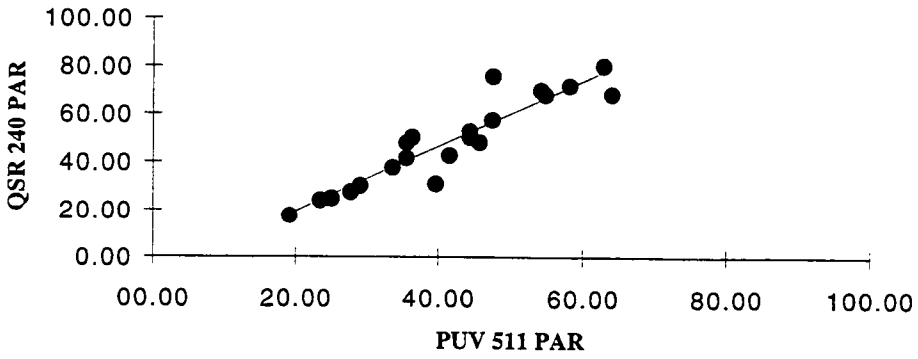

Appendix B : Comparison between three measurements of PAR for RSP²95 PUV 511 and QSR 240 are radiometers, the Model is that of Legendre et al. (1993).

APPENDIX C

Key for Appendix C

PA	*Phaeocystis* sp.
PD	Pennate diatoms
CD	Centric diatoms
DIN	Dinoflagellates
CR	Cryptomonads
CH	Choanoflagellates
SGFs	small green flagellates
DCY	Dinoflagellate cysts
SI	Silicoflagellates
PR	Prasinophytes
T.Cells	Total Cells

Appendix C : Ross Sea 1994 - UV Experiment Microscopy Data.																	
#	EXP.	TIME	screen	FOVs	Vol(ml)	PA	PD	CD	DIN	CR	CH	SGFs	DCY	SI	PR	T. CELLS	CELLS/L
1	1	24	0	228	4	518	5		2	4						529	3.463E+06
2	1	24	1	262	2	522	4	2	3	2						533	6.074E+06
3	1	24	2	240	2	541	3	1	2	2		2	2			553	6.879E+06
4	2	48	0	185	2	520	2	3	3							528	8.521E+06
5	2	48	1	170	2	546	2		1	3					1	553	9.712E+06
6	2	48	2	152	2	559	7	1		3		11				581	1.141E+07
7	2	96	0	76	2	486	1	2	1	1		4				495	1.945E+07
8	2	96	1	94	2	514	3	9	1	1	1	8				537	1.706E+07
9	2	96	2	64	2	523	7		2				1			533	2.486E+07
10	2	144	0	54	2	551	4	1	2			2			1	561	3.102E+07
11	2	144	1	61	2	573	8			1						582	2.848E+07
12	2	144	2	49	2	702	2					1			1	706	4.302E+07
13	2	192	0	70	2	556	6	2								564	2.405E+07
14	2	192	1	28	2	506	6	2				6				520	5.545E+07
15	2	192	2	28	2	700	6					1				707	7.538E+07
16	3	0	o	275	3	54	91		10	21		4	1			181	1.310E+06
17	3	24	0	502	3	37	227	5	10	32		7	2			320	1.269E+06
18	3	24	1	304	3	18	260	1	14	29			1			305	1.997E+06
19	3	24	2	247	5	24	285	3	5	35		4			1	357	1.726E+06
20	4	0	o	109	3	442	1		5	1		2				451	8.235E+06
21	4	24	0	172	3	334	1	1	5	3			1			345	3.992E+06
22	4	24	1	198	3	290	2	2	3	6			3			306	3.076E+06
23	4	24	2	125	3	329				2		2				333	5.302E+06
24	5	0	o	62	3	673	12		3	8	1			1		698	2.241E+07
25	5	24	0	100	3	477	20	1	5	1			1		1	506	1.007E+07
26	5	24	1	68	3	545	22		2	2			1			572	1.674E+07
27	5	24	2	93	3	645	26		4	5						680	1.455E+07
28	6	0	o	128	3	52	505	2	2	9	2					572	8.894E+06
29	6	0	o	90	3	41	348		4	9						402	8.890E+06
30	6	96	0	149	3	85	469	2	2							558	7.454E+06
31	6	96	1	154	3	44	774	4	8	1	1	1			2	835	1.079E+07
32	6	96	2	146	3	23	781	1	4	2	1	1			2	815	1.111E+07
33	6	168	0	217	3	49	458	5	8				2			522	4.788E+06
34	6	168	0	252	3	110	474	2	9					2	1	598	4.723E+06
35	6	168	1	106	3	85	711	3	9	1	4		1			814	1.528E+07
36	6	168	1	107	3	78	721	2	5	1	1	6	2			816	1.518E+07
37	6	168	2	90	3	95	696	1	2						1	795	1.758E+07
38	6	168	2	112	3	136	833	5	9	1	2	1	3		1	991	1.761E+07

APPENDIX D

Key for Appendix D

CODE	PHYTOPLANKTON TYPE	CODE	PHYTOPLANKTON TYPE
PA	*Phaeocystis* sp. (colonial)	DI	Dinoflagellate sp. I
PB	*Phaeocystis* sp. (solitary)	DM	Dinoflagellate sp. M
NA	*Nitzschia seriata* type	DN	Dinoflagellate sp. N
NB	*Nitzschia subcurvata*	RA	*Rhizoselenia* sp. A
NC	*Nitzschia closterium*	RC	*Rhizoselenia alata*
ND	*Nitzschia curta*	RE	*Rhizoselenia rhombus*
NE	med. chain forming *Nitzschia sp.* (>20µm)	RK	*Rhizoselenia* sp. K
NF	lge. chain forming *Nitzschia sp.* (>50µm)	RS	*Rhizoselenia styliformis*
NG	*Nitzschia pseudonana*	CTA	*Chaetoceros* sp. A
NG2	sm. chain forming *Nitzschia sp.* (<20µm)	CTB	*Chaetoceros* sp. B
NJ	*Nitzschia* sp. J	CTC	*Chaetoceros* sp. C
SF	small flagellates	CTD	*Chaetoceros* sp. D
CC	*Corethron criophilum*	CTE	*Chaetoceros* sp. E
CR	Cryptomonads	CTF	*Chaetoceros* sp. F
CH	Choanoflagellates	CTG	*Chaetoceros dichaeta*
PR	Prasinophytes	CTH	*Chaetoceros* sp. H
RGT	Round green things	CTK	*Chaetoceros* sp. K
SI	Silicoflagellates	CTL	*Chaetoceros neogracile*
EA	*Eucampia antarctica*	CTN	*Chaetoceros neglectum*
DA	Dinoflagellate sp. A	CTU	*Chaetoceros* unknown
DB	Dinoflagellate sp. B	UCE	unknown centric
DC	Dinoflagellate sp. C	UD	wide. *Dactyliosylen* sp.
DD	Dinoflagellate sp. D	UE	narrow. *Dactyliosylen* sp.
DE	Dinoflagellate sp. E	UF	suspected Chaonoflagellate
DF	Dinoflagellate sp. F	UG	sm. flagellate with long flagella
DG	Dinoflagellate sp. G	UK	Unknown diatom K

APPENDIX D : RSP² 95/96 MICROSCOPY [UV : o = time 0; 0 = total light; 1 = no UV-B; 2 = partial UV-B] PAGE 1																											
#	EXP.	TIME (h)	VOL (s)	UV	REP #	# FOVs	cells/L	Tot. cells	PA	PB	NA	NB	NC	ND	NE	NF	NG	NG2	NJ	SF	CC	CR	CH	PR	RGT	SI	EA
1	A	0	2	o	1	65	3.18E+07	721	199		7	444		5	29	2				16	1	3	13				
2	A	0	2	o	2	71	3.48E+07	861	249	1	3	526		2	30	8				20		1	13				
3	A	0	2	o	3	66	3.04E+07	700	220		11	392	1	5	44	5				12		2	4				
4	A	24	2	0	1	73	2.76E+07	703	136		3	488		10	37					11		3	4				
5	A	24	2	0	2	69	2.85E+07	685	134		7	457		8	54		1			11			6	1			
6	A	24	2	0	3	78	3.25E+07	884	169		3	622		2	51	8				19			1				
7	A	24	2	1	1	76	2.96E+07	783	138			565		3	42	3				7		1	2	1			
8	A	24	2	1	2	86	2.89E+07	866	159	1	2	618		1	39	2				16		1	6				
9	A	24	2	1	3	73	2.72E+07	691	122		4	486			40	3				15			5				
10	A	24	2	2	1	81	2.55E+07	721	134		3	525		4	17	2				9			3				
11	A	24	2	2	2	82	2.85E+07	814	176		5	555	1	7	27	2				14	1	1	4	1			
12	A	24	2	2	3	80	2.77E+07	772	163			548	2	2	18	4				2		3	2				
13	B	0	2	o	1	75	3.96E+07	1035	196	2	11	711			4					58		1	33				
14	B	0	2	o	2	75	4.33E+07	1131	257	8	4	719			2					79			41				
15	B	0	2	o	3	74	3.58E+07	922	185	4	4	581			3		7			83			32				
16	B	24	2	0	1	94	2.66E+07	872	186	7	12	559			4	4				60			4				
17	B	24	2	0	2	99	2.30E+07	792	92		9	585			3					57	1	1	12		4		
18	B	24	2	0	3	92	2.78E+07	892	250		9	545		2	5					49			6		3		
19	B	24	2	1	1	93	2.85E+07	925	198		6	625		2	3					46			11		7		
20	B	24	2	1	2	89	2.51E+07	777	107		18	576			1	4				35		2	8		2		
21	B	24	2	1	3	89	2.59E+07	804	86	1	9	600			7					50			10		5		
22	B	24	2	2	1	89	1.96E+07	607	109	4	8	426			4					20	1		2		5		
23	B	24	2	2	2	90	1.95E+07	612	65	3	3	464			2					28		1	11		3		
24	B	24	2	2	3	93	2.06E+07	668	129	5	5	435			7	4				31		1	10		2		
25	C	0	2	o	1	94	2.21E+07	725	152	1	4	409			4					115			8		5		
26	C	0	2	o	2	95	1.86E+07	616	118	1		344								112		1	7		2		
27	C	0	2	o	3	104	1.83E+07	664	141		2	364								99		1	12		12		
28	C	24	1.9	0	1	100	2.72E+07	901	342	1		430		1	4					83		1	3		6		
29	C	24	2	0	2	95	2.92E+07	966	514		1	340			5					67		1	2		1	1	
30	C	24	2	0	3	97	1.66E+07	560	91	12		320			6					92			1		3		
31	C	24	2	1	1	101	1.77E+07	624	151	19	1	314			2					78		2	1		9		
32	C	24	2	1	2	102	1.98E+07	703	131	25	1	391		8	1					104			1		4		
33	C	24	2	1	3	98	2.16E+07	737	150	16		412			6					102		1	2		5		
34	C	24	2	2	1	93	1.71E+07	553	55	9	1	351			2					75		3	4		3		
35	C	24	2	2	2	101	1.94E+07	683	133	7	2	377		2	2					105			4	8			
36	C	24	2	2	3	101	2.04E+07	717	86	5	1	444			10					104		4	6		9		
37	D	0	2	o	1	90	2.92E+07	917	252	8		494			18	6				80		2	4		7	1	
38	D	0	2	o	2	102	2.77E+07	986	114			714			17					95			1		2		
39	D	0	2	o	3	100	3.34E+07	1163	313	1		681		4	17					88		2	5		1		
40	D	3	2	0	1	112	3.78E+07	1477	151	4	1	1187			33					46					1		
41	D	3	1.9	0	2	99	4.68E+07	1535	239		1	1199			23					20					2		
42	D	3	2	0	3	96	4.12E+07	1378	172	2	2	1078			32					32					9	1	

APPENDIX D : RSP' 95/96 MICROSCOPY [UV : o = time 0; 0 = total light;1 = no UV-B; 2 = partial UV-B] PAGE 2

#	EXP.	UV	DA	DB	DC	DD	DE	DF	DG	DI	DM	DN	RA	RC	RE	RK	RS	CTA	CTB	CTC	CTD	CTE	CTF	CTG	CTH	CTK	CTL	CTN	CTU	UCE	UD	UE	UF	UG	UK
1	A	o	1																																
2	A	o	1										1					4																		
3	A	o	1																																
4	A	0		1		1													1	3										1					
5	A	0	1																											1					
6	A	0																												1	1	1			
7	A	1	4																													1	8		
8	A	1	1																	1	1	1										1	7		
9	A	1	2	1																													2	1	
10	A	2	1																2				2										7		
11	A	2	1																														6		
12	A	2	3																1		2										1		7		
13	B	o	1	2																	1									1			1		
14	B	o	3	1															2													1			
15	B	o	3		2																			1	1							1			
16	B	0	4	2	1	2	1							1											8							1			
17	B	0	6			1																			1					1		2			
18	B	0	3																													2			
19	B	1	3																		1				1							2			
20	B	1	1																													2			
21	B	1	1	1				1												11															
22	B	2	2																				1									1			
23	B	2	2		1																			3								1			
24	B	2	5															1						1	4					1		1			
25	C	o																					1									1			
26	C	o	3		1																											1			
27	C	o	2															1						1						1		1			
28	C	0					1																							1					
29	C	0	2					1						1											1										
30	C	0						1																1						2		1			
31	C	1							1										1	12										1					
32	C	1	1	1																										1		1			
33	C	1	1																									6				2			
34	C	2	1																						1			10		1		1			
35	C	2	3																												1	2			
36	C	2	3	1				1																				3				2			
37	D	o	4					2																						1		1			
38	D	o	1																									3				1			
39	D	o	2		1	2																					2			1	1	3			
40	D	0	3						1																		3			1	1	5			
41	D	0	3					3																						1		3			
42	D	0	2			2		1																							1	2			

APPENDIX D : RSP' 95/96 MICROSCOPY [UV : o = time 0; 0 = total light;1 = no UV-B; 2 = partial UV-B] PAGE 3																										
#	EXP.	TIME (h)	VOL (s)	UV	REP #	# FOVs	cells/L	Tot. cells	PA	PB	NA	NB	NC	ND	NE	NF	NG	NG2	NJ	SF	CC	CR	CH	PR	RGT	SI	EA
43	D	3	2	1	1	98	4.04E+07	1380	192			1087			9					40						1	
44	D	3	2	1	2	92	4.17E+07	1338	211			1023			21					23							
45	D	3	2	1	3	98	4.09E+07	1398	168	2	1	1123			17					34					2		
46	D	3	2	2	1	96	4.34E+07	1451	171	1	1	1140		4	34					37					3		
47	D	3	2	2	2	101	4.25E+07	1496	182		2	1163		16	30	6				32					1		
48	D	3	2	2	3	92	4.60E+07	1474	158	4		1184			28	4				27		1			1		
49	D	5	1.9	0	1	91	5.07E+07	1527	391	1		1024		4	16					34					1		
50	D	5	2	0	2	98	4.73E+07	1615	326			1162			25	4				41		1			1		
51	D	5	2	0	3	93	4.63E+07	1501	283			1095			30					33		1					
52	D	5	1.9	1	1	90	6.89E+07	2053	314		1	1549			31					96		1					
53	D	5	2	1	2	85	6.06E+07	1794	272		3	1310		3	26					111							
54	D	5	2	1	3	93	6.37E+07	2064	318	2		1543	1		30	4			1	98						1	
55	D	5	2	2	1	84	5.37E+07	1511	300		1	1031			36					73		2				1	
56	D	5	2	2	2	100	4.51E+07	1511	245	1		1103		4	33					52		1			1		
57	D	5	2	2	3	98	5.58E+07	1833	380			1312			23					52		1			2		
58	E	0	2	o	1	116	2.40E+07	931	20	1	8	704		4	13					110		3					
59	E	0	2	o	2	104	2.49E+07	868	9	1	1	642			8					137		2	1		1		
60	E	0	2	o	3	99	2.71E+07	900	4	1	5	665		4	11					134		4		1	1		
61	E	24	2	0	1	97	1.58E+07	534	14		5	382			12					47					2		
62	E	24	2	0	2	97	1.45E+07	490	8	1	3	341			12					43		4	1		4		
63	E	24	2	0	3	112	1.57E+07	611	7	1	5	424			13					76		1		1	2		
64	E	24	2	1	1	101	1.71E+07	602	6		2	438		1	12					58		1	1		2		
65	E	24	2	1	2	93	1.62E+07	524	9	1	4	385			11					37	3	1			2		
66	E	24	2	1	3	102	1.63E+07	579	5		2	430			7					49		1			6		
67	E	24	2	2	1	111	1.45E+07	561	13		4	388		2	20	1				60							
68	E	24	2	2	2	116	1.65E+07	669	22		1	475			17					69					4		
69	E	24	2	2	3	111	1.58E+07	610	12		4	460			15					33					1		
70	F	0	2		1	96	2.03E+07	678	70		5	279			64					159		7	5		2		
71	F	0	2		2	93	2.42E+07	785	217		9	241		2	64	1				156	1	6	6		1		
72	F	0	2		3	96	2.20E+07	735	160		4	274		5	40					156		3	5		1		
73	F	24	2	0	1	98	1.98E+07	676	45		3	299			49	4				178		4	4		4	1	
74	F	24	2	0	2	90	2.02E+07	633	25		9	247		3	56					203		2	5		4		
75	F	24	2	0	3	92	2.03E+07	651	74		3	234		4	42	3			1	193		2	3		1		
76	F	24	2	1	1	86	2.20E+07	658	77		6	263	1	5	40				1	161		3	4		1		
77	F	24	2	1	2	88	2.70E+07	829	102		7	341		5	54		1			216		2	5		3		
78	F	24	2	1	3	87	2.76E+07	836	147		1	331		4	49		1	2		200		2	6				
79	F	24	2	2	1	99	2.48E+07	822	158		6	333		8	56				1	170		1	4				
80	F	24	2	2	2	101	2.59E+07	875	254		9	298		6	55					155		2	4		1		
81	F	24	2	2	3	96	2.04E+07	655	91		9	259	1	2	37	2				153		3	3		3		1
82	G	0	2		1	97	1.44E+07	486	106		4	186	1	1	42					47		1	11		1		
83	G	0	2		2	97	1.67E+07	565	145		8	173	1	6	65					55		5	5		2		
84	G	0	2		3	92	1.55E+07	497	85		3	171		6	66					64		2	6		3		

APPENDIX D : RSP² 95/96 MICROSCOPY {UV : o = time 0; 0 = total light; 1 = no UV-B; 2 = partial UV-B} PAGE 4

#	EXP.	UV	DA	DB	DC	DD	DE	DF	DG	DI	DM	DN	RA	RC	RE	RK	RS	CTA	CTB	CTC	CTD	CTE	CTF	CTG	CTH	CTK	CTL	CTN	CTU	UCE	UD	UE	UF	UG	UK
43	D	1				1																		1							1	4			
44	D	1						2	1																		3					9			
45	D	1	1			1		1																								2			
46	D	2	2			2		2																						1		5			
47	D	2	5					2							1															2	1	4			
48	D	2	2		2			2										1						1			1			1		7			
49	D	0	1			1																					3				1	1			
50	D	0	1																					1								3			
51	D	0	1			1		2																						1		3			
52	D	1	1					1																2						1		3			
53	D	1				1													1								10			1		2			
54	D	1			1	2																										8			
55	D	2	3					1																						2		4			
56	D	2	2																					1			1					9			
57	D	2												1																		3			
58	E	o						2		1																						5		2	
59	E	o						1																1								4		1	
60	E	o	2					1							2																	1		4	
61	E	0	2					3																1			2			2	1				
62	E	0			1	2		1	1																							6			
63	E	0	4					3	2															1								7		1	
64	E	1	2					3		1														2							1	5		2	
65	E	1						1																								2		2	
66	E	1				1																		1	3					1	1	2		3	
67	E	2	4																																
68	E	2				1		2	1																					2		5			
69	E	2	1			1		2	1																					3		5		1	
70	F		1		1																			3							1	10		1	
71	F		2			1		1		1													1	1							1	2			
72	F		2																					1							1	11			
73	F	0				2																		1					4			5			
74	F	0						1																					1			3			
75	F	0						3																2					1	1	1	8			
76	F	1	1		1	1		3	1					1										2								9			
77	F	1	1					1	1	1														4			1		2			4			
78	F	1	1	1																				1		2				1	2	5			1
79	F	2						1																								3			
80	F	2						1										1											1			6			
81	F	2						1																		1			1		2	3			
82	G							1																					1			2			
83	G		3					6								1								1						2		2		1	1
84	G							1								1															1	4			

APPENDIX D : RSP¹ 95/96 MICROSCOPY [UV : o = time 0; 0 = total light;1 = no UV-B; 2 = partial UV-B] PAGE 5																											
#	EXP.	TIME (h)	VOL (s)	UV	REP #	# FOVs	cells/L	Tot. cells	PA	PB	NA	NB	NC	ND	NE	NF	NG	NG2	NJ	SF	CC	CR	CH	PR	RGT	SI	EA
85	G	3	2	0	1	107	1.23E+07	459	67		5	159	1		46					70		4	12				
86	G	3	2	0	2	99	1.11E+07	384	64		3	145	4	3	19					48			3		1		
87	G	3	2	0	3	101	1.15E+07	406	42		4	143	3	1	40		1			58		4	9		3	1	
88	G	3	2	1	1	99	2.74E+07	946	531		9	172	1	1	60		1			54		1	7		4		
89	G	3	2	1	2	93	1.92E+07	622	164		6	192	4	4	75	8	1			41	1	2	12		3		1
90	G	3	2	1	3	95	1.69E+07	559	163		5	178	3		58					40		1	10				
91	G	3	2	2	1	88	1.88E+07	576	176		6	178	1	2	45			4		46		3	6		3		
92	G	3	2	2	2	88	2.63E+07	808	398		3	187	2	1	46					49			10	1	1		
93	G	3	2	2	3	92	1.67E+07	534	143		11	174	1	3	44					36		1	8		2		
94	G	5	2	0	1	100	2.36E+07	823	339		2	207	3	4	63					90			4		1		
95	G	5	2	0	2	88	2.64E+07	810	436		5	103	3	2	79	1	4			59			6		1		
96	G	5	2	0	3	87	2.52E+07	764	298		4	187	2	3	76		5			83			4				
97	G	5	2	1	1	88	3.18E+07	975	490		10	187		4	66	4				90		1	13		1		
98	G	5	2	1	2	93	2.38E+07	771	313		3	197	1	1	62	2	5			73			10				
99	G	5	2	1	3	90	2.54E+07	797	282		7	225	3		72	2				77			11		2		
100	G	5	2	2	1	91	2.29E+07	727	280		2	180	5	5	52					76		1	6		1		
101	G	5	2	2	2	89	2.54E+07	787	337		9	172	5	5	52	16				58			12		3		
102	G	5	2	2	3	88	2.36E+07	723	281		7	180	1		58	2				64			13		1		
103	H	0	4		1	121	5.04E+06	425	4		34	23		1	33	71				121		3	6		6		
104	H	0	4		2	119	5.65E+06	469	7		35	19		3	64	64				106		3	3		12		
105	H	0	4		3	126	5.63E+06	494			45	20			77	101	1			95		6	8		8		1
106	H	24	4	0	1	125	5.57E+06	485	8		63	19		2	62	109				75		4	6		11		
107	H	24	4	0	2	142	5.38E+06	532	6		77	16	1	4	56	113				78	2	8	2		18		
108	H	24	4	0	3	124	5.47E+06	473	1		61	7	7	4	74	92	1			63		5	6		16		
109	H	24	4	1	1	136	4.74E+06	449	1		75	12			36	115				49		2	5		11	1	
110	H	24	4	1	2	148	3.95E+06	407	3		76	10		1	51	73				47		4	3		5	1	
111	H	24	4	1	3	128	4.83E+06	431			69	9			50	91				46					8		
112	H	24	4	2	1	135	4.91E+06	462	2		50	11	1	4	51	116				53		5	3		8		1
113	H	24	4	2	2	113	5.75E+06	453	3		61	12		4	69	80				62		9	2		8		1
114	H	24	4	2	3	166	4.81E+06	557	1		77	13		3	54	157				71		7	2		18		

APPENDIX D : RSP' 95/96 MICROSCOPY [UV : o = time 0; 0 = total light;1 = no UV-B; 2 = partial UV-B] PAGE 6

#	EXP.	UV	DA	DB	DC	DD	DE	DF	DG	DI	DM	DN	RA	RC	RE	RK	RS	CTA	CTB	CTC	CTD	CTE	CTF	CTG	CTH	CTK	CTL	CTN	CTU	UCE	UD	UE	UF	UG	UK
85	G	0	1					1								1															1	5			1
86	G	0	2		1			1																								4			
87	G	0	2					1																	1				1			4		1	
88	G	1	1			1																		3						2	1	8			
89	G	1	4										2											1		3						2	4			2
90	G	1	1		1											1								1								6			
91	G	2						3																4								6			
92	G	2	2										1											2		1						10			
93	G	2			1													1						2		1				2		8			1
94	G	0	2					1																3		1					1	8			
95	G	0	2																				1								1	11			1
96	G	0	2																										1	1		2			
97	G	1	2																							1			2	1		4			1
98	G	1																						2								3			
99	G	1	1		1			1																1			2		1	1	1	6		1	
100	G	2	3		3			1																1		1						8			
101	G	2	2																					2								10			1
102	G	2	1													1								5			1				1	3			
103	H		3		6	2									2		2													1		1		3	
104	H		4		1			23			1				3												11			5				1	
105	H		1		3			11		1					5	1														4		1			
106	H	0	2		2	2		6				2					3													2				1	
107	H	0	8		2	1		19		2		4				1	4													1		2			
108	H	0	2			4		14		1	2						3													1		1			
109	H	1	6		2			9			5				6															3				1	
110	H	1	5					12							4												1								
111	H	1	6			1		27			2				5	1								2			1							1	
112	H	2	2		2	3		22		2	1	1					5													4				1	
113	H	2	6		3			8									3							2			3		1			1			
114	H	2	7		4	1		16		1		2				1	3	1												1				1	

VITA

Naomi Parker was born in Owen, South Australia and attended Owen Primary School and Balaklava High School, graduating from High School in December, 1988. In February 1989 she began a Bachelor of Science at the Flinders University of South Australia and graduated with a B.Sc in Plant and Environmental Biology in 1991. In February 1992 she began a Graduate diploma of Antarctic and Southern Ocean studies with honors at the University of Tasmania, graduating the same year. She then spent a year and a half working in Hobart, Tasmania for the University of Tasmania, CSIRO division of Fisheries, and the Australian Antarctic Division. In July of 1994 she began a masters degree at the University of Tennessee and completed this in May, 1997. She will be commencing her PhD at the University of Tasmania studying bloom dynamics of phytoplankton in the Huon estuary and their impact on aquaculture in March of 1997.